

SPRINGER BRIEFS IN STATISTICS  
JSS RESEARCH SERIES IN STATISTICS

Yoko Tanokura  
Genshiro Kitagawa

# Indexation and Causation of Financial Markets Nonstationary Time Series Analysis Method



 Springer

# **SpringerBriefs in Statistics**

JSS Research Series in Statistics

## **Editor-in-chief**

Naoto Kunitomo  
Akimichi Takemura

## **Series editors**

Genshiro Kitagawa  
Tomoyuki Higuchi  
Nakahiro Yoshida  
Yutaka Kano  
Toshimitsu Hamasaki  
Shigeyuki Matsui  
Manabu Iwasaki

The current research of statistics in Japan has expanded in several directions in line with recent trends in academic activities in the area of statistics and statistical sciences over the globe. The core of these research activities in statistics in Japan has been the Japan Statistical Society (JSS). This society, the oldest and largest academic organization for statistics in Japan, was founded in 1931 by a handful of pioneer statisticians and economists and now has a history of about 80 years. Many distinguished scholars have been members, including the influential statistician Hirotugu Akaike, who was a past president of JSS, and the notable mathematician Kiyosi Itô, who was an earlier member of the Institute of Statistical Mathematics (ISM), which has been a closely related organization since the establishment of ISM. The society has two academic journals: the Journal of the Japan Statistical Society (English Series) and the Journal of the Japan Statistical Society (Japanese Series). The membership of JSS consists of researchers, teachers, and professional statisticians in many different fields including mathematics, statistics, engineering, medical sciences, government statistics, economics, business, psychology, education, and many other natural, biological, and social sciences.

The JSS Series of Statistics aims to publish recent results of current research activities in the areas of statistics and statistical sciences in Japan that otherwise would not be available in English; they are complementary to the two JSS academic journals, both English and Japanese. Because the scope of a research paper in academic journals inevitably has become narrowly focused and condensed in recent years, this series is intended to fill the gap between academic research activities and the form of a single academic paper.

The series will be of great interest to a wide audience of researchers, teachers, professional statisticians, and graduate students in many countries who are interested in statistics and statistical sciences, in statistical theory, and in various areas of statistical applications.

More information about this series at <http://www.springer.com/series/13497>

Yoko Tanokura · Genshiro Kitagawa

# Indexation and Causation of Financial Markets

Nonstationary Time Series Analysis Method

 Springer

Yoko Tanokura  
Graduate School of Advanced Mathematical  
Sciences  
Meiji University  
Nakano-ku, Tokyo  
Japan

Genshiro Kitagawa  
Research Organization of Information  
and Systems  
Minato-ku, Tokyo  
Japan

ISSN 2191-544X  
SpringerBriefs in Statistics  
ISSN 2364-0057  
JSS Research Series in Statistics  
ISBN 978-4-431-55275-8  
DOI 10.1007/978-4-431-55276-5

ISSN 2191-5458 (electronic)  
ISSN 2364-0065 (electronic)  
ISBN 978-4-431-55276-5 (eBook)

Library of Congress Control Number: 2015959580

© The Author(s) 2015

This work is subject to copyright. All rights are reserved by the Publisher, whether the whole or part of the material is concerned, specifically the rights of translation, reprinting, reuse of illustrations, recitation, broadcasting, reproduction on microfilms or in any other physical way, and transmission or information storage and retrieval, electronic adaptation, computer software, or by similar or dissimilar methodology now known or hereafter developed.

The use of general descriptive names, registered names, trademarks, service marks, etc. in this publication does not imply, even in the absence of a specific statement, that such names are exempt from the relevant protective laws and regulations and therefore free for general use.

The publisher, the authors and the editors are safe to assume that the advice and information in this book are believed to be true and accurate at the date of publication. Neither the publisher nor the authors or the editors give a warranty, express or implied, with respect to the material contained herein or for any errors or omissions that may have been made.

Printed on acid-free paper

This Springer imprint is published by SpringerNature  
The registered company is Springer Japan KK

# Preface

Financial markets can be found in nearly all countries throughout the world. As a result of the integration of a country's local financial system with international financial markets, people's daily lives in such countries, as well as the countries themselves, have become more exposed to cross-border risks, such as financial and economic risks. The financial crisis triggered by the US subprime loan crisis in 2007 eventually led to a global economic crisis that affected simultaneously not only emerging countries but also developed countries all over the world. In order to determine the mechanism of the crisis, a market overview is indispensable, especially when the market is influential on business and economy.

One means to express the overall perspective of a market is to construct an index as a proxy measure. However, unlike an established market, in which the index is officially defined and announced, for a newly developed financial instrument experiencing its rapid market growth, it is not easy to construct an appropriate index due to the lack of information. Moreover, in order to fully reflect the price movements of a financial asset, the index should reflect their distributions. However, these distributions are often heavy-tailed and possibly skewed, and identifying them directly is not easy.

This book develops through the use of nonstationary non-Gaussian multivariate time series analysis a new practical method for constructing an index of prices of a financial asset for which the distributions are skewed and heavy-tailed. In order to facilitate the identification of non-Gaussian distributions, we propose to transform the price observations by the Box-Cox transformation. Then, the long-term trend of the distributions of the optimal Box-Cox transformed observations is estimated by fitting a trend model in which observation noises have a time-varying variance. The parameter of the optimal transformation is determined by the AIC. By applying state-space modeling, the estimation is performed and missing observations are automatically interpolated. Finally, the index is defined by taking the inverse Box-Cox transformation of the optimal long-term trend. The new index becomes impartial, regardless of the price distribution, and is referred to as a distribution-free index.

Economic and financial time series often exhibit a gradually changing long-term fluctuation, i.e., a trend, which may sometimes form a pattern due to an event specific to the attribute of the time series such as fundamental and economic factors. On the other hand, the short-term cyclical fluctuations around the trend can be sensitively influenced by short-term cyclical fluctuations of any other economic and financial time series, regardless of their specific characteristics. In fact, contagious phenomena of short-term fluctuations of financial markets have often been observed worldwide due to the globalization of the financial system. In order to detect such causations, this book proposes the application of the generalized power contribution, which extends the original Akaike's power contribution by decomposing a variance covariance matrix of noises. The frequency-wise effect of multidimensional noise sources on the fluctuation of each variable with feedback loops is thus revealed.

In order to investigate the effectiveness of a distribution-free index, this book applies the construction method of a distribution-free index to financial and economic time series data and analyzes the causations using power contributions. For example, applying this method to the sovereign credit default swap markets, in which the spread distributions are often heavy-tailed and the number of observations varies over time due to immaturity, the worldwide spillover effects of the European debt crisis are detected. Another example shows the clear polarization between advanced and emerging regions by constructing the GDP growth distribution-free indices.

These applications confirm that applying our indexation method to markets with insufficient information, such as fast-growing or immature markets, can be effective. Therefore, wider applicable area of our method can be expected.

Although this book has been made to be as self-contained as possible, the reader may benefit from some of the referenced literature.

This book is intended for anyone who is interested in the practical use of statistical methods in solving real-world problems. We hope that our method will prove useful in analyzing practical problems in finance and economics.

Tokyo, Japan  
August 2015

Yoko Tanokura  
Genshiro Kitagawa

## Acknowledgments

The research in this book was supported in part by Grants-in-Aid for Scientific Research (C) No. 22500270, (C) No. 25330044, and (A) No. 22240030. We express our gratitude to Prof. Hiroshi Tsuda of Doshisha University and to Prof. Seisho Sato of the University of Tokyo for their helpful discussions. Also, we are deeply grateful to Mr. Nizam Hamid for his valuable comments on the applications. Finally, we thank Mr. Yasuaki Fujine and Ms. Kozue Inamura for their support in building the database.

# Contents

<b>1</b>	<b>Introduction</b>	1
1.1	Indexation of Financial Markets	1
1.2	Causation of Financial Markets	3
1.3	Nonstationarity of Financial Time Series	5
1.4	State-Space Modeling	8
1.5	Organization of the Book and Related Web Information	10
	References	10
<b>2</b>	<b>Method for Constructing a Distribution-Free Index</b>	13
2.1	Nonstationary Time Series Modeling	13
2.1.1	Trend Estimation	13
2.1.2	Time-Varying Variance Modeling	16
2.1.3	Seasonal Adjustment Modeling	19
2.1.4	Non-Gaussian Distribution Modeling	22
2.2	Transformation of Non-Gaussian Distributed Prices of a Financial Market	27
2.3	Construction of a Distribution-Free Index	30
	References	33
<b>3</b>	<b>Power Contribution Analysis of a Multivariate Feedback System</b>	35
3.1	Akaike's Power Contribution and Its Generalization	35
3.2	Algorithm for Decomposing a Variance Covariance Matrix	40
3.3	Example of Power Contribution Analysis	43
	References	46

<b>4 Application to Financial and Economic Time Series Data</b> . . . . .	49
4.1 Detecting Crisis Spillovers in Terms of Sovereign CDS Distribution-Free Indices . . . . .	49
4.1.1 SCDS Regional Distribution-Free Index Construction . . . . .	50
4.1.2 Role of the SCDS Distribution-Free Index . . . . .	56
4.1.3 Causation Between SCDS Regional Distribution-Free Indices . . . . .	59
4.2 Measuring the Impact of the US Subprime Crisis on Japanese Financial Markets . . . . .	64
4.2.1 Japanese Corporate CDS Market and Rating Classes . . . . .	65
4.2.2 Japanese CDS Rating-Based Distribution-Free Index Construction . . . . .	67
4.2.3 Causation Between Japanese Financial Markets . . . . .	72
4.3 Other Applications: Usability of the Distribution-Free Index . . . . .	78
4.3.1 Constructing a GDP Growth Regional Distribution-Free Index . . . . .	79
4.3.2 Constructing a Japanese SCDS Distribution-Free Index Using SCDS Curves . . . . .	90
References . . . . .	99
<b>Index</b> . . . . .	101

# Chapter 1

## Introduction

**Abstract** This book presents a new practical method for constructing an index of prices of a financial asset for the case in which the distributions are skewed and heavy-tailed, using nonstationary non-Gaussian multivariate time series analysis. In order to facilitate the identification of the distribution, the observations are transformed by the Box-Cox transformation. A new distribution-free index is defined by taking the inverse Box-Cox transformation of the optimal long-term trend, which is estimated by fitting a trend model with time-varying observation noises. In order to detect causations between financial markets which are mostly entangled and may cause inextricable difficulties, such as financial crises, this book proposes the application of the generalized power contribution, which reveals the frequency-wise effect of multidimensional noise sources on the power of fluctuation of each variable in a multivariate feedback system. Applications to financial and economic time series data are used to investigate the effectiveness of the new index by power contribution analysis, and confirm that applying our indexation method to markets with insufficient information, such as fast-growing or immature markets, can be effective.

**Keywords** Heavy-tailed · Box-Cox transformation · Trend model with time-varying observation noises · Power contribution · Distribution-free index

### 1.1 Indexation of Financial Markets

Financial markets can be found in nearly all countries throughout the world. Some of these markets are extremely small in terms of market size and have only a few participants, whereas others, such as the New York Stock Exchange and the foreign exchange markets, trade significant assets. Financial news is reported globally, and the direct or indirect influences of financial markets on people's daily lives, as well as on countries, are considered daily.

One means for expressing the overall perspective of a market is to use an index as a proxy measure. For an established market, such as a listed stock market, the index is officially defined and announced. Various types of methods can be used to compute an index, depending on its purpose. On the other hand, for a newly developed financial instrument forming its market rapidly, it is not easy to construct an appropriate index due to a lack of information. For example, the number of price observations varies

over time and may even become zero at certain times. However, a market overview is indispensable for financial products that may influence business and economy.

A good example of such a market is the credit default swap (CDS) market. The attention to credit risk, which measures the exposure to loss resulting from failure of a corporation or government to fulfill its debt obligations, has become noticeable since recent financial crises such as the global financial crisis triggered by the US subprime loan crisis in 2007 and the European debt crisis revealed in 2009. The CDS is an over-the-counter derivative contract first introduced in 1997, that is designed to isolate the credit risk of an underlying asset without selling the asset itself. In particular, the sovereign CDS (SCDS) spread for dealing with sovereign risk on a government bond can be regarded as the market evaluation of the credit risk of that country. Even though the SCDS market is not mature, the market trend for SCDS has become significantly influential on the global economy.

Although the assumption that the distributions of prices or returns of financial assets are Gaussian has been commonly used in theoretical finance, some studies in the 1960s failed to validate this assumption and found heavier tails than would be present in a Gaussian distribution (Mandelbrot 1963; Fama 1965). The tails consisting of extreme values of prices or returns that are caused by sharply soaring or plunging asset prices, are more likely to occur than expected by a Gaussian distribution. In particular, distributions of stock returns have been discussed in many studies such as Paraez (1972), Madan and Seneta (1990), and Linden (2001). However, an exact identification of such distributions remains an open question.

The distribution of CDS spreads is often significantly heavy-tailed and has numerous missing observations at certain times, especially for early trade dates. Although identifying a heavy-tailed distribution directly is not easy, in order to fully incorporate the overall price movements of the market, the index should reflect their distributions.

In order to address the above problems, this book proposes a new practical method for constructing an index of prices of a financial asset for which the distributions are skewed and heavy-tailed, using nonstationary non-Gaussian multivariate time series analysis. First, in order to facilitate the identification of such a distribution, we transform the price observations by the Box-Cox transformation (Box and Cox 1964). This transformation has been applied in various areas of finance and expresses most major transformations, such as the inverse transformation, the reciprocal square root transformation, the logarithmic transformation, the square root, and no transformation, according to the value of the parameter. Second, we estimate the long-term trend of the distributions of the optimal Box-Cox transformed prices by fitting a trend model with time-varying observation noises. The parameter of the optimal Box-Cox transformation is determined by minimizing the AIC (Akaike 1998; Konishi and Kitagawa 2008) with respect to the original price data. By applying a state-space representation and the Kalman filter/fixed interval smoothing algorithm, the estimation is performed and missing observations are automatically interpolated (Kitagawa 2010). Finally, the index is defined by taking the inverse Box-Cox transformation of the optimal long-term trend. Then, the index becomes impartial regardless of price distribution, which is referred to as a distribution-free index.

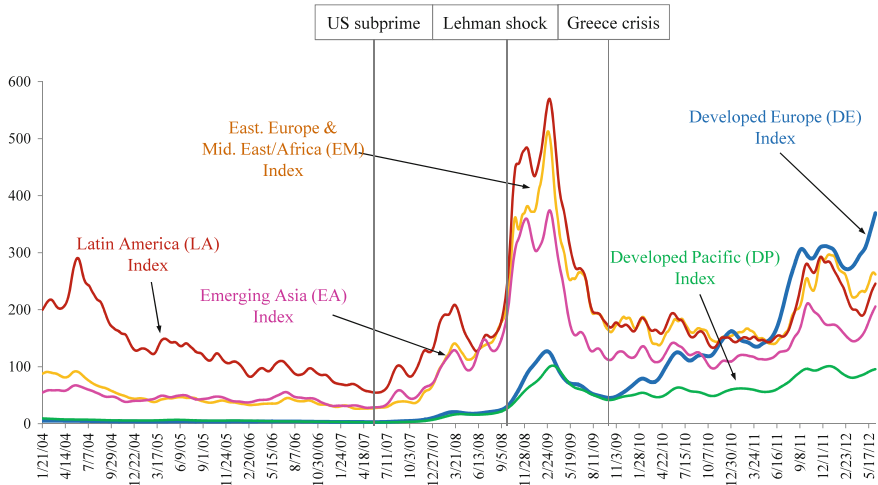


**Fig. 1.1** Five SCDS regional distribution-free indices. *Source* Bloomberg LP

Tanokura et al. (2012) proposed a method based on trend estimation with Cauchy observation noises that are dependent on the number of observations. This book presents further improvement to the trend model with Gaussian observation noises with the time-varying variance proposed in Kitagawa (1987). To our knowledge, there have been few studies on estimating heavy-tailed distributions using a variable transformation and the AIC.

In this book, various examples of distribution-free indices are analyzed. For example, by applying the indexation method to SCDS spreads by region, the SCDS regional distribution-free indices are constructed. Figure 1.1 shows a sharp increase of the Developed Europe (DE) index (blue line), representing the sovereign risk of the developed Europe, as compared to those of the other regional indices, since the revelation of the Greece debt crisis in the fall of 2009. The spillover effects of the European debt crisis are observed. We analyze these SCDS regional distribution-free indices in Chap. 4.

## 1.2 Causation of Financial Markets

Due to the globalization of the financial system, contagious phenomena of price fluctuations of financial markets have often been observed worldwide. Financial markets are mostly diversified and entangled, which may cause inextricable difficulties. In fact, the global economy has remained more or less sluggish since the global economic crisis driven by the bankruptcy of Lehman Brothers in 2008. In order to cope with difficulties in controlling spillovers and policy planning, it is necessary to clarify the mechanisms behind contagious phenomena. In particular, since the prices of

financial assets fluctuate with both serial correlations and time series correlations, identifying the dynamic structure, i.e., measuring the degree and direction of influence between markets, is significant.

Economic and financial time series often exhibit a gradually changing long-term fluctuation, which is referred to as a trend. A trend may sometimes form a pattern due to an event specific to the attribute of the time series such as fundamental and economic factors. On the other hand, the short-term cyclical fluctuations around the trend can sensitively be influenced by short-term cyclical fluctuations of any other economic and financial time series, regardless of their specific characteristics. Such a short-term cyclical fluctuation may lead to a future change in the trend direction. In this book, we treat causations which arise from short-term cyclical fluctuations.

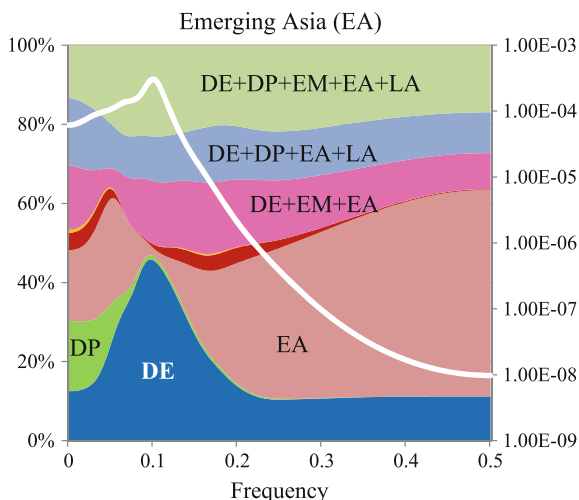
As a causation measure for this purpose, we focus on the concept of relative power contribution through multivariate autoregressive (AR) modeling, which was proposed by Akaike (1968) for analyzing a multivariate feedback system. This measure is referred to as Akaike's power contribution.

The presence of feedback in a multivariate dynamic system, namely, the influence of an input variable on an output variable with a time lag, can be expressed directly by the time-domain approach. On the other hand, by the frequency domain approach, periodic variations of repetitive and regular movements, which are often observed in financial and economic time series, can be expressed in the form of trigonometric functions, however, there are practically difficulties in capturing feedback loops. Akaike's power contribution expresses frequency-wise causations including feedback through the multivariate AR modeling framework.

Akaike's power contribution has been applied to various real-world problems (Akaike and Nakagawa 1988; Akaike and Kitagawa 1999; Ohtsu et al. 1981, 2015). However, because of the independence assumption between the noises of variables, Akaike's power contribution is not applicable to time series in economics and finance because significant correlations between the noises of variables are often observed. In order to address this problem, the generalized power contribution was proposed by decomposing a variance covariance matrix of the noises of variables (Tanokura and Kitagawa 2004). This modeling reveals the frequency-wise effect of multidimensional noise sources on the power of the fluctuation of each variable in a multivariate feedback system. In other words, it becomes possible to simultaneously measure the degree of influence between various combinations of the noises of variables. Therefore, multidirectional causations between variables can be evaluated. The applicable area is significantly widened (Tanokura 2006). Moreover, since we ensure the stability of Akaike's original power contribution in the generalized power contribution, the concept of power contribution is strengthened and improved.

Other related studies on detecting noise sources can be found in various areas such as neuroscience and econometrics. In particular, based on a well-known causality concept defined by Granger (1969), frequency-wise measures of causality for two stationary time series proposed in Geweke (1982) and Hosoya (1991) were extended to those measures for three series in Geweke (1984) and Hosoya (2001), respectively. Although their interests are similar to ours, their approaches are fundamentally different from Akaike's (as noted in Hosoya 1991).

**Fig. 1.2** Power contributions (%) and the log-transformed power spectrum (*white line*) for the Emerging Asia (EA) index, which is the SCDS distribution-free index of the emerging Asia. The SCDS regional distribution-free indices contributing to the fluctuations of the EA index are the Developed Europe (DE), Developed Pacific (DP), Eastern Europe and Middle East/Africa (EM), and Latin America (LA) indices. *Source* Bloomberg LP



To our knowledge, there have been no practical studies on the analysis of measuring multidirectional influences from multidimensional noise sources simultaneously, based on the direct decomposition of a variance covariance matrix of the noises of variables in order to quantitatively evaluate the degree of influences.

This book conducts a power contribution analysis for short-term cyclical fluctuations of financial and economic time series data, including distribution-free indices that we constructed, and investigates the effectiveness of the method for constructing a distribution-free index.

Figure 1.2 shows the power contributions (%) and the power spectrum (white line) for the Emerging Asia (EA) index, which is the SCDS distribution-free index of the emerging Asia. The peak of the contribution from the Developed Europe (DE) index (blue area) representing the sovereign risk of the developed Europe, around the frequency of 0.1 (approximately 10-day cycle of fluctuation), sharply penetrates the contribution from the EA index itself (light pink area). This implies a significantly rooted spillover effect from the European debt crisis on the emerging Asia. The analysis is presented in Chap. 4.

### 1.3 Nonstationarity of Financial Time Series

A time series is a record of a randomly fluctuating phenomenon. Data used in financial markets and economics, such as stock prices, foreign exchange rates, and economic growth rates, are often collected in the form of a series of observations recorded at a conventionally equally spaced time interval, such as daily, monthly, and quarterly intervals.

The primary purpose of time series analysis is generally to capture both time series correlations and serial correlations across several time series. Since such fluctuating phenomena in the real world often entail uncertainties, the time series is expressed by a stochastic model. Therefore, the observed phenomenon is regarded as a realization of the model.

In order to measure the dependency of a time series, we define the following statistics. We denote a univariate time series as  $y_n$ ,  $n = 1, \dots, N$ . The mean value function of the time series is defined as

$$\mu_n = E(y_n), \quad (1.1)$$

where  $E(y)$  denotes the expectation with respect to the distribution of  $y$ .

The auto-covariance of the time lag  $k$  between the time series  $y_n$  and  $y_{n-k}$  is defined as

$$C_{n,n-k} = Cov(y_n, y_{n-k}) = E\{(y_n - \mu_n)(y_{n-k} - \mu_{n-k})\}. \quad (1.2)$$

Note that the variance of the time series,  $Var(y_n)$ , is obtained when  $k = 0$ .

When a phenomenon is regarded as a realization of a stochastic model with a time-invariant structure, i.e., when a time series  $y_n$  satisfies the following conditions:

$$E(y_n) = E(y_{n-k}), \quad (1.3)$$

$$Var(y_n) = Var(y_{n-k}), \quad (1.4)$$

$$Cov(y_n, y_m) = Cov(y_{n-k}, y_{m-k}), \quad n \neq m \quad (1.5)$$

for an arbitrary integer  $k$ , we refer to the time series as weakly stationary. In this book, a stationary time series refers to a weakly stationary time series, which is often useful in applications to real-world phenomena.

For a stationary time series, the mean value function becomes a constant, i.e.,

$$\mu = E(y_n), \quad (1.6)$$

which is referred to as the mean of the time series  $y_n$ . Then, the auto-covariance of the lag  $k$  becomes

$$C_{n,n-k} = Cov(y_n, y_{n-k}) = E\{(y_n - \mu)(y_{n-k} - \mu)\}, \quad (1.7)$$

which is expressed as a function of  $k$  and is referred to as the auto-covariance function.

The fluctuation of a time series often correlates to that of another time series. The statistics for such a multivariate time series are defined as follows.

We denote  $y_n = (y_n(1), \dots, y_n(l))^t$ ,  $n = 1, \dots, N$ , as an  $l$ -dimensional time series, where  $x^t$  is the transposed form of a vector  $x$ . The mean of the  $i$ th time series  $y_n(i)$  is defined as

$$\mu(i) = E\{y_n(i)\}, \quad i = 1, \dots, l. \quad (1.8)$$

The cross-covariance of the time lag  $k$  between the time series  $y_n(i)$  and another time series  $y_{n-k}(j)$  is defined as

$$C_k(i, j) = Cov(y_n(i), y_{n-k}(j)) = E[\{y_n(i) - \mu(i)\}\{y_{n-k}(j) - \mu(j)\}^t]. \quad (1.9)$$

Then, a matrix  $C_k = (C_k(i, j))$  is referred to as the cross-covariance matrix of the lag  $k$  (Box and Jenkins 1970; Akaike and Nakagawa 1988). When  $C_k$  is regarded as a function of  $k$ ,  $C_k$  is referred to as a cross-covariance function of the lag  $k$ . The diagonal element  $C_k(i, i)$  is the auto-covariance function of the  $i$ th time series  $y_n(i)$ .

The estimations of (1.1) and (1.2) for a univariate time series, and those of (1.8) and (1.9) for an  $l$ -dimensional time series are, respectively, given by

$$\hat{\mu} = \frac{1}{N} \sum_{n=1}^N y_n, \quad (1.10)$$

$$\hat{C}_{n,n-k} = \frac{1}{N} \sum_{n=k+1}^N (y_n - \hat{\mu})(y_{n-k} - \hat{\mu}), \quad (1.11)$$

$$\hat{\mu}(i) = \frac{1}{N} \sum_{n=1}^N y_n(i), \quad (1.12)$$

$$\hat{C}_k(i, j) = \frac{1}{N} \sum_{n=k+1}^N (y_n(i) - \hat{\mu}(i))(y_{n-k}(j) - \hat{\mu}(j)). \quad (1.13)$$

Economic and financial time series are often observed to be nonstationary. A time series has a trend, namely, a mean value function that slowly moves upward or downward, a time series has short-term cyclical fluctuations, namely, time-varying fluctuations around the mean value, and a time series has both a trend and short-term cyclical fluctuations. For example, Fig. 1.3 shows a Japanese equity index, the Nikkei 225 provided by the Nikkei, of which the long-term fluctuation moved upward and downward. In this book, we focus on such financial phenomena. In Sect. 2.1, we provide several methods for modeling nonstationary time series.



**Fig. 1.3** Transition of the Nikkei 225. *Source* the Nikkei

## 1.4 State-Space Modeling

The estimations of the time series models provided in this book are obtained through state-space modeling, which provides a unified method for solving various practical problems. Moreover, state-space modeling is appropriate for analyzing immature financial markets with insufficient information, because missing observations can be interpolated. Here, we provide the definition of the standard state-space model treated in this book.

Suppose that an  $l$ -dimensional time series  $y_n$  is expressed as the following state-space model:

$$x_n = Fx_{n-1} + Gv_n \quad : \text{system model}, \quad (1.14)$$

$$y_n = Hx_n + w_n \quad : \text{observation model}, \quad (1.15)$$

where the  $k$ -dimensional vector  $x_n$  is referred to as a state vector, and  $F$ ,  $G$ , and  $H$  are  $k \times k$ ,  $k \times m$ , and  $l \times k$  matrices, respectively. An  $m$ -dimensional system noise  $v_n$  in (1.14) is a white noise that follows a Gaussian distribution with the  $m$ -dimensional mean vector  $0$  and an  $m \times m$  variance covariance matrix  $Q$ . An  $l$ -dimensional observation noise  $w_n$  in (1.15) is a white noise that follows a Gaussian distribution with the  $l$ -dimensional mean vector  $0$  and an  $l \times l$  variance covariance matrix  $R$ . In this book, for convenience,  $v_n$  and  $w_n$  are assumed to be independent.

In state-space modeling, the system evolution over time is determined by the state vector in the system model (1.14), and the observation is expressed as the transition of the state vector following the observation model (1.15). The estimation of the state vector is equivalent to identifying its conditional distribution, which is assumed to be Gaussian. Therefore, the conditional means and conditional variance covariance matrices of the state vector can recursively be obtained using the Kalman filter.

The concept of state-space originally comes from engineering. The state is unobservable but can be estimated based on the past behavior of the system. Further details can be found in Kitagawa and Gersch (1996).

Time series models can generally be expressed through state-space modeling. For example, consider fitting an autoregressive (AR) model of order  $m$  to a given univariate time series  $y_n$ :

$$y_n = \sum_{i=1}^m a_i y_{n-i} + v_n, \quad (1.16)$$

where  $a_i$  is an AR coefficient, and  $v_n$  is the Gaussian white noise with mean 0 and variance  $\sigma^2$ . If we define the state vector as  $x_n = (y_n, y_{n-1}, \dots, y_{n-m+1})^t$ , then, by setting an  $m \times m$  matrix  $F$  and an  $m$ -dimensional vector  $G$  as follows:

$$F = \begin{bmatrix} a_1 & a_2 & \cdots & a_m \\ 1 & & & \\ & \ddots & & \\ & & 1 & 0 \end{bmatrix}, \quad G = \begin{bmatrix} 1 \\ 0 \\ \vdots \\ 0 \end{bmatrix}, \quad (1.17)$$

the system model (1.14) is obtained. Moreover, by setting an  $m$ -dimensional vector  $H$  as  $H = [1, 0, \dots, 0]$ , the observation model (1.15) is attained. Note that, in the case of an AR model, the observation noise becomes zero. In other words, this is a special case in the sense that the state vector is exactly determined by the observations until the time  $n$ .

Generally, the representation of state-space modeling is not uniquely determined. Moreover, the representation of the state vector is also not uniquely determined. For example, the state vector is defined as  $x_n = (y_n, \tilde{y}_{n+1|n-1}, \dots, \tilde{y}_{n+m-1|n-1})^t$ , where  $\tilde{y}_{n+i|n-1} = \sum_{j=i+1}^m a_j y_{n+i-j}$ ,  $i = 1, \dots, m-1$ . This expression describes the state-space related to the observations until time  $n-1$  of the one-step-ahead predictor of  $y_{n+i}$ , i.e.,  $y_{n+i|n-1} = \sum_{j=1}^m a_j y_{n+i-j}$ . Then, by setting matrix  $F$  and vectors  $G$  and  $H$  as follows:

$$F = \begin{bmatrix} a_1 & 1 & & \\ a_2 & & \ddots & \\ \vdots & & & 1 \\ a_m & & & 0 \end{bmatrix}, \quad G = \begin{bmatrix} 1 \\ 0 \\ \vdots \\ 0 \end{bmatrix}, \quad H = [1, 0, \dots, 0], \quad (1.18)$$

another state-state model is obtained. Details are provided in Kitagawa (2010).

The time series models treated in this book, such as the trend component model and the seasonal component model, are expressed as a state-space model in the form of (1.18). The details are presented in Chap. 2.

## 1.5 Organization of the Book and Related Web Information

This book consists of two parts. Chapters 2 and 3 present theoretical background for our method, and Chap. 4 presents an application of our method.

Chapter 2 proposes a method for constructing a distribution-free index. First, we briefly review nonstationary time series modeling, which is closely related to our indexation method. Then, a distribution-free index is defined by taking the inverse Box-Cox transformation of the optimal long-term trend, which is estimated by fitting a trend model with time-varying observation noises to the Box-Cox transformed observations.

In Chap. 3, as a tool for detecting causations between financial markets, we review the generalized power contribution, which reveals the frequency-wise effect of multidimensional noise sources on the power of the fluctuation of each variable in a multivariate feedback system.

Applications of our method for constructing a distribution-free index to financial and economic time series data highlighting the recent sequential financial crises are presented in Chap. 4. The causations are investigated through power contribution analysis. In addition, the usability of a distribution-free index is examined. These applications verify the effectiveness of a distribution-free index and confirm that applying our indexation method to markets with insufficient information, such as fast-growing or immature markets, can be effective. Therefore, wider applicable area of our method can be expected.

For more information on this research, visit our website: Statistical Financial Risk Monitor (StatFiRM) on <http://home.mims.meiji.ac.jp/~tanokura/statfirmHomeJ.html>. The web site was set up to disclose information related to the method for constructing a distribution-free index and its applications. In particular, the SCDS regional distribution-free indices are periodically updated to show the current trends of regional sovereign risks in terms of the SCDS market.

In addition, the seasonal adjustment model (Gersch and Kitagawa 1983; Kitagawa and Gersch 1984) reviewed in Sect. 2.1.3, is also freely available as web-based time series analysis software, Web DECOMP, at [http://ssnt.ism.ac.jp/inets/inets\\_eng.html](http://ssnt.ism.ac.jp/inets/inets_eng.html), which was developed by the Institute of Statistical Mathematics. In this book, Web DECOMP is used to extract a detrended cyclical component of a time series in order to detect causations between short-term fluctuations of financial and economic time series by power contribution analysis.

## References

- Akaike, H.: On the use of a linear model for the identification of feedback systems. *Ann. Inst. Statist. Math.* **20**, 425–439 (1968)
- Akaike, H.: Information theory and an extension of the maximum likelihood principle. In: Parzen, E., Tanabe, K., Kitagawa, G. (eds.) *Selected Papers of Hirotugu Akaike*, pp. 199–213. Springer, New York (1998)

- Akaike, H., Nakagawa, T.: *Statistical Analysis and Control of Dynamic System*. KTK Scientific Publishers, Tokyo (1988)
- Akaike, H., Kitagawa, G. (eds.): *The Practice of Time Series Analysis*. Springer, New York (1999)
- Box, G.E.P., Cox, D.R.: An analysis of transformations. *J. Roy. Stat. Soc. Ser. B* **26**(2), 211–252 (1964)
- Box, G.E.P., Jenkins, G.M.: *Time Series Analysis: Forecasting and Control*. Holden-Day, San Francisco (1970)
- Fama, E.F.: The behavior of stock market prices. *J. Bus.* **38**(1), 34–105 (1965)
- Gersch, W., Kitagawa, G.: The prediction of time series with trends and seasonalities. *J. Bus. Econ. Stat.* **1**(3), 253–264 (1983)
- Geweke, J.: Measurement of linear dependence and feedback between multiple time series. *J. Am. Stat. Assoc.* **77**(378), 304–324 (1982)
- Geweke, J.: Measures of conditional linear dependence and feedback between time series. *J. Am. Stat. Assoc.* **79**(388), 907–915 (1984)
- Granger, C.W.J.: Investigating causal relations by econometric models and cross-spectral methods. *Econometrica* **37**, 424–438 (1969)
- Hosoya, Y.: The decomposition and measurement of interdependency between second-order stationary processes. *Probab. Theory Relat. Fields* **88**, 429–444 (1991)
- Hosoya, Y.: Elimination of third-series effect and defining partial measures of causality. *J. Time Ser. Anal.* **22**(5), 537–554 (2001)
- Kitagawa, G.: Non-Gaussian state space modeling of nonstationary time series. *J. Am. Stat. Assoc.* **82**(400), 1032–1041 (1987)
- Kitagawa, G.: *Introduction to Time Series Modeling*. CRC Press, Boca Raton (2010)
- Kitagawa, G., Gersch, W.: A smoothness priors-state space modeling of time series with trend and seasonality. *J. Am. Stat. Assoc.* **79**(386), 378–389 (1984)
- Kitagawa, G., Gersch, W.: *Smoothness Priors Analysis of Time Series*. Lecture Notes in Statistics, vol. 116. Springer, New York (1996)
- Konishi, S., Kitagawa, G.: *Information Criteria and Statistical Modeling*. Springer, New York (2008)
- Linden, M.: A model for stock return distribution. *Int. J. Financ. Econ.* **6**, 159–169 (2001)
- Madan, D.B., Seneta, E.: The variance gamma (V. G.) model for share market returns. *J. Bus.* **63**(4), 511–524 (1990)
- Mandelbrot, B.: The variation of certain speculative prices. *J. Bus.* **36**(4), 394–419 (1963)
- Ohtsu, K., Horigome, M., Kitagawa, G.: A new ship's auto pilot design through a stochastic model. *Automatica* **15**, 255–268 (1981)
- Ohtsu, K., Peng, H., Kitagawa, G.: *Time Series Modeling for Analysis and Control*. Advanced Autopilot and Monitoring Systems. Springer Series in Statistics. Springer, Tokyo (2015)
- Pariez, P.D.: The distribution of share price changes. *J. Bus.* **45**(4), 49–55 (1972)
- Tanokura, Y.: Detection of the international sector comovements (in Japanese). Japanese Association of Financial Econometrics and Engineering Journal: Econometrics on financial engineering and security markets 2006, 155–178 Toyokeizai sinposha, Tokyo (2006)
- Tanokura, Y., Kitagawa, G.: Modeling influential correlated noise sources in multivariate dynamic systems. In: Hamza, M.H. (ed.) *Modelling and Simulation: Fifteenth IASTED International Conference Proceedings*, pp. 19–24. ACTA Press, CA (2004)
- Tanokura, Y., Tsuda, H., Sato, S., Kitagawa, G.: Constructing a credit default swap index and detecting the impact of the financial crisis. In: Bell, W.R., Holan, S.H., McElroy, T.S. (eds.) *Economic Time Series: Modeling and Seasonality*, pp. 359–380. CRC Press, Boca Raton (2012)

# Chapter 2

## Method for Constructing a Distribution-Free Index

**Abstract** Nonstationary financial time series often observed in the real world, include a time series with a slowly shifting mean value function, a time series with time-varying variations around the mean value, and a time series with both a moving mean value and changing waveforms around the mean value. First, we briefly review nonstationary time series modeling, such as trend estimation, time-varying variance modeling, seasonal adjustment modeling, and non-Gaussian distribution modeling, which is closely related to our method for constructing a distribution-free index. Since the distribution of prices of a financial market is often non-Gaussian, we propose to transform the price observations by the Box–Cox transformation. Then, a distribution-free index is defined by taking the inverse Box–Cox transformation of the optimal long-term trend, which is estimated by fitting a trend model with time-varying observation noises to the Box–Cox transformed observations. The new index becomes impartial, regardless of the price distributions.

**Keywords** Trend model · Nonstationary non-Gaussian time series · Time-varying variance · Distribution-free index · Box-Cox transformation

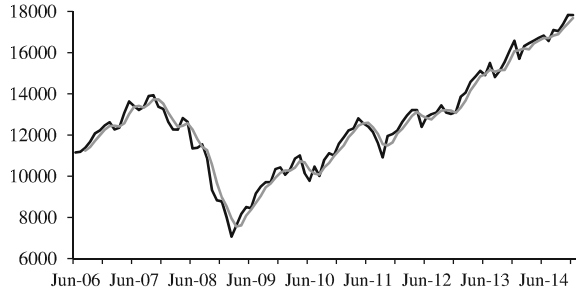
## 2.1 Nonstationary Time Series Modeling

### 2.1.1 Trend Estimation

Economic and financial time series often exhibit a slowly increasing or decreasing shift of the mean values over certain periods. We refer to a relatively long-term shift of the mean value as a trend. A trend may sometimes form a pattern due to an event specific to the attribute of the time series. These trends are important because economic and financial events influence all of our lives to a certain degree. Therefore, modeling a trend appropriately is important.

In order to capture the trend of a financial time series, for example, by calculating moving averages as in Fig. 2.1, which shows the 3-month moving averages of the Dow Jones Industrial Average, we practically attempt to draw a line or a curve as the trend. However, the delay of the point in time at which a trend changes cannot

**Fig. 2.1** Dow Jones Industrial Average (*black line*) and its 3-month moving averages (*gray line*). Source S&P Dow Jones Indices LLC



be ignored. This delay becomes longer as the period of taking moving averages becomes longer. In this book, we regard a trend as locally connected polynomials with stochastic fluctuations defined on short-term periods, which express gradual changes.

Next, consider a univariate observed time series,  $y_n$ ,  $n = 1, \dots, N$ , which is expressed as

$$y_n = t_n + w_n, \quad (2.1)$$

where  $t_n$  is referred to as the trend component, and  $w_n$  is a white noise following a Gaussian distribution with mean 0 and variance  $\sigma^2$  (Kitagawa 2010). Then,  $y_n$  follows a Gaussian distribution with mean  $t_n$  and variance  $\sigma^2$ .

The trend component can be expressed in various forms (Kitagawa and Gersch 1984, 1996; Kitagawa 2010). Here, we define the trend component model as

$$\Delta^k t_n = v_n, \quad (2.2)$$

where  $k$  is the trend order, and  $v_n$  is a Gaussian white noise with mean 0 and variance  $\tau^2$ .  $\Delta$  is defined as the time difference operator satisfying

$$\Delta t_n = t_n - t_{n-1}. \quad (2.3)$$

We collectively refer to the pair of models (2.1) and (2.2) as the trend model. As the variance  $\tau^2$  of the noise  $v_n$  becomes smaller, the trend component model realizes smoother and more sensitive tendencies to the actual long-term fluctuations, as shown in Fig. 2.2.

When  $k = 1$ , (2.2) becomes a random walk model

$$t_n - t_{n-1} = v_n,$$

and the trend becomes locally constant. When  $k = 2$ , (2.2) becomes

$$t_n = 2t_{n-1} - t_{n-2} + v_n,$$

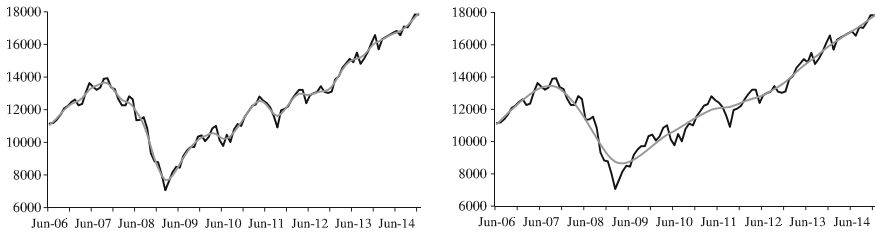


**Fig. 2.2** Dow Jones Industrial Averages (*black*) and their estimated trends (*gray*). *Left-hand panel*  $\tau^2 = 0.34$ , *right-hand panel*  $\tau^2 = 0.15$ . *Source* S&P Dow Jones Indices LLC

and the trend is locally linear. Moreover, when  $k = 3$ , (2.2) is

$$t_n = 3t_{n-1} - 3t_{n-2} + t_{n-3} + v_n,$$

where the trend is locally quadratic. In the general case of  $k$ , by using the lag operator  $B$  defined by  $B t_n = t_{n-1}$ , the time difference operator of the  $k$ th order can be expressed as a binary expansion

$$\Delta^k = (1 - B)^k = \sum_{i=0}^k {}_k C_i (-B)^i. \quad (2.4)$$

Denoting the binomial coefficients  $c_i = (-1)^{i+1} {}_k C_i$ , the trend component model is written as

$$t_n = \sum_{i=1}^k c_i t_{n-i} + v_n, \quad (2.5)$$

which is formally an AR model. However, the trend component model is nonstationary because the roots of the characteristic equation lie on the unit circle.

The trend model given by (2.1) and (2.5) can be expressed by the following state-space model:

$$x_n = F x_{n-1} + G v_n \quad (2.6)$$

$$y_n = H x_n + w_n, \quad (2.7)$$

where  $x_n$  is a  $k$ -dimensional state vector,  $F$  is a  $k \times k$  matrix, and  $G$  and  $H$  are  $k$ -dimensional vectors defined by

$$x_n = \begin{bmatrix} t_n \\ t_{n-1} \\ \vdots \\ t_{n-k+1} \end{bmatrix}, \quad F = \begin{bmatrix} c_1 & c_2 & \cdots & c_k \\ 1 & 0 & \cdots & 0 \\ & \ddots & \ddots & \vdots \\ & & 1 & 0 \end{bmatrix}, \quad G = \begin{bmatrix} 1 \\ 0 \\ \vdots \\ 1 \end{bmatrix}, \quad (2.8)$$

$$H = [1, 0, \dots, 0].$$

The variances  $\tau^2$  and  $\sigma^2$  of the noises are estimated by the maximum likelihood method, and the smoothed estimates of the state vector are calculated by the Kalman filter/fixed interval smoothing algorithm (Kitagawa 2010). The trend order  $k$  of the trend component model can be determined by the AIC (Akaike 1998; Konishi and Kitagawa 2008). Note that, in practice, the trend order  $k$  is usually selected as either 1 or 2.

When  $k = 1$ , the binomial coefficient in (2.5) is  $c_1 = 1$ , and the state-space model is obtained as

$$x_n = t_n, \quad F = G = H = 1. \quad (2.9)$$

When  $k = 2$ ,  $c_1 = 2$  and  $c_2 = -1$  in (2.5), and the state-space model is obtained as

$$x_n = \begin{bmatrix} t_n \\ t_{n-1} \end{bmatrix}, \quad F = \begin{bmatrix} 2 & -1 \\ 1 & 0 \end{bmatrix}, \quad G = \begin{bmatrix} 1 \\ 0 \end{bmatrix}, \quad H = [1, 0]. \quad (2.10)$$

Moreover, the state-space model can also be obtained as

$$x_n = \begin{bmatrix} t_n \\ -t_{n-1} \end{bmatrix}, \quad F = \begin{bmatrix} 2 & 1 \\ -1 & 0 \end{bmatrix}, \quad G = \begin{bmatrix} 1 \\ 0 \end{bmatrix}, \quad H = [1, 0]. \quad (2.11)$$

We will use this representation (2.11) in the subsequent sections.

More details on the trend estimation can be found in Kitagawa and Gersch (1984, 1996) and Kitagawa (2010).

### 2.1.2 Time-Varying Variance Modeling

Nonstationary time series with time-varying fluctuations around the mean value can often be found in financial markets. In other words, the variance and the autocovariance function of such a time series change over time. In fact, as we sometimes hear the soar of the stock market volatility, such nonstationary phenomena always make us realize the existence of increased risk. Note that the estimation of a time-varying variance is equivalent to that of a stochastic volatility in financial time series analysis (Kitagawa 1987, 2010).

Estimating a time-varying variance directly is not easy. We estimate a time-varying variance using an approximated Gaussian distribution (Davis and Jones 1968) in the following manner. The advantage of this method is that the estimation of a time-varying variance can be realized by the simple estimation of the trend of a transformed time series.

Consider that a univariate time series,  $y_n$ ,  $n = 1, \dots, N$ , is the realization of a white noise that follows a Gaussian distribution with mean 0 and time-varying variance  $\sigma_n^2$ . We define the squared time series as follows:

$$s_n = y_n^2, \quad n = 1, \dots, N. \quad (2.12)$$

Then,  $s_n$  follows a  $\chi^2$  (Chi-squared) distribution with one degree of freedom. Therefore, the probability density function of  $s_n$  is given by

$$f(s) = \frac{1}{\sqrt{2\pi\sigma^2}} s^{-\frac{1}{2}} \exp\left(-\frac{s}{2\sigma^2}\right). \quad (2.13)$$

Next, by the logarithmic transformation, we transform  $s_n$  to obtain

$$z_n = \log(s_n). \quad (2.14)$$

Then, since the inverse transformation of the logarithm is given by  $s_n = e^{z_n}$ , the probability density function of  $z_n$  is given by

$$g(z) = \left| \frac{de^z}{dz} \right| f(e^z) = \frac{1}{\sqrt{2\pi\sigma^2}} \exp\left\{ \frac{1}{2} \left( z - \frac{e^z}{\sigma^2} \right) \right\}. \quad (2.15)$$

Since this  $g(z)$  can be written as

$$g(z) = \frac{1}{\sqrt{2\pi}} \exp\left[ \frac{1}{2} \{ (z - \log \sigma^2) - \exp(z - \log \sigma^2) \} \right], \quad (2.16)$$

$z_n$  can be expressed as

$$z_n = \log \sigma_n^2 + w_n. \quad (2.17)$$

The noise  $w_n$  in (2.17) follows a double exponential distribution, the probability density function of which is expressed as

$$h(w) = \frac{1}{\sqrt{2\pi}} \exp\left[ \frac{1}{2} \{ w - \exp(w) \} \right]. \quad (2.18)$$

The mean and the variance of this distribution are given by  $-(\gamma + \log 2) = -(0.57722 + 0.69315) = -1.27036$  ( $\gamma$ : Euler constant) and  $\pi^2/2$ , respectively.

Therefore, by approximating the double exponential distribution as a Gaussian distribution with mean  $-(\gamma + \log 2)$  and variance  $\pi^2/2$ , the estimation of the logarithm of the variance  $\sigma_n^2$  of the original time series  $y_n$  can be reduced to that of the following trend model:

$$\Delta^k t_n = v_n \quad (2.19)$$

$$z_n = t_n + w_n, \quad (2.20)$$

where  $k$  is the trend order, and the system noise  $v_n$  follows a Gaussian distribution with mean 0 and variance  $\tau^2$ .

By applying state-space modeling as described in the previous section, the trend component  $t_n$  is estimated by the Kalman filter/fixed interval smoothing algorithm (Kitagawa 2010). Since the smoothed estimates of  $\log \sigma_n^2$  are obtained by

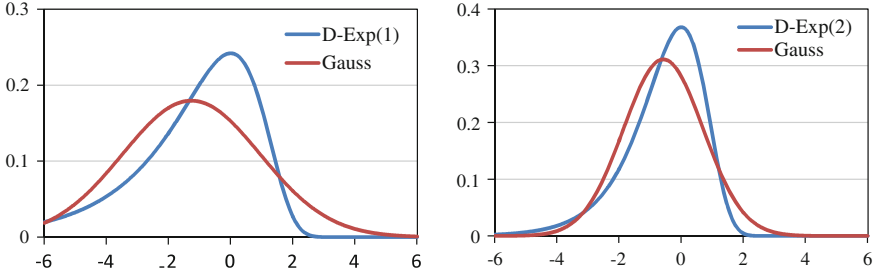


**Fig. 2.3** Double exponential (D-Exp) distributions (*blue*) and their Gaussian approximations (*red*). *Left-hand panel* one degree of freedom, *Right-hand panel* two degrees of freedom

$$t_n + \gamma + \log 2, \quad n = 1, \dots, N, \quad (2.21)$$

$\exp(t_n + \gamma + \log 2)$  is the estimate of the time-varying variance.

However, as shown in the left panel of Fig. 2.3, the double exponential distribution derived from the  $\chi^2$  distribution with one degree of freedom (blue line) is highly skewed and the variance is large, and so the approximation by the Gaussian distribution (red line) is not so good.

Therefore, in order to mitigate this problem in the actual estimation of the time-varying variance, we usually define the following time series:

$$s_m = \frac{1}{2} (y_{2m-1}^2 + y_{2m}^2), \quad m = 1, \dots, N/2. \quad (2.22)$$

Then,  $s_m$  follows a  $\chi^2$  distribution with two degrees of freedom, i.e., an exponential distribution. Using a similar argument to that above, the density function of the logarithm of (half of) the  $\chi^2$  distribution with two degrees of freedom is given by

$$g(z) = \frac{1}{\sigma^2} \exp\left(z - \frac{e^z}{\sigma^2}\right) = \exp\{(z - \log \sigma^2) - \exp(z - \log \sigma^2)\}. \quad (2.23)$$

In this case, the noise  $w_m$ , replacing  $n$  with  $m$  in (2.17), follows a double exponential distribution in which the probability density function is expressed as

$$h(w) = \exp\{w - \exp(w)\}. \quad (2.24)$$

The mean and the variance are given by  $-\gamma = -0.57722$  ( $\gamma$ : Euler constant) and  $\pi^2/6$ , respectively, as shown in the right panel of Fig. 2.3.

In this method of time-varying variance estimation, the number of the observations is halved. On the other hand, the noise distribution  $h(w)$  in (2.24) is closer to a Gaussian distribution than that in the original (2.18), and the variance of the observation noise becomes a third of that of the original approximation. Therefore, if the variance does not change abruptly over time and the assumption that  $\sigma_{2m-1}^2 = \sigma_{2m}^2$  is

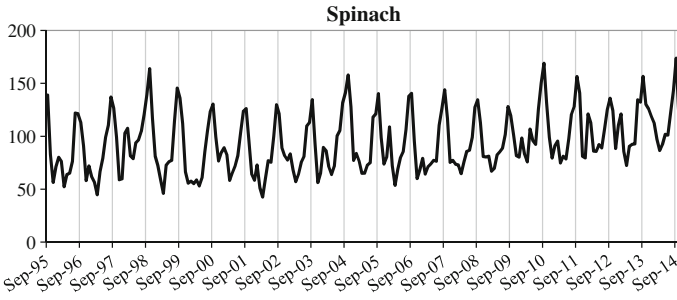


**Fig. 2.4** Japanese consumer price index for spinach. *Source* Statistics Bureau of Japan

reasonable, the accuracy of the estimation of  $\log \sigma_n^2$  can be expected to increase by approximately 50 %, i.e., the variance becomes  $2 \times 1/3 = 2/3$ . Several examples of the estimation of a time-varying variance are presented in Chap. 4.

Note that direct estimation can be performed by applying a non-Gaussian filter/smoothing algorithm without the assumption of  $\sigma_{2m-1}^2 = \sigma_{2m}^2$  (Kitagawa 2010).

### 2.1.3 Seasonal Adjustment Modeling

Some economic time series that are closely related to financial markets tend to reflect seasonal factors, i.e., exhibit a similar pattern of fluctuations around the same season every year. Familiar examples of such time series are the prices of vegetables, wages, and unemployment rates. Figure 2.4 shows the Japanese consumer price index for spinach. A clear seasonal pattern with a yearly peak in September exists. These time series may influence not only financial markets but also economies.

This section briefly introduces a seasonal adjustment model proposed by Gersch and Kitagawa (1983), and Kitagawa and Gersch (1984, 1996).

When a component  $s_n$  of a time series cyclically fluctuates on a yearly basis, this component can be expressed as

$$s_n \approx s_{n-p}, \tag{2.25}$$

where  $p$  is the period length of the component. For example, in the case of monthly data, set  $p = 12$ . Then,  $s_n$  is referred to as a seasonal component or seasonality, which has a more or less regular fluctuation with a period of 1 year. Note that this seasonal component can be applied to other regular patterns, such as the weekly pattern in daily data ( $p = 7$ ) or the daily pattern in hourly data ( $p = 24$ ).

For an observed univariate time series  $y_n$  with a regular seasonal pattern of fluctuations, a seasonal adjustment model is expressed as

$$y_n = t_n + s_n + p_n + w_n. \tag{2.26}$$

In other words, the observation comprises the following four components.

A trend component  $t_n$  is estimated by the trend component model with the trend order  $k$

$$\Delta^k t_n = v_{n1}, \quad v_{n1} \sim N(0, \tau_1^2), \quad (2.27)$$

which was presented in the previous section.

A seasonal component  $s_n$ , which slowly forms seasonal fluctuations, is expressed by the following seasonal component model with a period length  $p$ :

$$\sum_{i=0}^{p-1} s_{n-i} = v_{n2}, \quad v_{n2} \sim N(0, \tau_2^2). \quad (2.28)$$

The details of this model will be explained later.

A stationary component  $p_n$  is estimated by the following stationary AR component model of order  $m$ :

$$p_n = \sum_{i=1}^m a_i p_{n-i} + v_{n3}, \quad v_{n3} \sim N(0, \tau_3^2), \quad (2.29)$$

which expresses relatively shorter cyclical fluctuations than the gradual long-term trend component (2.27). Finally, the distribution of the observation noise  $w_n$  in (2.26) is given by

$$w_n \sim N(0, \sigma^2). \quad (2.30)$$

Economic time series with seasonality often accompany a trend expressing gradually shifting mean value functions, such as the consumer price index. For such series, the observation model is naturally considered as a form of decomposition: a trend component plus a seasonal component. In order to obtain a smoother trend, we introduce a seasonal adjustment model to which a stationary AR component expressing shorter cyclical fluctuations than a trend is added.

Let us now explain the seasonal component model (2.28). Using the lag operator  $B$  introduced in Sect. 2.1.1, we obtain

$$B^p s_n = s_{n-p}. \quad (2.31)$$

Therefore, (2.25) approximately satisfies

$$(1 - B^p) s_n \approx 0. \quad (2.32)$$

Similar to the trend component model presented in Sect. 2.1.1, a seasonal component with period  $p$ , can approximately be defined as

$$(1 - B^p) s_n = v_{n2}, \quad (2.33)$$

where  $v_{n2}$  is a white noise following a Gaussian distribution with mean 0 and unknown variance  $\tau_2^2$ .

However, in practice, this seasonal component model (2.33) may not work well within the framework of the seasonal adjustment model (2.26) due to the existence of the factor  $(1 - B)$ , which is common to both the trend and seasonal component models. Since, as compared with the lag operator expression (2.4) of the trend model in Sect. 2.1.1, the following expansion

$$1 - B^p = (1 - B)(1 + B + \cdots + B^{p-1}), \quad (2.34)$$

is obtained for the seasonal component model (2.33).

Next, any arbitrary constant  $e_n = c$  satisfies the difference equation

$$(1 - B)e_n = 0. \quad (2.35)$$

Therefore, if we define other components  $t'_n$  and  $s'_n$  as

$$\begin{aligned} t'_n &= t_n + e_n \\ s'_n &= s_n - e_n, \end{aligned}$$

then these components satisfy (2.27), (2.33), and

$$y_n = t'_n + s'_n + p_n + w_n. \quad (2.36)$$

Therefore, apart from the stationary AR component  $p_n$ , we have two methods by which to decompose the time series  $y_n$  into  $t_n$  and  $s_n$  with the same noises  $v_{n1}$ ,  $v_{n2}$ , and  $w_n$ , and there is nothing to choose between them. Using the common factor in the component models of  $t_n$  and  $s_n$  within the seasonal adjustment modeling framework, the uniqueness of decomposition is lost.

From the expansion (2.34), as the sufficient condition for  $1 - B^p = 0$  is  $1 + B + \cdots + B^{p-1} = 0$ , when  $\sum_{i=0}^{p-1} B^i s_n \approx 0$  is satisfied,

$$s_n \approx s_{n-p}$$

is also satisfied. Therefore, in order to avoid the above problem of the nonuniqueness of the decomposition, define the following seasonal component model:

$$\sum_{i=0}^{p-1} B^i s_n = v_{n2}, \quad v_{n2} \sim N(0, \tau_2^2). \quad (2.37)$$

Therefore, (2.28) is obtained.

Equivalently, since the seasonal component model (2.37) can be written as

$$s_n = - \sum_{i=1}^{p-1} B^i s_n + v_{n2}, \quad (2.38)$$

this model can formally be regarded as a special case of an AR model.

As in the case of the trend model, the state-space model is obtained as

$$\begin{aligned} x_n &= \begin{bmatrix} s_n \\ s_{n-1} \\ \vdots \\ s_{n-p+2} \end{bmatrix}, \quad F = \begin{bmatrix} -1 & -1 & \cdots & -1 \\ 1 & & & \\ & \ddots & & \\ & & & 1 \end{bmatrix}, \quad G = \begin{bmatrix} 1 \\ 0 \\ \vdots \\ 0 \end{bmatrix}, \\ H &= [1, 0, \dots, 0]. \end{aligned} \quad (2.39)$$

The details and an extension to a higher seasonal order model can be found in Kitagawa (2010).

Considering the models mentioned above, we now return to the seasonal adjustment model (2.26). Each component model can be expressed in state-space model form. Therefore, in the same manner as for each component model, the state-space model used for the seasonal adjustment model (2.26) consisting of (2.27)–(2.29) is obtained in the following composite form:

$$\begin{aligned} x_n &= \begin{bmatrix} x_{1n} \\ x_{2n} \\ x_{3n} \end{bmatrix}, \quad F = \begin{bmatrix} F_1 & & \\ & F_2 & \\ & & F_3 \end{bmatrix}, \quad G = \begin{bmatrix} G_1 & 0 & 0 \\ 0 & G_2 & 0 \\ 0 & 0 & G_3 \end{bmatrix}, \\ H &= [H_1 \ H_2 \ H_3], \quad Q = \begin{bmatrix} \tau_1^2 & 0 & 0 \\ 0 & \tau_2^2 & 0 \\ 0 & 0 & \tau_3^2 \end{bmatrix}. \end{aligned} \quad (2.40)$$

Here,  $F_i$ ,  $G_i$ , and  $H_i$  correspond to the matrices in the state-space representation for each component model. Similarly,  $Q$  is composed of the set of the variances of the system noises.

The above-mentioned seasonal adjustment model is freely available as web-based time series analysis software, Web DECOMP, at [http://ssnt.ism.ac.jp/inets/inets\\_eng.html](http://ssnt.ism.ac.jp/inets/inets_eng.html), which was developed by the Institute of Statistical Mathematics. In Chap. 4, DECOMP is used to extract a detrended cyclical component of a time series in order to detect causations between short-term fluctuations of financial and economic time series by power contribution analysis.

As an example of applying the seasonal adjustment model provided by DECOMP, Fig. 2.5 shows a decomposition of the Japanese consumer price index for spinach illustrated in Fig. 2.4, into the trend, seasonal, stationary AR, and noise components. The highly visible seasonality is detected.

### 2.1.4 Non-Gaussian Distribution Modeling

In the Gaussian state-space modeling presented in the previous sections, the gradual changes of fluctuation structures of nonstationary time series are well captured. However, in financial time series, time-varying fluctuation structures, occasionally

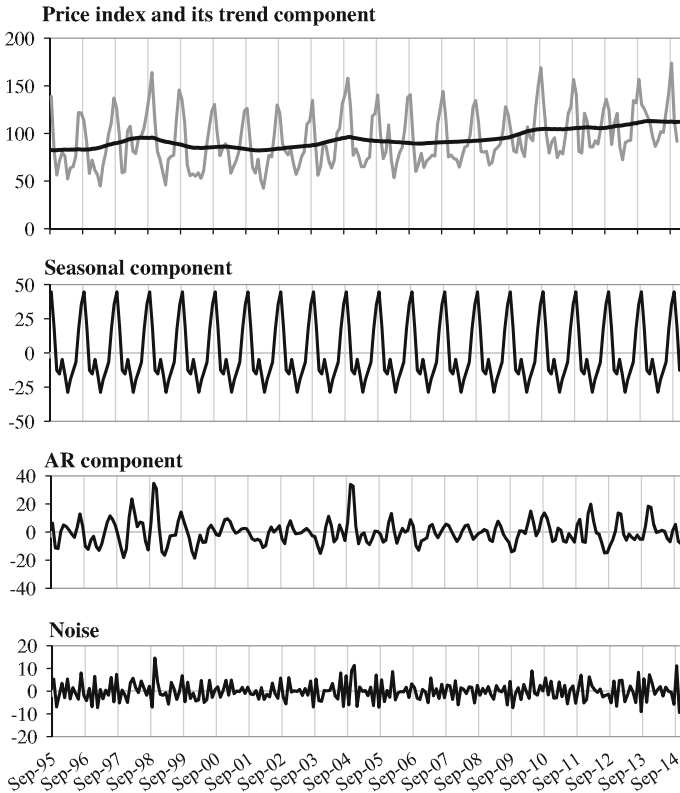


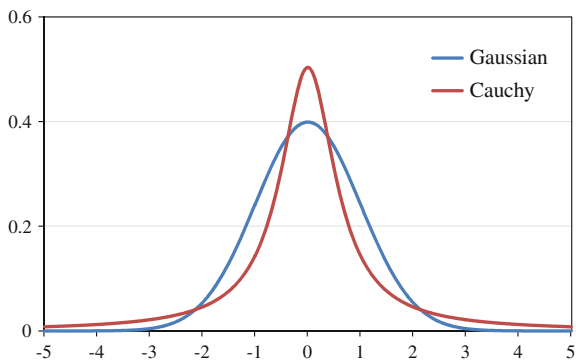
**Fig. 2.5** Decomposition of the Japanese consumer price index for spinach (gray line) into the trend (top), seasonal (second from top), AR (second from bottom), and noise (bottom) components. Source Statistics Bureau of Japan

including both gradual and sudden changes, can often be observed. The recent outstanding example of a sudden change can be the occurrence of the Lehman Brothers’ bankruptcy in 2008. Actually, the possibility of a sudden drastic change has recently expanded and recognizing indicators of such change are crucial.

As an extension of Gaussian state-space modeling, a non-Gaussian state-space model is naturally considered, by assuming a non-Gaussian distribution of the system noise, a non-Gaussian distribution of the observation noise, or non-Gaussian distributions of both. For example, when a heavy-tailed distribution, such as the Cauchy distribution (red line) shown in Fig. 2.6, is assumed for the system noise, a time series including gradual changes with high probabilities and sudden changes with low probabilities, can be modeled. Furthermore, note that the estimation of a time-varying variance in Sect. 2.1.2 can be directly performed using the noise distribution (2.18) without using the Gaussian approximation.

In order to extend the standard state-space model (1.14) and (1.15) mentioned in the introductory chapter, we recall again that

**Fig. 2.6** Gaussian (blue) and Cauchy (red) distributions



$$x_n = Fx_{n-1} + Gv_n \quad (2.41)$$

$$y_n = Hx_n + w_n, \quad (2.42)$$

where  $x_n$  is the state vector at time  $n$ . Here, the density functions  $q(v)$  and  $r(w)$  of the system noise  $v_n$  and the observation noise  $w_n$  are not necessarily Gaussian. Then, the state distribution generally becomes non-Gaussian.

In Gaussian state-space modeling, since the state distribution is Gaussian, the conditional means and the conditional variance covariance matrices are obtained recursively by the Kalman filter. However, in non-Gaussian state-space modeling, as the conditional distribution of the state cannot be specified only by the conditional mean and the conditional variance covariance matrix, computing the state distribution is necessary.

In order to address this problem, various algorithms, such as the extended Kalman filter (Anderson and Moore 2012), and the non-Gaussian filter/smoothing algorithm which numerically approximates non-Gaussian distributions by using a step function or a piecewise linear function (Kitagawa 1987), have been proposed. The development of various non-Gaussian approximating algorithms is reported in Kitagawa and Gersch (1996).

Denoting the set of observations by time  $t$  as  $Y_t \equiv \{y_1, \dots, y_t\}$ , in general for the non-Gaussian state-space model (2.41) and (2.42), the conditional distribution of the state  $p(x_n|Y_t)$  is obtained by the following recursive formula:

$$\begin{aligned} p(x_n|Y_{n-1}) &= \int p(x_n|x_{n-1})p(x_{n-1}|Y_{n-1})dx_{n-1} \\ p(x_n|Y_n) &= \frac{p(y_n|x_n)p(x_n|Y_{n-1})}{p(y_n|Y_{n-1})}, \end{aligned} \quad (2.43)$$

where  $p(y_n|Y_{n-1}) = \int p(y_n|x_n)p(x_n|Y_{n-1})dx_n$ .

Using this non-Gaussian filter/smoothing algorithm, it is possible to estimate a time-varying variance of a time series without approximating the double exponential distribution by a Gaussian distribution, i.e., by directly using the time-varying variance model

$$\begin{aligned} t_n &= t_{n-1} + v_n \\ x_n &= t_n + w_n, \end{aligned} \tag{2.44}$$

where the trend order is one, and the noise distribution is expressed as  $h(w_n) = (2\pi)^{1/2} \exp\{(w_n - \exp(w_n))/2\}$  in Sect. 2.1.2. Moreover, note that in this method, the system noise  $v_n$  is not restricted to be Gaussian. By using a heavy-tailed distribution for the system noise, sudden changes in variance can be detected (Kitagawa 1987, 2010).

This non-Gaussian filter/smoothing algorithm can also be applied to a nonlinear state-space model

$$\begin{aligned} x_n &= f(x_{n-1}, v_n) \\ y_n &= h(x_n, w_n). \end{aligned} \tag{2.45}$$

In this nonlinear modeling framework, the time-varying variance model can be expressed as

$$\begin{aligned} s_n &= s_{n-1} + v_n \\ y_n &= e^{s_n} w_n. \end{aligned} \tag{2.46}$$

Therefore, using this method, we can estimate the time-varying variance, even without defining the squared time series, as in Sect. 2.1.2 (Kitagawa 2010).

For the more general case, Kitagawa (1996) proposed a significantly practical simulation-based estimation method, i.e., the sequential Monte Carlo filter, for a nonlinear non-Gaussian state-space representation further extending to nonlinearities of the state and (or) the observation models. This filter approximates a distribution by several (for example, 10,000 or more) particles that can be regarded as independent realizations from the distribution (Gordon et al. 1993; Kitagawa 1996, 2010; Doucet et al. 2001).

Next, we briefly outline the sequential Monte Carlo filter. For the set of observations by time  $t$ ,  $Y_t$ , we will evaluate the conditional distribution of the state  $p(x_n|Y_t)$ , which is referred to as a predictor when  $n > t$ , as a filter when  $n = t$ , and as a smoother when  $n < t$ .

The initial state  $x_0$  is assumed to follow the density  $p_0(x)$ , and, for the above three cases, each distribution is expressed using  $m$  particles, as follows:

$$\begin{aligned} \{p_n^{(1)}, \dots, p_n^{(m)}\} &\sim p(x_n|Y_{n-1}) && \text{for the predictor,} \\ \{f_n^{(1)}, \dots, f_n^{(m)}\} &\sim p(x_n|Y_n) && \text{for the filter,} \\ \{s_{n|t}^{(1)}, \dots, s_{n|t}^{(m)}\} &\sim p(x_n|Y_t) && \text{for the smoother.} \end{aligned}$$

When  $m$  particles  $\{p_n^{(1)}, \dots, p_n^{(m)}\}$  from the predictor  $p(x_n|Y_{n-1})$  are given, the distribution is approximated by the empirical distributions determined by the  $m$  particles. In other words, the distribution is approximated by the probability mass function

$$\Pr(x_n = p_n^{(j)} | Y_{n-1}) = \frac{1}{m}, \quad j = 1, \dots, m.$$

Then, a set of realizations expressing the one step ahead predictor  $p(x_n | Y_{n-1})$  and the filter  $p(x_n | Y_n)$  can be obtained recursively in the following manner:

1. Generate a random number  $f_0^{(j)} \sim p_0(x)$  for  $j = 1, \dots, m$ .
2. Repeat the following steps for  $n = 1, \dots, t$ .
  - a. Generate random numbers  $v_n^{(j)} \sim q(v)$  for  $j = 1, \dots, m$ , to obtain independent realizations of the system noise  $v_n$  in (2.41) following the distribution with density function  $q(v)$ .
  - b. Compute  $p_n^{(j)} = Ff_{n-1}^{(j)} + Gv_n^{(j)}$  for  $j = 1, \dots, m$ .
  - c. Compute  $\alpha_n^{(j)} = r(y_n - Hp_n^{(j)})$  for  $j = 1, \dots, m$ , where  $r(w)$  is the density function of the observation noise  $w_n$  in (2.42).
  - d. Generate  $f_n^{(j)}$  for  $j = 1, \dots, m$ , by resampling  $p_n^{(1)}, \dots, p_n^{(m)}$  with weights proportional to  $\alpha_n^{(1)}, \dots, \alpha_n^{(m)}$ .

For a parameter set  $\theta$  of the state-space model such as the variances of the noises, the likelihood of the model is given by

$$L(\theta) = p(y_1, \dots, y_t | \theta) = \prod_{n=1}^t p(y_n | Y_{n-1}),$$

where  $p(y_1 | Y_0) = p_0(y_1)$ . For applying the sequential Monte Carlo filter, we use the approximation

$$\begin{aligned} p(y_n | Y_{n-1}) &= \int p(y_n | x_n) p(x_n | Y_{n-1}) dx_n \\ &\cong \frac{1}{m} \sum_{j=1}^m p(y_n | p_n^{(j)}) = \frac{1}{m} \sum_{j=1}^m \alpha_n^{(j)}. \end{aligned}$$

The maximum likelihood estimate can be obtained by maximizing the log-likelihood:

$$\log L(\theta) = \sum_{n=1}^t \log p(y_n | Y_{n-1}) \cong \sum_{n=1}^t \log \left( \sum_{j=1}^m \alpha_n^{(j)} \right) - t \log m.$$

The sequential Monte Carlo filter is described in detail in Kitagawa (2010), Kitagawa and Gersch (1996), and Doucet et al. (2001).

The application of the sequential Monte Carlo filter is shown in Chap. 4.

## 2.2 Transformation of Non-Gaussian Distributed Prices of a Financial Market

Financial markets are discussed daily in the news throughout the world. The movement of some markets can influence business and economy, and such markets may replace each other over time. Since we usually observe financial market indices such as the S&P 500, one means by which to express the overall perspective of a market is to use the index as a proxy measure. Unlike an established market, in which the index is officially defined and announced, for a newly developed financial instrument forming its market with rapid growth, it is not easy to construct an appropriate index due to a lack of information, such as missing observations at certain times. Moreover, in order to fully reflect the price movements of a financial asset, the index should reflect the price distributions.

Although the assumption that the distributions of prices or returns of financial assets are Gaussian has been commonly used in theoretical finance, some studies in the 1960s failed to validate this assumption and found heavier tails than would be present in a Gaussian distribution (Mandelbrot 1963; Fama 1965). The tails consisting of extreme values of prices or returns that are caused by sharply soaring or plunging asset prices are more likely to occur than expected by a Gaussian distribution. In particular, distributions of stock returns have been discussed in many studies such as Paraez (1972), Madan and Seneta (1990), and Linden (2001). However, an exact identification of such distributions remains an open question.

The distribution of Credit Default Swap (CDS) spreads is often significantly heavy-tailed. For example, Fig. 2.7 shows histograms of the Japanese corporate CDS spreads referencing 327 companies. From back to front, the distributions are heavily skewed to the right. An analysis of this market is provided in Chap. 4.

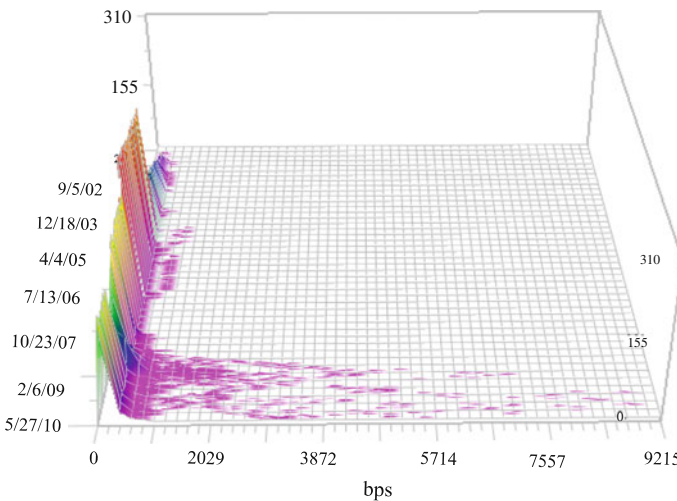


**Fig. 2.7** Japanese corporate CDS spread histograms. *Source* Bloomberg LP

In order to facilitate the identification of such a distribution, Tanokura et al. (2012) proposed transforming the observations in the following manner:

Let  $p_i(n)$ ,  $i = 1, \dots, j(n)$ , denote the prices of issues of a financial market with a non-Gaussian price distribution at time  $n$ ,  $n = 1, \dots, N$ . The number of observations  $j(n)$  varies over time and can be zero at certain times, and  $p_i(n)$  is positive. In order to transform a skewed non-Gaussian distribution of the prices to an approximately Gaussian distribution, we consider the Box–Cox transformation (Box and Cox 1964):

$$q_{i,\lambda}(n) = h(p_i(n)) = \begin{cases} \lambda^{-1}\{p_i(n)^\lambda - 1\} & \lambda \neq 0 \\ \log p_i(n) & \lambda = 0. \end{cases} \quad (2.47)$$

This transformation has been applied in various areas of finance and includes most major transformations, as well as no transformation, as follows: Ignoring a constant term, the Box–Cox transformation becomes the inverse transformation for  $\lambda = -1$ , the reciprocal square root transformation for  $\lambda = -0.5$ , the logarithm for  $\lambda = 0$ , the square root for  $\lambda = 0.5$ , and no transformation for  $\lambda = 1$ .

Now, for each  $\lambda$ , since there are  $j(n)$  observations at time  $n$ , consider the following average time series of the Box–Cox transformed prices  $q_{i,\lambda}(n)$ :

$$y_\lambda(n) = \frac{1}{j(n)} \sum_{i=1}^{j(n)} q_{i,\lambda}(n), \quad n = 1, \dots, N, \quad (2.48)$$

which is often observed to be nonstationary. Then, we fit the following trend model: to  $y_\lambda(n)$ :

$$\Delta^k t_\lambda(n) = v_\lambda(n), \quad v_\lambda(n) \sim N(0, \tau_\lambda^2) \quad (2.49)$$

$$y_\lambda(n) = t_\lambda(n) + w_\lambda(n), \quad w_\lambda(n) \sim D(0, \sigma_\lambda^2), \quad (2.50)$$

where  $k$  is the trend order, and  $\Delta t_\lambda(n) = t_\lambda(n) - t_\lambda(n-1)$ . Here,  $D(0, \sigma_\lambda^2)$  denotes a general distribution with location parameter 0 and unknown scale parameter  $\sigma_\lambda$ .

This is an extension of the trend model with the Gaussian observation noises shown in Sect. 2.1.1 to the trend model with general observation noises. In other words, the case of a non-Gaussian observation noise distribution can also be considered.

In order to consider a rapidly growing or immature financial market with a significantly changing number of observations over time, it might be reasonable to assume that  $\sigma_\lambda^2$  in (2.50) is inversely proportional to the number of observations. In other words, we replace (2.50) in the above trend model with the following expression:

$$y_\lambda(n) = t_\lambda(n) + w_\lambda(n), \quad w_\lambda(n) \sim D(0, \sigma_\lambda^2/j(n)). \quad (2.51)$$

Tanokura et al. (2012) considered the trend model with Cauchy observation noises in (2.51), which is generally useful for modeling the large deviation of noises that are often observed in financial markets. For convenience, we refer to this trend estimation

model based on Cauchy observation noises as the Cauchy trend estimation model, whereas the model based on Gaussian observation noises is referred to as the Gaussian trend estimation model.

In this book, as a further improvement, we also treat the case of Gaussian observation noises with a time-varying variance. In this case, we replace the observation model (2.51) with the following model:

$$y_\lambda(n) = t_\lambda(n) + w_\lambda(n), \quad w_\lambda(n) \sim N(0, \sigma_\lambda^2(n)/j(n)). \quad (2.52)$$

Note that  $\sigma_\lambda^2(n)$  varies over time  $n$  and is estimated by the time-varying variance model reviewed in Sect. 2.1.2. We refer to this trend estimation model based on Gaussian observation noises with a time-varying variance (GTV) as the GTV trend estimation model.

Each extended trend model (2.49) with (2.51) or (2.52) can be expressed as a state-space model as follows:

$$x_\lambda(n) = Fx_\lambda(n-1) + Gv_\lambda(n) \quad (2.53)$$

$$y_\lambda(n) = Hx_\lambda(n) + w_\lambda(n). \quad (2.54)$$

For example, for the trend order  $k = 1$ , the state vector is defined as  $x_\lambda(n) = t_\lambda(n)$ , and the matrices are defined as  $F = G = H = 1$ . For  $k = 2$ ,  $x_\lambda(n)$ ,  $F$ ,  $G$ , and  $H$  are respectively defined as

$$x_\lambda(n) = \begin{bmatrix} t_\lambda(n) \\ t_\lambda(n-1) \end{bmatrix}, \quad F = \begin{bmatrix} 2 & -1 \\ 1 & 0 \end{bmatrix}, \quad G = \begin{bmatrix} 1 \\ 0 \end{bmatrix}, \quad H = [1, 0].$$

Given a parameter  $\lambda$  of the Box–Cox transformation, the estimation of the state vector is performed in the following manner. When we assume that the observation noise distribution is Gaussian, i.e., either the Gaussian trend estimation model (2.51) or the GTV trend estimation model (2.52), the conditional means and conditional variance covariance matrices for the state can be calculated recursively by the Kalman filter. On the other hand, when the observation noise distribution is assumed to be non-Gaussian, e.g., a Cauchy distribution in (2.51), the state vector is estimated by a non-Gaussian filter or the sequential Monte Carlo filter presented in Sect. 2.1.4. In both cases, the parameters such as the variances of noises are estimated by the maximum likelihood method, and the missing observations, namely, observations that are not available for at certain points in time, can be interpolated by a smoothing algorithm (Anderson and Moore 2012; Kitagawa and Gersch 1996; Kitagawa 2010). The trend order  $k$  is selected using the AIC (Akaike 1998; Konishi and Kitagawa 2008). In addition, although the type of the observation noise distribution is entirely dependent on the observations, it can also be determined using the AIC.

One application in Chap. 4 compares Gaussian, Cauchy, and GTV observation noises using the data that was originally used in Tanokura et al. (2012).

This book proposes a trend model with Gaussian observation noises with a time-varying variance (GTV trend estimation model).

### 2.3 Construction of a Distribution-Free Index

The estimation method for the trend component  $t_\lambda(n)$  in the trend model was presented in the previous section. Now, we have to search for an optimal  $\lambda$  in order to construct a distribution-free index for a financial market with non-Gaussian price distributions. Distribution-free means being impartial, regardless of the observation distributions.

For each  $\lambda$ , as mentioned in the previous section, assume that the average time series  $y_\lambda(n)$ ,  $n = 1, \dots, N$ , in (2.48), of the Box–Cox transformed prices  $q_{i,\lambda}(n)$  of the original prices  $p_i(n)$ ,  $i = 1, \dots, j(n)$ , in (2.47), is modeled by the trend model (2.49) and (2.52).

Then, the one-step-ahead predictive density function of  $y_\lambda(n)$  is given by

$$p(y_\lambda(n)|Y_{\lambda,n-1}) = \left\{ \frac{j(n)}{2\pi\sigma_\lambda^2(n)} \right\}^{\frac{1}{2}} \exp \left[ -\frac{j(n)\{y_\lambda(n) - t_\lambda(n)\}^2}{2\sigma_\lambda^2(n)} \right], \quad (2.55)$$

where  $Y_{\lambda,n-1} = \{y_\lambda(1), \dots, y_\lambda(n-1)\}$ . The log-likelihood and the AIC of the trend model for  $y_\lambda(n)$  are respectively obtained as

$$\ell_\lambda = \sum_{n=1}^N \log p(y_\lambda(n)|Y_{\lambda,n-1}) \quad (2.56)$$

$$\begin{aligned} \text{AIC}_\lambda &= -2\ell_\lambda + 2(\text{number of parameters}) \\ &= -2\ell_\lambda + 2(k+2). \end{aligned} \quad (2.57)$$

The optimal parameter  $\lambda$  should be determined with respect to the original prices. Therefore, the average time series  $y_\lambda(n)$  is transformed back to  $z_\lambda(n)$  by the following inverse Box–Cox transformation:

$$z_\lambda(n) = h_\lambda^{-1}(y_\lambda(n)) = \begin{cases} \{1 + \lambda y_\lambda(n)\}^{1/\lambda} & \lambda \neq 0 \\ \exp y_\lambda(n) & \lambda = 0. \end{cases} \quad (2.58)$$

Using the density function (2.55) of the trend model for  $y_\lambda(n)$ , the density function of the corresponding model for  $z_\lambda(n)$  is given by

$$p(z_\lambda(n)|Z_{\lambda,n-1}) = \left| \frac{dh_\lambda}{dz} \right| p(y_\lambda(n)|Y_{\lambda,n-1}), \quad (2.59)$$

where  $Z_{\lambda,n-1} = \{z_\lambda(1), \dots, z_\lambda(n-1)\}$ , and  $dh_\lambda/dz$  is the Jacobian of the Box–Cox transformation (2.47), which is obtained as  $dh_\lambda/dz = z_\lambda(n)$ . Then, the log-likelihood of the model evaluated on  $z_\lambda(n)$ ,  $n = 1, \dots, N$ , is obtained as

$$\ell_\lambda^0 = \sum_{n=1}^N \log p(y_\lambda(n)|Y_{\lambda,n-1}) + \sum_{n=1}^N \log \left| \frac{dh_\lambda}{dz} \right|. \quad (2.60)$$

Moreover,  $AIC_\lambda$  is modified to  $AIC_\lambda^0$ , which is the AIC value of the corresponding model for  $z_\lambda(n)$ , and is evaluated as

$$AIC_\lambda^0 = AIC_\lambda - 2 \sum_{n=1}^N \log \left| \frac{dh_\lambda}{dz} \right|_{z=z_\lambda(n)} \quad (2.61)$$

(Kitagawa 2010).

Therefore, the optimal  $\lambda$  can be determined by minimizing  $AIC_\lambda^0$  values, and the optimal trend component  $t_\lambda(n)$ ,  $n = 1, \dots, N$ , in (2.52) is obtained.

Finally, returning to the original observations, the distribution-free index  $i(n)$ ,  $n = 1, \dots, N$ , is defined as the inverse Box–Cox transformed values of the optimal trend component  $t_\lambda(n)$ , as follows:

$$i(n) = \begin{cases} \{1 + \lambda t_\lambda(n)\}^{1/\lambda} & \lambda \neq 0 \\ \exp t_\lambda(n) & \lambda = 0. \end{cases} \quad (2.62)$$

Let us observe the effect of using the Box–Cox transformation (2.47). Figure 2.8 shows the histograms of the Box–Cox transformed observations of the Japanese corporate CDS spreads illustrated in Fig. 2.7, where the optimal  $\lambda$  is given by  $-0.5$ . From back to front, the distribution at each point in time becomes closely symmetric and approximately Gaussian. When the mean is subtracted from the distribution at each point in time, the Box–Cox transformed distributions become easily understandable, as shown in Fig. 2.9. From back to front, the distribution at each point in time can approximately be regarded as Gaussian, even though the dispersion around the center largely varies over time. That is why the time-varying variance model is applied.

Note that the method for constructing a distribution-free index can be applied to general observations, such as the rate of return and the economic growth rate, which can be negative, although the Box–Cox transformation (2.47) is defined for observations taking positive values. Since the purpose of using the Box–Cox transformation is to search for an appropriate transformation close to a Gaussian distribution, the Box–Cox transformation can be applied to transformed observations in a positive domain by an appropriate distribution invariant function, say, a parallel transformation. In this way, we construct a distribution-free index for real GDP growth in Chap. 4.

In addition, since various transformations can be obtained by changing the parameter  $\lambda$  of the Box–Cox transformation, it is possible to examine the observation

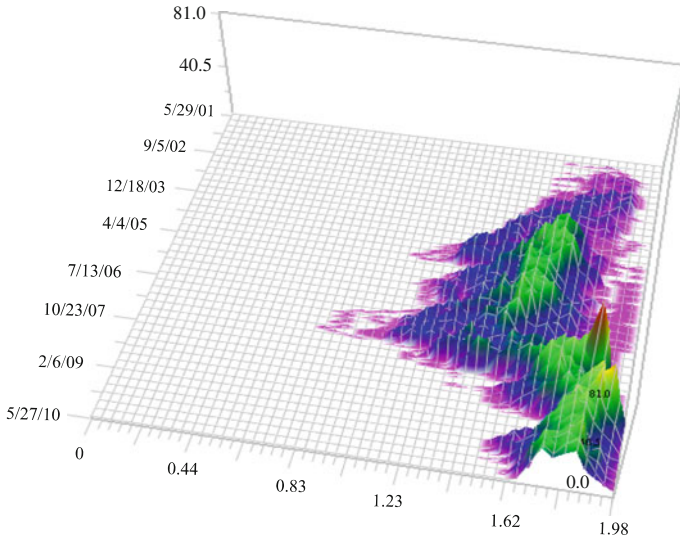


**Fig. 2.8** Histograms of the Box–Cox transformed Japanese corporate CDS spreads, where  $\lambda = -0.5$

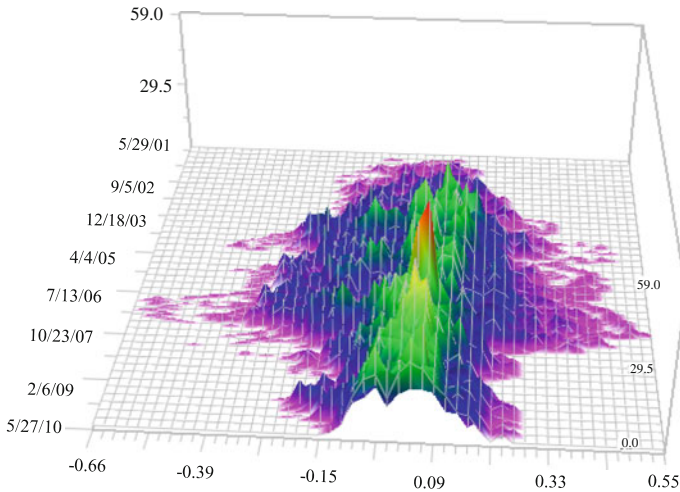


**Fig. 2.9** Histograms of the mean subtracted at each point in time from the Box–Cox transformed Japanese corporate CDS spreads

distribution to be analyzed, namely, to determine how far the distribution is from a Gaussian distribution by  $AIC_{\lambda}^0$  values in (2.61). Moreover, this method can also be used to estimate the trend of a single time series.

We briefly describe a computation procedure for constructing a distribution-free index based on the trend model with Gaussian observation noises with a time-varying

variance (GTV trend estimation model). The estimates of variances of  $\tau_\lambda^2$  and  $\sigma_\lambda^2$  are obtained by the maximum likelihood method.

First, a trend order  $k$  is fixed.

1. Given a parameter  $\lambda \in \{\lambda_1, \dots, \lambda_m\}$  of the Box–Cox transformation.
  - a. Transform the observations by the Box–Cox transformation (2.47).
  - b. Estimate the parameters of the fitted trend model to the Box–Cox transformed observations by the Kalman filter.
  - c. Compute the residual of the trend component.
  - d. Estimate the time-varying variance by fitting the time-varying variance model in Sect. 2.1.2 to the residuals.
  - e. Estimate the trend model with Gaussian observation noises with the above time-varying variance and compute  $AIC_\lambda^0$  in (2.61).
2. Determine the optimal  $\lambda$  by minimizing  $AIC_\lambda^0$ .
3. Obtain the optimal trend model with the Gaussian observation noises with the time-varying variance.
4. The distribution-free index is obtained by the inverse Box–Cox transformation of the optimal trend component (2.62).

If necessary, the trend order  $k$  can be changed, and the above procedure can be repeated. As a reference, the standard trend estimation in Kitagawa (2010) can be helpful.

## References

- Akaike, H.: Information theory and an extension of the maximum likelihood principle. In: Parzen, E., Tanabe, K., Kitagawa, G. (eds.) *Selected Papers of Hirotugu Akaike*, pp. 199–213. Springer, New York (1998)
- Anderson, B.D.O., Moore, J.B.: *Optimal Filtering*. Courier Dover Publications, Mineola (2012)
- Box, G.E.P., Cox, D.R.: An analysis of transformations. *J. Roy. Stat. Soc. Ser. B* **26**(2), 211–252 (1964)
- Davis, H.T., Jones, R.H.: Estimation of the innovations variance of a stationary time series. *J. Am. Stat. Assoc.* **63**, 141–149 (1968)
- Doucet, A., de Freitas, N., Gordon, N.: *Sequential Monte Carlo Methods in Practice*. Springer, New York (2001)
- Fama, E.F.: The behavior of stock market prices. *J. Bus.* **38**(1), 34–105 (1965)
- Gersch, W., Kitagawa, G.: The prediction of time series with trends and seasonalities. *J. Bus. Econ. Stat.* **1**(3), 253–264 (1983)
- Gordon, N.J., Salmond, D.J., Smith, A.F.M.: Novel approach to nonlinear/non-Gaussian Bayesian state estimation. *IEEE Proc.-F* **140**, 107–113 (1993)
- Kitagawa, G.: Non-Gaussian state-space modeling of nonstationary time series. *J. Am. Stat. Assoc.* **82**(400), 1032–1041 (1987)
- Kitagawa, G.: Monte Carlo filter and smoother for non-Gaussian nonlinear state space models. *J. Comput. Graph. Stat.* **5**(1), 1–25 (1996)
- Kitagawa, G.: *Introduction to Time Series Modeling*. CRC Press, Boca Raton (2010)

- Kitagawa, G., Gersch, W.: A smoothness priors-state space modeling of time series with trend and seasonality. *J. Am. Stat. Assoc.* **79**(386), 378–389 (1984)
- Kitagawa, G., Gersch, W.: *Smoothness Priors Analysis of Time Series*. Lecture Notes in Statistics, vol. 116. Springer, New York (1996)
- Konishi, S., Kitagawa, G.: *Information Criteria and Statistical Modeling*. Springer, New York (2008)
- Linden, M.: A model for stock return distribution. *Int. J. Financ. Econ.* **6**, 159–169 (2001)
- Madan, D.B., Seneta, E.: The variance gamma (V. G.) model for share market returns. *J. Bus.* **63**(4), 511–524 (1990)
- Mandelbrot, B.: The variation of certain speculative prices. *J. Bus.* **36**(4), 394–419 (1963)
- Paraez, P.D.: The distribution of share price changes. *J. Bus.* **45**(4), 49–55 (1972)
- Tanokura, Y., Tsuda, H., Sato, S., Kitagawa, G.: Constructing a credit default swap index and detecting the impact of the financial crisis. In: Bell, W.R., Holan, S.H., McElroy, T.S. (eds.) *Economic Time Series: Modeling and Seasonality*, pp. 359–380. CRC Press, Boca Raton (2012)

# Chapter 3

## Power Contribution Analysis of a Multivariate Feedback System

**Abstract** The globalization of financial and economic systems has brought attention to the significant ramifications of price fluctuations in both domestic and international financial markets, which may cause inextricable difficulties such as the global economic crisis triggered by the bankruptcy of Lehman Brothers in 2008. In order to detect such causations, we propose the application of the generalized power contribution, which extends the original Akaike's power contribution by decomposing a variance covariance matrix of the noises. This application reveals the frequency-wise effect of multi-dimensional noise sources on the power of the fluctuation of each variable in a multivariate feedback system. Therefore, multi-directional causations between variables can simultaneously be evaluated. The causations detected by power contribution analysis verify the effectiveness of a distribution-free index and provide valuable information flows.

**Keywords** Power contribution · Decomposition of a variance and covariance matrix · Information flow · Feedback system · Correlated noise

### 3.1 Akaike's Power Contribution and Its Generalization

A multivariate dynamic system with a feedback structure in which the comprising variables influence each other simultaneously or after short intervals, can often be found in the real world, such as ship motions and commodity price fluctuations. In our lives, we are interested in global financial market information such as the closing and current values of stock indices and foreign exchange rates, which are broadcast regularly, because this information may reflect current local financial markets. Generally, it is not easy to capture causations between variables in such a system.

The presence of feedback loops, namely, the influence of an input variable on an output variable with a time lag, can be expressed directly by the time domain approach. On the other hand, periodic variations of repetitive and regular movements, which are often observed in financial and economic time series, can be expressed in the form of trigonometric functions by the frequency domain approach. However, there are practically difficulties in capturing feedback loops by the frequency domain

approach, which requires being uncorrelated with the noises of the input variable in spectral analysis.

For analyzing a multivariate dynamic system with feedback, Akaike (1968) introduced a time domain approach to the frequency domain framework by defining the concept of relative power contribution through multivariate autoregressive (AR) modeling. Here, we briefly introduce Akaike's power contribution and its generalized version in order to detect causations between economic and financial time series.

Assume that an  $l$ -dimensional stationary time series  $y_n = (y_n(1), y_n(2), \dots, y_n(l))^t$ ,  $n = 1, \dots, N$ , is expressed as the following multivariate AR model with order  $m$ :

$$y_n = \sum_{j=1}^m A_j y_{n-j} + v_n, \quad (3.1)$$

where  $A_j$  is an  $l \times l$  AR coefficient matrix, where its  $(r, s)$ -component is written as  $a_j(r, s)$ . An  $l$ -dimensional white noise  $v_n$  satisfies the following conditions:

$$\begin{aligned} E(v_n) &= [0, \dots, 0]^t, & E(v_n v_n^t) &= W, \\ E(v_n v_h^t) &= O \quad (n \neq h), & E(v_n y_h^t) &= O \quad (n > h). \end{aligned}$$

Here,  $O$  is the  $l \times l$  zero matrix, and  $W = (\sigma_{rs})$  is a symmetric positive definite matrix (i.e.,  $\sigma_{rs} = \sigma_{sr}$ ) that is referred to as the variance covariance matrix of the noises.

The Fourier transform of the cross-covariance function  $C_k(r, s)$  presented in the introductory chapter, is given by

$$\begin{aligned} P_{rs}(f) &= \sum_{k=-\infty}^{\infty} C_k(r, s) e^{-2\pi i k f} \\ &= \sum_{k=-\infty}^{\infty} C_k(r, s) \cos 2\pi k f - i \sum_{k=-\infty}^{\infty} C_k(r, s) \sin 2\pi k f, \end{aligned} \quad (3.2)$$

which is referred to as the cross-spectral density function, or simply the cross spectrum. Here,  $f$  is a frequency satisfying  $-1/2 \leq f \leq 1/2$ , and  $i$  is the imaginary unit.

We define the cross spectrum matrix as the following  $l \times l$  matrix:

$$P(f) = \begin{bmatrix} P_{11}(f) & \cdots & P_{1l}(f) \\ \vdots & \ddots & \vdots \\ P_{l1}(f) & \cdots & P_{ll}(f) \end{bmatrix}.$$

The diagonal element  $P_{rr}(f)$  is referred to as the power spectral density function, or simply the power spectrum.

Then, the following relations between the cross spectrum matrix and the cross-covariance matrix hold:

$$P(f) = \sum_{k=-\infty}^{\infty} C_k e^{-2\pi i k f},$$

$$C_k = \int_{-1/2}^{1/2} P(f) e^{2\pi i k f} df.$$

The details can be found in Kitagawa (2010).

The cross spectrum matrix  $P(f)$  can be obtained as

$$P(f) = A(f)^{-1} W (A(f)^{-1})^*, \quad (3.3)$$

where  $A(f)$  is the  $l \times l$  complex matrix with its  $(r, s)$ -component  $A_{rs}(f)$ , and  $A^*$  denotes the complex conjugate of a matrix  $A$ . Here,  $A_{rs}(f)$  is defined as the Fourier transform of the coefficients  $a_j(r, s)$  in the multivariate AR model (3.1):

$$A_{rs}(f) = \sum_{j=0}^m a_j(r, s) e^{-2\pi i j f}, \quad (3.4)$$

where  $a_0(r, r) = -1$ , and  $a_0(r, s) = 0$  for  $r \neq s$  (Whittle 1963; Akaike and Nakagawa 1988). For simplicity, denoting  $A(f)^{-1}$  as  $B(f) = (b_{rs}(f))$ , (3.3) is given by

$$P(f) = B(f) W B(f)^*. \quad (3.5)$$

In the original definition in Akaike (1968), the components of the noise  $v_n$  are assumed to be mutually uncorrelated:  $\sigma_{rs} = 0$ ,  $r \neq s$ . Then, the variance covariance matrix of the noises is expressed as

$$W = \text{diag}\{\sigma_{11}, \dots, \sigma_{ll}\}. \quad (3.6)$$

Therefore, from (3.5) the power spectrum of the  $r$ th component  $y_n(r)$  of the time series  $y_n$  at a frequency  $f$  can be simply expressed as

$$P_{rr}(f) = \sum_{s=1}^l b_{rs}(f) \sigma_{ss} b_{rs}(f)^* \equiv \sum_{s=1}^l |b_{rs}(f)|^2 \sigma_{ss}. \quad (3.7)$$

That is, the power spectrum of  $y_n(r)$  at a frequency  $f$  is composed of  $l$  noise influences, and the degree of influence from the  $s$ th noise component  $v_n(s)$  on the fluctuation of  $y_n(r)$  is evaluated by  $|b_{rs}(f)|^2 \sigma_{ss}$  for  $s = 1, \dots, l$ .

Therefore, Akaike's power contribution is defined as

$$r_{rs}(f) = \frac{|b_{rs}(f)|^2 \sigma_{ss}}{P_{rr}(f)}, \quad (3.8)$$

which expresses the proportion of the fluctuation of  $y_n(r)$  caused by the  $s$ th noise component  $v_n(s)$  at a frequency  $f$ .

In practice, the variance covariance matrix of the noises is rarely diagonal. Therefore, Akaike suggested carefully examining the estimated noise correlations and seeking a possible practical solution in checking whether these correlations could be ignored. Akaike's power contribution has been applied to various real-world problems (Akaike and Nakagawa 1988; Akaike and Kitagawa 1999; Ohtsu et al. 1981, 2015). However, in the analysis of economic and financial time series with significant correlations between noises, Akaike's power contribution is not applicable, or at least may yield significant bias as a result of ignoring the presence of such correlations.

In order to address this problem, a generalized power contribution based on modeling correlations of general order, i.e., correlations between two variables, three variables, . . . , all variables of a multivariate time series, was proposed in Tanokura and Kitagawa (2004).

We next consider decomposing an  $l \times l$  variance covariance matrix  $W = (\sigma_{rs})$  into a sum of matrices with rank one in the following manner.

$$\begin{aligned} W = & q_l \mathbf{I}_0 \mathbf{I}_0^t + \sum_{j_1=1}^l q_{l-1, j_1} \mathbf{I}_{j_1} \mathbf{I}_{j_1}^t + \sum_{j_1=2}^l \sum_{j_2=1}^{j_1-1} q_{l-2, j_1 j_2} \mathbf{I}_{j_1 j_2} \mathbf{I}_{j_1 j_2}^t + \cdots \\ & + \sum_{j_1=l-1}^l \sum_{j_2=l-2}^{j_1-1} \cdots \sum_{j_{l-1}=1}^{j_{l-2}-1} q_{l-(l-1), j_1 \dots j_{l-1}} \mathbf{I}_{j_1 \dots j_{l-1}} \mathbf{I}_{j_1 \dots j_{l-1}}^t, \end{aligned} \quad (3.9)$$

where  $\mathbf{I}_0$  is the  $l$ -dimensional unit vector, and  $\mathbf{I}_{j_1 \dots j_k}$  is an  $l$ -dimensional vector, where the  $j_1$ th to the  $j_k$ th components are 0 and the remaining components are 1 for  $k = 1, \dots, l-1$ . Note that each term on the right-hand side of (3.9) expresses a range of variables consisting of correlations in descending order.

This decomposition is not unique in general, but can be uniquely determined when we specify each matrix with rank one according to descending order of correlation, i.e., from the first term to the last term in (3.9).

We assume that the common influence of all the variables is derived from the smallest correlation coefficient. When  $q_l$  of the first term of (3.9) is taken as an off-diagonal component with the smallest absolute value, say,  $\sigma_{l1}$ , the second term  $\sum_{j_1=1}^l q_{l-1, j_1} \mathbf{I}_{j_1} \mathbf{I}_{j_1}^t$  of (3.9) has only two possible values that are non-zero. Similarly, the third term  $\sum_{j_1=2}^l \sum_{j_2=1}^{j_1-1} q_{l-2, j_1 j_2} \mathbf{I}_{j_1 j_2} \mathbf{I}_{j_1 j_2}^t$  of (3.9) has three possible non-zero values, and so on, where the  $l$ th term of (3.9) has  $l$  possible non-zero values.

Finally, the variance covariance matrix is expressed as a sum of at most  $l(l+1)/2$  terms:

$$\begin{aligned}
 W &= q_{l,1} \mathbf{I}_{H_1(0)} \mathbf{I}_{H_1(0)}^t + \sum_{j=1}^2 q_{l-2+j,j} \mathbf{I}_{H_j(1)} \mathbf{I}_{H_j(1)}^t + \cdots \\
 &\quad + \sum_{j=1}^l q_{l-l+j,j} \mathbf{I}_{H_j(l-1)} \mathbf{I}_{H_j(l-1)}^t \\
 &= \sum_{k=0}^{l-2} \sum_{j=1}^{k+1} q_{l-(k+1)+j,j} \mathbf{I}_{H_j(k)} \mathbf{I}_{H_j(k)}^t + \sum_{j=1}^l q_{jj} \mathbf{I}_{H_j(l-1)} \mathbf{I}_{H_j(l-1)}^t, \quad (3.10)
 \end{aligned}$$

where  $\mathbf{I}_{H_j(k)} = [i_{jk}(1), \dots, i_{jk}(l)]$  is an  $l$ -dimensional vector, of which  $k$  components are 0 and  $(l-k)$  components are either 1 or  $-1$ , depending on the signs of correlations for  $k = 0, \dots, l-1$ ;  $j = 1, \dots, k+1$ . Here,  $H_j(k)$ , the suffix of  $\mathbf{I}_{H_j(k)}$ , is a subset  $H_j(k) = \{h_{j,1}, \dots, h_{j,k}\}$  of  $H = \{1, \dots, l\}$  and indicates the components of 0 of  $\mathbf{I}_{H_j(k)}$ . Note that the last term of (3.10) can be expressed as  $\text{diag}\{q_{11}, \dots, q_{ll}\}$ .

Then, by (3.5), the cross spectrum matrix can be decomposed as

$$\begin{aligned}
 P(f) &= \sum_{k=0}^{l-2} \sum_{j=1}^{k+1} q_{l-(k+1)+j,j} B(f) \mathbf{I}_{H_j(k)} \mathbf{I}_{H_j(k)}^t B(f)^* \\
 &\quad + B(f) \text{diag}\{q_{11}, \dots, q_{ll}\} B(f)^*. \quad (3.11)
 \end{aligned}$$

Therefore, the power spectrum of its  $r$ th component is expressed as

$$\begin{aligned}
 P_{rr}(f) &= \sum_{k=0}^{l-2} \sum_{j=1}^{k+1} q_{l-(k+1)+j,j} \sum_{h=1, h \neq r}^l \sum_{n=1, n \neq r}^l c_{rjk}(h) c_{rjk}(n)^* \\
 &\quad + \sum_{j=1}^l q_{jj} |b_{rj}(f)|^2, \quad (3.12)
 \end{aligned}$$

where  $c_{rjk}(h) = i_{jk}(h) b_{rh}(f)$ .

This expression implies that the power spectrum  $P_{rr}(f)$  can generally be decomposed into two terms. The first term expresses the  $l(l-1)/2$  common influences from  $l$  noise components, i.e., the influences resulting from correlations between  $l$  noise components. The second term expresses the  $l$  influences from single noise components, i.e., the influences resulting from the diagonal matrix of the noises. The first term is referred to as correlated noise, and the second term is referred to as independent noise.

Note that (3.12) is the general form of (3.7), i.e., (3.12) becomes (3.7) when  $q_{rs} = 0$  for  $r \neq s$ . In other words, according to the original Akaike's power contribution

(3.8),  $P_{rr}(f)$  is decomposed into  $l$  terms corresponding to the second term of (3.12) under the assumption of the independence of the noises.

Finally, the generalized power contribution is defined as

$$\tilde{r}_{rjk}(f) = \begin{cases} \frac{q_{l-(k+1)+j,j} \sum_{h=1, h \neq r}^l \sum_{n=1, n \neq r}^l c_{rjk}(h) c_{rjk}(n)^*}{P_{rr}(f)} & (k = 0, \dots, l-2; j = 1, \dots, k+1) \\ \frac{q_{l-(k+1)+j,j} |b_{rj}(f)|^2}{P_{rr}(f)} & (k = l-1; j = 1, \dots, l). \end{cases} \quad (3.13)$$

Note that the power contribution is usually expressed as a ratio to the power spectrum.

This modeling reveals the frequency-wise effect of multi-dimensional noise sources on the power of the fluctuation of each variable in a multivariate feedback system. In other words, it becomes possible to simultaneously measure the degree of influence between various combinations of the noises of variables. Therefore, multi-directional causations between variables can be evaluated. The applicable area is significantly widened (Tanokura 2006). Moreover, since we ensure the stability of Akaike's original power contribution in the generalized power contribution in Sect. 3.3, the concept of power contribution is strengthened and improved.

Other related studies on detecting noise sources can be found in various areas such as neuroscience and econometrics. In particular, based on a well-known causality concept defined by Granger (1969), frequency-wise measures of causality for two stationary time series proposed in Geweke (1982) and Hosoya (1991), were extended to those measures for three series in Geweke (1984) and Hosoya (2001), respectively. Although their interests are similar to ours, their approaches are fundamentally different from Akaike's (as noted in Hosoya 1991).

## 3.2 Algorithm for Decomposing a Variance Covariance Matrix

Rather than directly decomposing an  $l$ -dimensional variance covariance matrix of the noises  $W = (\sigma_{ij})$ , we decompose the following correlation matrix:

$$R = (\rho_{ij}), \quad \rho_{ij} = \frac{\sigma_{ij}}{\sqrt{\sigma_{ii}\sigma_{jj}}}, \quad (3.14)$$

where  $\rho_{ij} = \rho_{ji}$  and  $|\rho_{ij}| < 1$ ,  $i \neq j$ . Finally, by the transformation

$$W = TRT \quad (3.15)$$

where  $T = \text{diag}\{\sqrt{\sigma_{11}}, \dots, \sqrt{\sigma_{ll}}\}$ , the decomposition of the original variance covariance matrix can be obtained.

This algorithm is based on the procedure of subtracting a specified matrix from the correlation matrix  $R$  to make its off-diagonal component zero, and this procedure is repeated until the remaining matrix becomes diagonal. Therefore, the number of repetitions is at most  $l(l-1)/2$ .

We denote a specified matrix by  $q\Pi'$  with rank one, where  $q$  takes the absolute value of an off-diagonal component of the correlation matrix  $R$ , which is referred to herein as the target. On the other hand,  $\mathbf{I} = [e_1, e_2, \dots, e_l]'$  is an  $l$ -dimensional vector, the component  $e_i$  of which takes a value of either 1,  $-1$ , or 0, depending on the sign of the target. The algorithm is as follows.

1. The off-diagonal component with the smallest absolute value, say,  $\rho_{ij}$  is determined as the target. Then, we take  $q = |\rho_{ij}|$ .
2. The  $i$ th component of  $\mathbf{I}$ , is taken to be  $e_i = 1$ , and the sign of the  $j$ th component  $e_j$  is set equal to that of the target  $\rho_{ij}$ . The other components of  $\mathbf{I}$ ,  $e_k$ ,  $k \neq i$ ;  $k \neq j$  are assumed to be 0.
3. In order to make the absolute values of the other off-diagonal components as small as possible after the subtraction, when three off-diagonal components  $\rho_{ki}$ ,  $\rho_{ij}$ , and  $\rho_{jk}$  for  $k \neq i$ ;  $k \neq j$  satisfy the condition:

$$\rho_{ki}\rho_{ij}\rho_{jk} > 0, \quad (3.16)$$

we set  $e_k = e_j$  if  $\rho_{jk} > 0$  and  $e_k = -e_j$  if  $\rho_{jk} < 0$ .

For the case in which the target  $\rho_{ij} > 0$ , the sign of  $\rho_{jk}$  is the same as that of  $\rho_{ki}$  and  $e_j = 1$ . If  $\rho_{jk} > 0$ , we set  $e_k = e_j = 1$ . Then, the component of the matrix  $\Pi'$  corresponding to  $\rho_{jk}$  becomes  $e_j e_k = 1$ , and the component of the matrix corresponding to  $\rho_{ki}$  becomes  $e_k e_i = 1$ . Therefore, both components approach 0 after the subtraction. If  $\rho_{jk} < 0$ , we set  $e_k = -e_j = -1$ . The component of the matrix  $\Pi'$  corresponding to  $\rho_{jk}$  becomes  $e_j e_k = -1$ , and the component of the matrix corresponding to  $\rho_{ki}$  becomes  $e_k e_i = -1$ . Therefore, both components approach 0 after the subtraction. The same result is obtained for the case in which  $\rho_{ij} < 0$ .

4. If the other off-diagonal component  $\rho_{hk}$ ,  $h = 2, \dots, l$ ,  $k = 1, \dots, h-1$ ;  $h$ ,  $k \neq i$ ;  $h, k \neq j$  is equal to 0 and neither  $e_h$  nor  $e_k$  is 0, then  $e_h$  or  $e_k$  is set to be 0, as follows. According to which of the subtracted diagonal components, either  $\rho_{ii}$  or  $\rho_{jj}$ , is larger, we calculate the following two values: the difference between  $\rho_{ii}$  and the sum of the other components on the same column ( $2\rho_{ii} - \sum_{m=1}^l \rho_{mi}$ ) and the difference between  $\rho_{jj}$  and the sum of the other components on the same column ( $2\rho_{jj} - \sum_{m=1}^l \rho_{mj}$ ). If the latter is smaller, we set  $e_k = 0$ , otherwise  $e_h = 0$ .
5. If the absolute value of the other off-diagonal component  $\rho_{hk}$  becomes larger after the subtraction, we set  $e_h = 0$ . Then, the  $l$ -dimensional vector  $\mathbf{I}$  is determined, and  $R - q\Pi'$  is calculated.
6. If the absolute values of all the other off-diagonal components increase after the calculation  $R - q\Pi'$ , return to step 1 to change the target. In other words, the

component with the second smallest absolute value for the target is adopted and steps 2 through 5 are repeated.

7. By repeating steps 1 through 5 at most  $l(l-1)/2$  times, the resulting matrix becomes diagonal, and the decomposition of the correlation matrix  $R$  is obtained. By transforming the decomposition of  $R$  by (3.15), the decomposition of the variance covariance matrix  $W$  is finally attained. Then, the generalized power contribution is calculated by (3.13).

In order to clarify the decomposing procedure and the generalized effect of Akaike's power contribution, we next present a simple numerical example. Assume that the three-dimensional variance covariance matrix of the noises is given as

$$W = \begin{bmatrix} 9.0 & 4.2 & 0.9 \\ 4.2 & 4.0 & 1.0 \\ 0.9 & 1.0 & 1.0 \end{bmatrix}. \quad (3.17)$$

Then the correlation matrix is calculated as

$$R = \begin{bmatrix} 1 & 0.7 & 0.3 \\ 0.7 & 1 & 0.5 \\ 0.3 & 0.5 & 1 \end{bmatrix}. \quad (3.18)$$

The target is the (3,1)-component, 0.3, which has the smallest absolute value among the correlation coefficients, and we take the vector  $I_1$  to be  $[1, 1, 1]^t$ . Calculating  $R_1 = R - 0.3 I_1 I_1^t$ ,

$$R_1 = \begin{bmatrix} 0.7 & 0.4 & 0 \\ 0.4 & 0.7 & 0.2 \\ 0 & 0.2 & 0.7 \end{bmatrix}, \quad (3.19)$$

is obtained, and the (3,1)-component becomes 0. From (3.19), the next target is the (3,2)-component, 0.2. Taking the vector  $I_2 = [0, 1, 1]^t$ , we calculate  $R_2 = R_1 - 0.2 I_2 I_2^t$ . Then,

$$R_2 = \begin{bmatrix} 0.7 & 0.4 & 0 \\ 0.4 & 0.5 & 0 \\ 0 & 0 & 0.5 \end{bmatrix} \quad (3.20)$$

is obtained. Similarly, taking the vector  $I_3 = [1, 1, 0]^t$ ,

$$R_3 = \begin{bmatrix} 0.3 & 0 & 0 \\ 0 & 0.1 & 0 \\ 0 & 0 & 0.5 \end{bmatrix} \quad (3.21)$$

is attained. As a result, we obtain the following decomposition of the correlation matrix  $R$ :

$$R = 0.3 I_1 I_1^t + 0.2 I_2 I_2^t + 0.4 I_3 I_3^t + R_3. \quad (3.22)$$

Therefore, the original variance covariance matrix is decomposed as follows:

$$\begin{aligned} W &= 0.3 T I_1 I_1^t T + 0.2 T I_2 I_2^t T + 0.4 T I_3 I_3^t T + T R_3 T \\ &= 0.3 \begin{bmatrix} 9 & 6 & 3 \\ 6 & 4 & 2 \\ 3 & 2 & 1 \end{bmatrix} + 0.2 \begin{bmatrix} 0 & 0 & 0 \\ 0 & 4 & 2 \\ 0 & 2 & 1 \end{bmatrix} + 0.4 \begin{bmatrix} 9 & 6 & 0 \\ 6 & 4 & 0 \\ 0 & 0 & 0 \end{bmatrix} \\ &\quad + \begin{bmatrix} 2.7 & 0 & 0 \\ 0 & 0.4 & 0 \\ 0 & 0 & 0.5 \end{bmatrix}, \end{aligned} \quad (3.23)$$

where  $T = \text{diag}\{3, 2, 1\}$ . This leads to the calculation of the generalized power contribution.

In (3.23), the first term corresponds to the influence from the correlated noise common to all three variables, and the second term corresponds to influences from the correlated noise between the second and third variables. Moreover, the third term corresponds to the influence from the correlated noise between the first and second variables, and the final term corresponds to the influence from the three independent noises. Note that the variable combination of each correlated noise depends on the variance covariance matrix. In this example, there is no influence from correlated noise between the first and third variables.

Since Akaike's power contribution is calculated by the following diagonal matrix, which ignores all of the off-diagonal components of the variance covariance matrix (3.17):

$$\begin{bmatrix} 9 & 0 & 0 \\ 0 & 4 & 0 \\ 0 & 0 & 1 \end{bmatrix}, \quad (3.24)$$

the first three terms corresponding to the influences from the correlated noises in (3.23) are a new addition to Akaike's power contribution.

### 3.3 Example of Power Contribution Analysis

This section provides an example of power contribution analysis for an artificial trivariate AR process of order two, which is generated by the following  $3 \times 3$  AR coefficient matrices satisfying the condition of stationarity for a multivariate AR process (e.g., Hamilton 1994):

$$A_1 = \begin{bmatrix} 1.50 & -0.10 & -0.39 \\ 0.31 & 0.90 & -0.13 \\ 0.17 & 0.21 & -1.20 \end{bmatrix} \text{ and } A_2 = \begin{bmatrix} -0.80 & 0.14 & 0.16 \\ -0.23 & -0.80 & 0.10 \\ -0.11 & 0.10 & -0.60 \end{bmatrix},$$

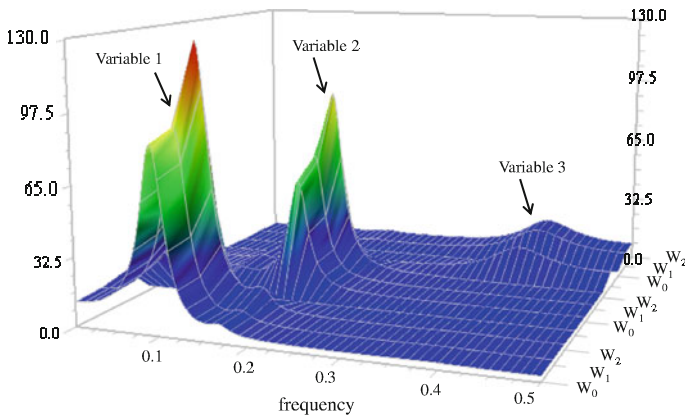
and three-dimensional normal random numbers with mean vector 0 and variance covariance matrix  $W$  that are generated using Cholesky decomposition. By changing the components of  $W$  as follows:

$$W_0 = \begin{bmatrix} 1 & 0 & 0 \\ 0 & 1 & 0 \\ 0 & 0 & 1 \end{bmatrix}, \quad W_1 = \begin{bmatrix} 1 & -0.1 & 0.1 \\ 0.1 & 1 & -0.1 \\ 0.1 & -0.1 & 1 \end{bmatrix}, \text{ and } W_2 = \begin{bmatrix} 1 & -0.6 & 0.3 \\ -0.6 & 1 & -0.1 \\ 0.3 & -0.1 & 1 \end{bmatrix},$$

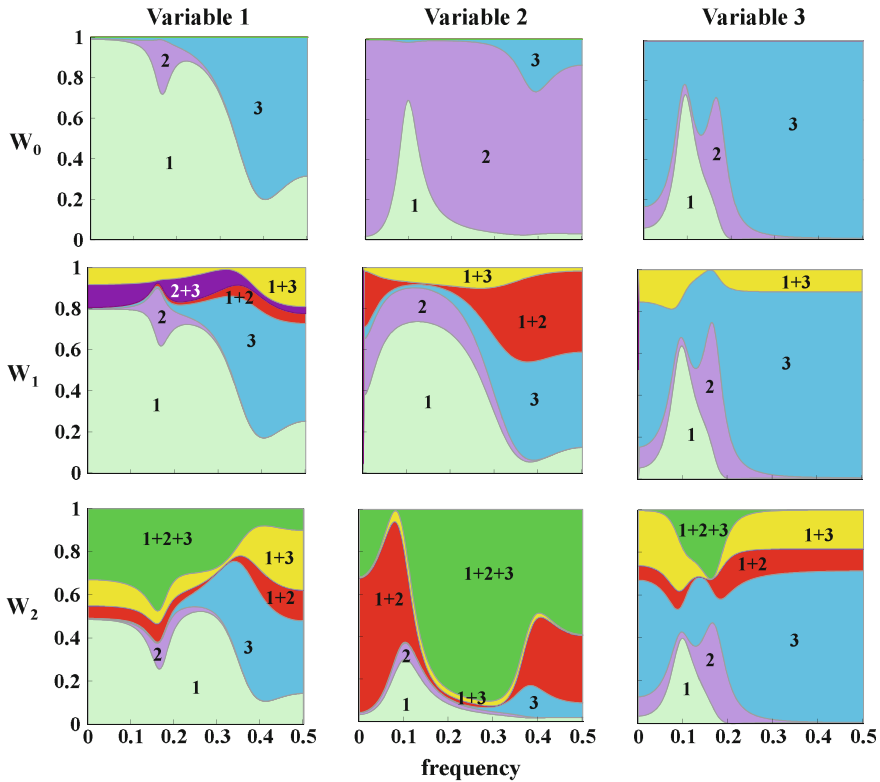
we can compare three stationary trivariate AR processes. Since  $W_0$ ,  $W_1$ , and  $W_2$  can be decomposed as the form (3.10), the generalized power contribution for each case is calculated.

Figure 3.1 shows the power spectrum of each variable for the three cases. The front, middle, and rear groups shows three power spectra for  $W_0$ ,  $W_1$ , and  $W_2$  of Variables 1, 2, and 3, respectively. For each variable, the peak of the power spectrum is sharper in the case of  $W_2$ , where the correlation coefficients are higher than those of  $W_0$  and  $W_1$ . For the most part, the shapes of the power spectra for each variable remain unchanged.

Figure 3.2 shows the generalized power contributions for each variance covariance matrix in the form of a graph matrix. The three graphs on the top row are for variance covariance matrix  $W_0$ , and the generalized power contributions of Variables 1, 2, and 3 are shown from left to right. Similarly, the graphs of the middle and bottom rows are for variance covariance matrices  $W_1$  and  $W_2$ , respectively. Figure 3.2 indicates that there are three primary types of noise influence. First, there are influences from



**Fig. 3.1** Power spectra of Variable 1 (*front*), Variable 2 (*middle*), and Variable 3 (*rear*) for the variance covariance matrices  $W_0$ ,  $W_1$ , and  $W_2$ .



**Fig. 3.2** Generalized power contributions of Variable 1, Variable 2, and Variable 3 for  $W_0$  (top),  $W_1$  (middle), and  $W_2$  (bottom)

the three independent noises (1, 2, and 3), corresponding to Variables 1, 2, and 3, respectively. The second type of noise influence is the influence of two correlated noises, e.g., the simultaneous influence of Variables 1 and 2 (1+2 in the figure). The third type of noise influence is the simultaneous influence of Variables 1, 2, and 3 (1+2+3 in the figure). Since  $W_0$  is diagonal and has no correlations among variables, each graph on the top row shows the influences from only the three independent noises for the variable concerned. Note that, based on (3.12), since the number of correlated noises is three, there may be one correlated noise that does not show up. In the three graphs of the middle row for the case of  $W_1$ , the three correlated noises are 1 + 2, 2 + 3, and 1 + 3. In the three graphs of the bottom row for the case of  $W_2$ , the three correlated noises are 1 + 2, 1 + 3, and 1 + 2 + 3. The revelation of a combination of variables of correlated noise depends on the values of the variance covariance matrix.

Moreover, in the case of high correlations, i.e., the case of  $W_2$ , the correlated noise influences can be misinterpreted as independent noise influences, as compared with the case of no correlations,  $W_0$ .

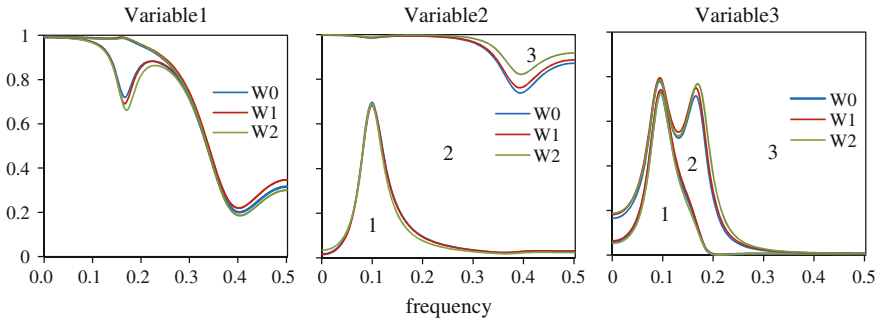


**Fig. 3.3** Akaike's power contribution of Variable 1, Variable 2, and Variable 3 for  $W_0$  (blue line),  $W_1$  (red line), and  $W_2$  (green line)

In Fig. 3.3, Akaike's power contribution of each variable for the case of  $W_0$  is shown along with the independent noise influences on the generalized power contributions for the cases of  $W_1$  and  $W_2$ . In each panel, the blue, red, and green lines represent Akaike's power contributions for  $W_0$  and the independent noise influences in the generalized power contributions for  $W_1$  and  $W_2$ , respectively. The changes between Akaike's power contributions and influences of independent noises on the generalized power contribution are significantly small. This implies the stability of Akaike's power contribution.

In addition, we applied the generalized power contribution to different trivariate AR processes that were generated by different AR coefficient matrices and three-dimensional normal random numbers with mean 0 and different variance covariance matrices  $W$ . The same results were obtained.

In the next chapter, which demonstrates the application of our indexation and causation method, the various relationships between financial and economic time series are observed.

## References

- Akaike, H.: On the use of a linear model for the identification of feedback systems. *Ann. Inst. Stat. Math.* **20**, 425–439 (1968)
- Akaike, H., Nakagawa, T.: *Statistical Analysis and Control of Dynamic System*. KTK Scientific Publishers, Tokyo (1988)
- Akaike, H., Kitagawa, G. (eds.): *The Practice of Time Series Analysis*. Springer, New York (1999)
- Granger, C.W.J.: Investigating causal relations by econometric models and cross-spectral methods. *Econometrica* **37**, 424–438 (1969)
- Geweke, J.: Measurement of linear dependence and feedback between multiple time series. *J. Am. Stat. Assoc.* **77–378**, 304–324 (1982)
- Geweke, J.: Measures of conditional linear dependence and feedback between time series. *J. Am. Stat. Assoc.* **79–388**, 907–915 (1984)
- Hamilton, J.D.: *Time Series Analysis*. Princeton University Press, Princeton (1994)

- Hosoya, Y.: The decomposition and measurement of interdependency between second-order stationary processes. *Probab. Th. Rel. Fields* **88**, 429–444 (1991)
- Hosoya, Y.: Elimination of third-series effect and defining partial measures of causality. *J. Time Ser. Anal.* **22**(5), 537–554 (2001)
- Kitagawa, G.: *Introduction to Time Series Modeling*. CRC Press, Boca Raton (2010)
- Ohtsu, K., Horigome, M., Kitagawa, G.: A new ship's auto pilot design through a stochastic model. *Automatica* **15**, 255–268 (1981)
- Ohtsu, K., Peng, H., Kitagawa, G.: *Time Series Modeling for Analysis and Control. Advanced Autopilot and Monitoring Systems*. Springer Series in Statistics, Springer, Tokyo (2015)
- Tanokura, Y.: Detection of the international sector comovements (in Japanese). *Japanese Association of Financial Econometrics and Engineering Journal: Econometrics on financial engineering and security markets 2006*, 155–178 Toyokeizai sinposha, Tokyo (2006)
- Tanokura, Y., Kitagawa, G.: Modeling influential correlated noise sources in multivariate dynamic systems. In: Hamza, M.H. (ed.) *Modelling and Simulation: Fifteenth IASTED International Conference Proceedings*, pp. 19–24. ACTA Press, Calgary (2004)
- Whittle, P.: On the fitting of multivariable autoregressions and the approximate canonical factorization of a spectral density matrix. *Biometrika* **50**, 129–134 (1963)

# Chapter 4

## Application to Financial and Economic Time Series Data

**Abstract** A method for constructing a distribution-free index is applied to financial and economic time series data and causations are analyzed based on power contributions. Highlighting the current sequential financial crises, the applications focus primarily on credit default swap (CDS) markets, which often have heavy-tailed spread distributions. The first application detects that the European debt crisis has already spilled over worldwide in terms of sovereign CDS (SCDS) markets. The second application measures the impact of the US subprime crisis on Japanese domestic markets. Finally, in order to examine the usability of a distribution-free index, the clear polarization between advanced and emerging regions by GDP growth regional distribution-free indices, and the importance of examining sovereign risks in estimating the economic growth, are observed. Moreover, the Japanese SCDS distribution-free index can be regarded as an underlying SCDS spread level reflecting a domestic credit strength. These applications verify the effectiveness of a distribution-free index and confirm that applying our method to markets with insufficient information, such as fast-growing or immature markets, can be effective.

**Keywords** Credit default swap · Sovereign risk · Crisis spillovers · GDP growth · Distribution-free index · Power contribution

### 4.1 Detecting Crisis Spillovers in Terms of Sovereign CDS Distribution-Free Indices

The sequential financial crises initially triggered by the US subprime loan crisis drastically influenced financial markets worldwide. Since then, in particular, attention to credit risk, which measures the exposure to loss resulting from failure of a corporation or government to fulfill their debt obligations, has come to the forefront. A credit default swap (CDS), the most widely used instrument among credit derivatives, is an over-the-counter contract designed to isolate the credit risk profile of an underlying asset without selling the asset itself. The buyer of a CDS periodically pays a premium quoted as an annual rate, usually in basis points (bps), to the seller for credit protection of a debt, and the seller will make a payment on the occurrence of a credit event of the reference entity. Due to this innovative advantage, the market

scale has rapidly expanded and a CDS can be regarded as a proxy for the credit risk of the issuer (Cossin et al. 2002).

Recently, a sovereign CDS (SCDS) dealing with credit risk on a government has been highlighted because of concerns about the European debt crisis starting with the Greece deficit crisis in the fall of 2009. Although the spread fluctuation of SCDS markets has become influential on the global economy, due to their shallow histories, fully exploiting the insufficient amount of information that is available for these markets has become essential.

This section attempts to detect the influences of the European debt crisis on the SCDS markets. First, we construct SCDS regional distribution-free indices focused on their spread distributions by applying the method for constructing a distribution-free index presented in Chap. 2. Second, we conduct the power contribution analysis (Akaike 1968; Tanokura and Kitagawa 2004), as described in Chap. 3, as a tool for detecting the multidimensional sources of fluctuations between SCDS regional distribution-free indices in terms of frequency domain properties. Then, the causal relations between regions for the periods of the post-subprime crisis, the post-Lehman shock, the post-Greece deficit crisis, and the crisis contagious phase are investigated.

Significant changes in SCDS spread fluctuations between regions are detected, revealing that the European debt crisis has already spilled over worldwide. Such prolonged phenomena would have a serious influence on the real economy.

#### ***4.1.1 SCDS Regional Distribution-Free Index Construction***

We focus on US dollar-denominated SCDS spreads of the 5-year contract, which is regarded as the standard and the most liquid contract in the market.

Figure 4.1 shows the time series of SCDS spread histograms, provided by Bloomberg LP. Each histogram consists of the middle composite SCDS spreads of at most 66 referencing countries in the sense that both bid and offer spreads exist during the period. From upper rear to lower front, the period is from January 21, 2004 to June 11, 2012 including the occurrences of the US subprime crisis and the European debt crisis.

As shown in Fig. 4.1, the SCDS spread distributions are skewed and heavy-tailed. For the purpose of constructing an index to represent the overall SCDS market behavior, simply taking an average spread at each point in time seems to be inappropriate because this causes bias and unevenly reflects the extreme spreads of the tails. Moreover, as shown in Fig. 4.2, the number of observations shows an increasing trend and then a gradual downturn.

Next, we apply the method for constructing a distribution-free index presented in Chap. 2 to SCDS spreads. Since SCDS spreads are often highly correlated over time with those within the same region, we construct a regional distribution-free index assuming that an SCDS spread follows the distribution specific to its region. We classify the 66 SCDS issues into eight regions, as shown in Table 4.1. The classification is based on the regional classifications by MSCI and Markit.

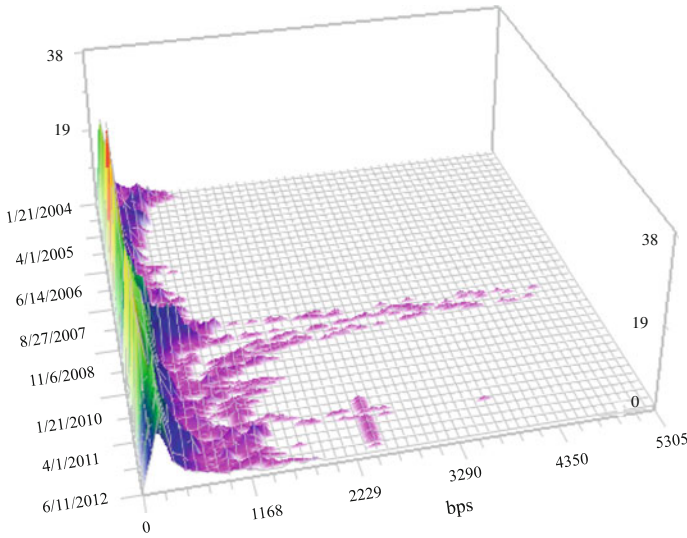


**Fig. 4.1** Sovereign CDS (SCDS) spread histograms. The SCDS spread in bps (from left to right), the time (from upper rear to lower front), and the number of observations (vertical scale). Source Bloomberg LP

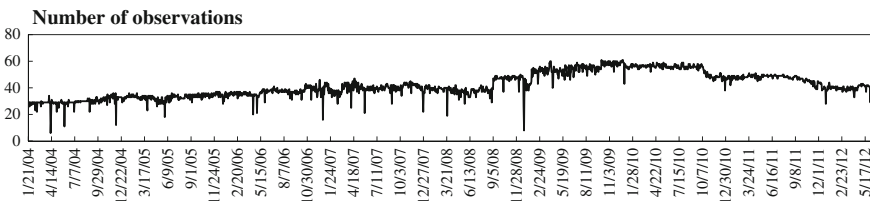


**Fig. 4.2** Number of SCDS spreads from January 21, 2004 to June 11, 2012

We determine the optimal  $\lambda$  for the Box-Cox transformation (2.47) in Chap. 2 (Box and Cox 1964). Note that the Box-Cox transformations are applicable as CDS spreads are generally positive. For each region, we calculate  $AIC_{\lambda}^0$  in (2.61) in Chap. 2, for  $\lambda = -1, -0.9, \dots, 0.9, 1$ , which is the AIC (Akaike 1998; Konishi and Kitagawa 2008) for the original SCDS spreads. From Table 4.2 showing the  $AIC_{\lambda}^0$  for major  $\lambda$ s for eight regions, the minimum value of  $AIC_{\lambda}^0$  for each region is obtained at either  $\lambda = 0, \lambda = -0.5$ , or  $\lambda = -1$ . Note that  $AIC_{\lambda}^0$  for the original spreads ( $\lambda = 1$ ) is the worst for all regions. Here, from the minimum value of the total  $AIC_{\lambda}^0$  on the rightmost column,  $\lambda = -0.5$  is selected for all eight regions, which yields a reciprocal root square transformation when the constant term is ignored.

Then, we estimate the optimal trend for each region. For example, the estimated trend for Southern Europe, which includes Greece and Spain, is shown in Fig. 4.3. From top to bottom, the estimated trend with  $\pm\sigma$ ; the residual term, which is the difference between the average of the Box-Cox transformed SCDS spreads and the smoothed value at each point of time; the estimated time-varying variance; and

**Table 4.1** List of SCDS issues of eight regions, with the number of countries in parentheses

Region	Country
Northern Europe (6)	Denmark, Finland, Ireland, Norway, Sweden, UK
Western Europe (6)	Austria, Belgium, France, Germany, Netherlands, Switzerland
Southern Europe (6)	Cyprus, Greece, Italy, Malta, Portugal, Spain
Eastern Europe (16)	Bulgaria, Croatia, Czech Republic, Estonia, Hungary, Kazakhstan, Latvia, Lithuania, Poland, Romania, Russia, Serbia, Slovakia, Slovenia, Turkey, Ukraine
Middle East/Africa (11)	Abu Dhabi, Bahrain, Dubai, Egypt, Iraq, Israel, Lebanon, Qatar, Saudi Arabia, South Africa, Tunisia
Developed Pacific (4)	Australia, Hong Kong, Japan, New Zealand
Emerging Asia (8)	China, Indonesia, Korea, Malaysia, Pakistan, Philippines, Thailand, Vietnam
Latin America (9)	Argentina, Brazil, Chile, Colombia, Ecuador, Mexico, Panama, Peru, Venezuela

**Table 4.2**  $AIC_{\lambda}^0$  for major  $\lambda$ s for eight regions

$\lambda$	North. Europe	West. Europe	South. Europe	East. Europe	Mid. East/Africa	Developed Pacific	Emerging Asia	Latin America	Total
1	14,401	11,053	17,069	17,826	20,316	12,196	16,085	21,633	130,579
0.5	10,374	9,164	14,281	16,122	19,484	11,122	15,207	19,519	115,273
0	7,618	8,287	13,236	15,539	18,891	10,841	14,528	17,902	106,841
-0.5	7,135	8,758	12,721	15,579	18,802	11,086	14,377	17,200	105,839
-1	7,085	9,623	14,204	16,378	19,715	11,652	13,965	16,494	109,115

the number of observations are shown. The number of observations often varies over time and vanishes for certain trading days. Although a relatively large residual term can occasionally be found when a sudden rise and fall of the observations occurs, the trend is estimated well as a whole. Note that the peak rise of the time-varying variance occurs at the time of the US subprime crisis exteriorization in mid-2007. Similar results are obtained for the other regions. As another example, the estimated results for Latin America are presented in Fig. 4.4. The frequent variations in the number of observations including missing observations, cause the sharp peaks of the residual terms. A steady increase in the time-varying variance in mid-2007 is also observed in this region. Thus, the impact of the US subprime crisis on the region cannot be ignored.

For each region, the SCDS regional distribution-free index is obtained by the inverse Box-Cox transformation of the optimal trend (2.62) in Chap. 2. As an example, Fig. 4.5 illustrates the relationship between the SCDS distribution-free index of Southern Europe (SE index) and the original SCDS spread distributions. For

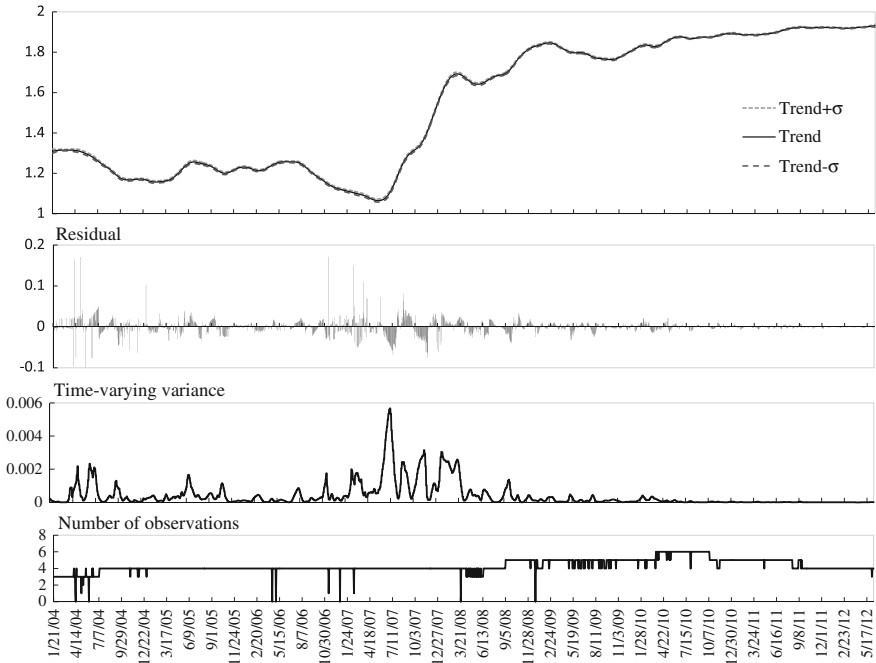


**Fig. 4.3** Visualization of the characteristics of the optimal trend for Southern Europe. From top to bottom, the estimated trend, the residual term, the time-varying variance, and the number of observations are shown

simplicity, the data based on the month-end are shown. Since the significantly sharp rises of all items have continued since the Lehman shock in the fall of 2008, as shown in the top panel, we divide the period as shown in the bottom panels. The upper tails become increasingly distorted after the US subprime crisis came to light in mid-2007, after the Lehman shock in the fall of 2008, and after the Greece deficit crisis revealed in late 2009. The SE index (blue line) is mostly located at more or less the 50 percentile (red dotted line) of the distributions. Moreover, as shown in the lower left panel of Fig. 4.6, for the case of Latin America, the trend is appropriately estimated when there are no observations. Similar results are obtained for the other regions. On the whole, each SCDS regional distribution-free index is positioned at a well-balanced place among individual SCDS spreads within the region.

Figure 4.7 shows the eight SCDS regional distribution-free indices. Four SCDS regional distribution-free indices in Europe and the SCDS distribution-free indices of four other regions are shown in the top and bottom panels, respectively. In the top panel, the continuous upward trend of the SE index from the end of 2009, i.e., the occurrence of the Greece debt crisis, is noteworthy. Based on this figure, these SCDS regional distribution-free indices are generally well balanced and reflect the market views on the regional sovereign risks.

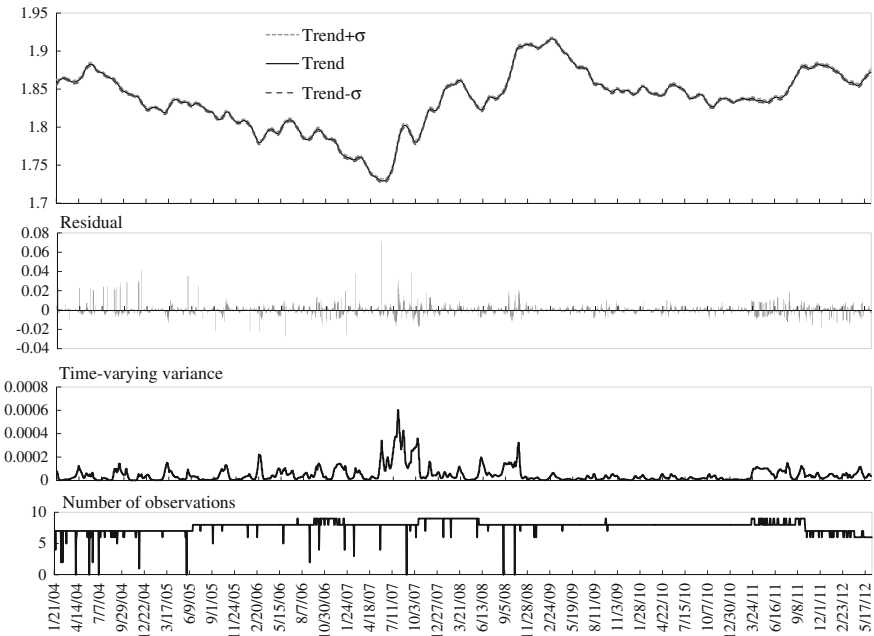


**Fig. 4.4** Visualization of the characteristics of the optimal trend for Latin America. From top to bottom, the estimated trend, the residual term, the time-varying variance, and the number of observations are shown

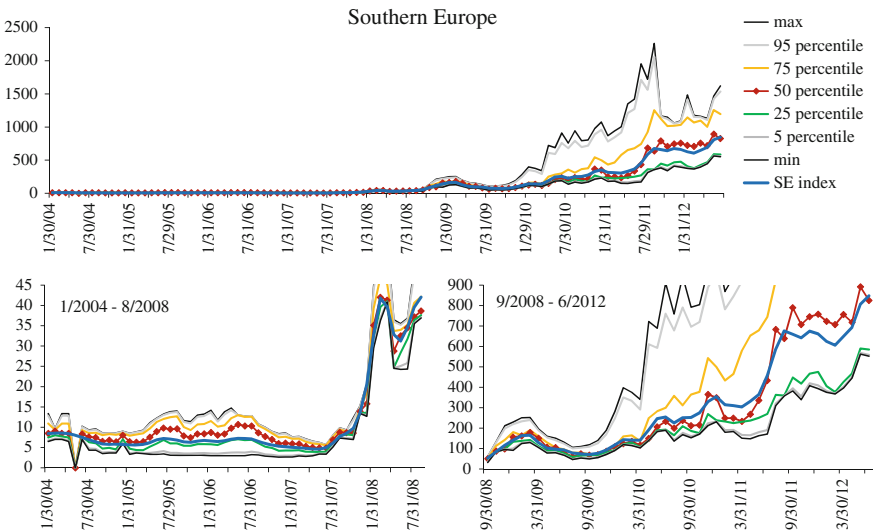


**Fig. 4.5** SCDS distribution-free index of Southern Europe (SE index) with the SCDS spread distributions for the entire period (*top*) and detailed periods of interest (*bottom*)

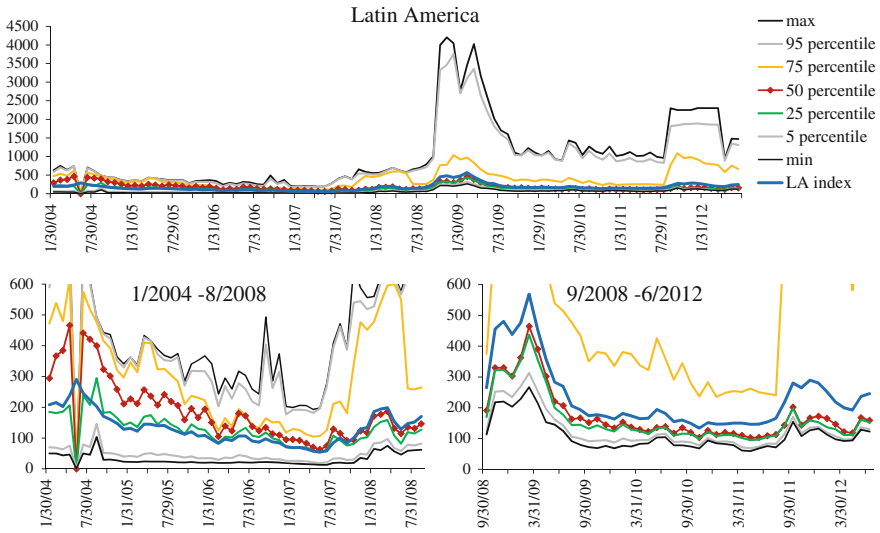


**Fig. 4.6** SCDS distribution-free index of Latin America (LA index) with the SCDS spread distributions for the entire period (*top*) and detailed periods of interest (*bottom*)

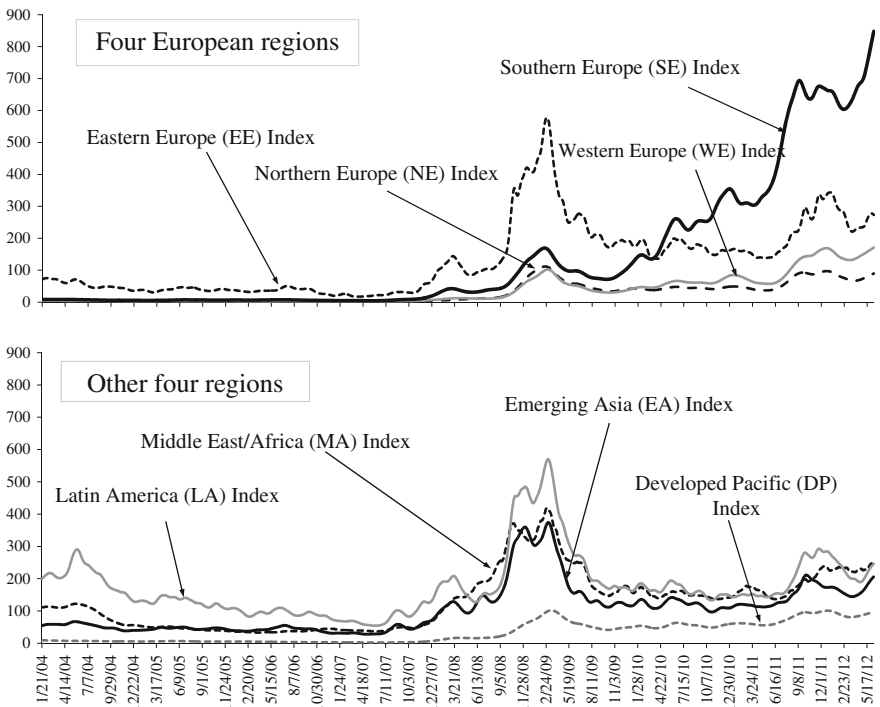


**Fig. 4.7** Eight SCDS regional distribution-free indices

The European debt crisis has impacted most of the developed countries in Europe. Therefore, we construct a composite index for the developed Europe, the DE index, from the NE index, the WE index, and the SE index in a regional-weighted form, which is the sum of the index value multiplied by the regional weight proportional to the numbers of countries included, as follows:

$$\text{DE index} = (\text{NE index} \times 33.3\%) + (\text{WE index} \times 33.3\%) + (\text{SE index} \times 33.3\%).$$

Similarly, we construct a composite index for Eastern Europe & Middle East/Africa, the EM index, from the EE index and the MA index, as follows:

$$\text{EM index} = (\text{EE index} \times 59.3\%) + (\text{MA index} \times 40.7\%).$$

Finally, we obtain five SCDS regional distribution-free indices: the Developed Europe (DE), Eastern Europe & Middle East/Africa (EM), Developed Pacific (DP), Emerging Asia (EA), and Latin America (LA) indices, as shown in Fig. 4.8. In the earlier period, the levels of the SCDS regional distribution-free index were split into three groups: the highest level includes the LA index (red line), the middle level includes the EM (yellow line) and EA (pink line) indices, and the lowest level includes the DP (green line) and DE (blue line) indices. Later, the EM and EA indices caught up with the highest LA index. In other words, these indices are polarized between the developed regions (the DE and DP indices) and the emerging regions (the EM, EA, and LA indices). In particular, both the LA and EM indices remained high until the end of 2010. On the other hand, the DE index (blue) gradually increased and departed from the level that includes the DP index since the fall of 2009, i.e., the disclosure of Greece deficit crisis. This implies that the DE index can be regarded as an indicator of the European debt crisis.

Since then, the DE index exhibited a consistent upward trend and reached the level of the LA and EM indices at the end of 2010. Eventually, the DE index climbed up to the top level around mid-2011. The parallel shifts of all distribution-free indices afterwards imply the spillovers from the European debt crisis.

### ***4.1.2 Role of the SCDS Distribution-Free Index***

There are existing SCDS indices provided by Markit, such as the iTraxx SovX Western Europe, for the purpose of hedging or taking credit risk on sovereign debt. They are generally equally weighted of selected names in their regions based on trading activities and are rolled every six months with membership changes. Therefore, the index may be biased due to the heavy-tailed spread distributions. In other words, the information on some issues can be unfairly diluted or weighted. Moreover, the data length of one series of an index is not sufficient for analyzing the relationship with other financial market indices, such as an equity index or a bond index. Fung et al. (2008) constructed an index in the same manner as the Dow Jones CDX

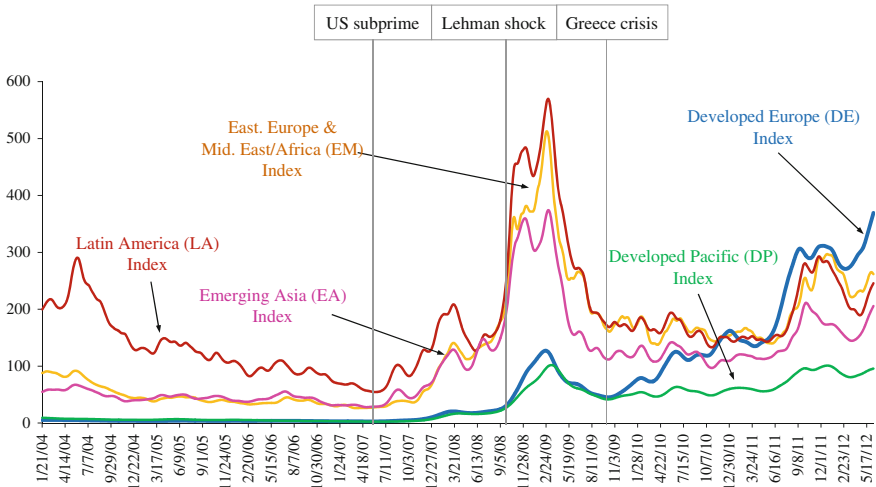


**Fig. 4.8** Five SCDS regional distribution-free indices

index (the US corporate CDS index provided by Markit) was constructed, and they connected the index to the existing series in order to cover the period examined.

On the other hand, in the distribution-free index construction method presented in Chap. 2, all existing information in the financial market can be fully exploited by considering the distributions, and the problem on the missing observations can be solved.

Figure 4.9 compares the SCDS regional distribution-free indices with the Markit iTraxx SovX indices, provided by Bloomberg LP, by region. In response to the data length of the Markit indices, the period of all three panels is set to be from September 1, 2009 to June 11, 2012. In the top panel, three series (Series 2, 6, and 7) of the iTraxx SovX Western Europe, the composite DE index based on three SCDS regional distribution-free indices, and the three SCDS regional distribution-free indices (the NE, WE, and SE indices), are shown. The DE index (red line) exhibits smooth fluctuations and appropriately complies with the three series of the iTraxx SovX Western Europe (green lines). Moreover, the breakdown of the sub-regional sovereign risk can be observed in the fluctuations of the SCDS regional distribution-free indices, i.e., the NE, WE, and SE indices (dashed lines). The middle panel compares two series (Series 3 and 7) of the iTraxx SovX CEEMA with the composite EM index and two SCDS regional distribution-free indices (the EE and MA indices). Note that a few sudden drops to zero of Series 3 of the iTraxx SovX CEEMA indicate missing observations. The members of Series 3 appear to have relatively high sovereign risks, and the EM index fluctuates between two series of the iTraxx SovX CEEMA in a balanced manner. In the bottom panel, two series (Series 4 and 6) of the iTraxx SovX Asia Pacific are compared with the composite AP index and two SCDS regional distribution-free indices (the DP and EA indices). Note that the composite AP index is defined as the number of weighted countries

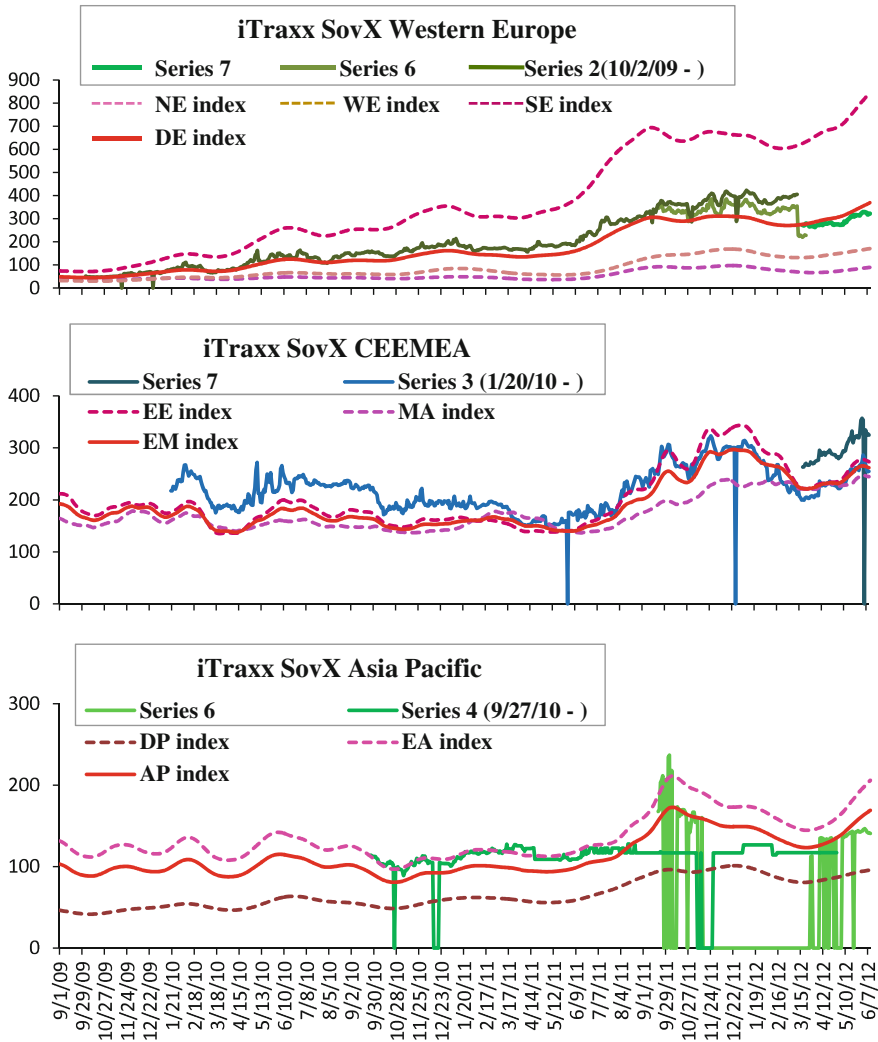


**Fig. 4.9** Comparison of the SCDS regional distribution-free indices with the Markit iTraxx SovX indices for developed Europe (*top*), Eastern Europe & Middle East/Africa (*middle*), and Asia Pacific (*bottom*). *Source* Bloomberg LP

of the DP and EA indices, in the same manner as the DE index. Similarly, we find that the AP index exhibits well-balanced fluctuations between the two series of the iTraxx SovX Asia Pacific.

In order to examine the SCDS markets, the information detected from the SCDS regional distribution-free indices may be useful to complement the information detected from existing Markit iTraxx SovX indices.

### 4.1.3 *Causation Between SCDS Regional Distribution-Free Indices*

Using five SCDS regional distribution-free indices, as shown in Fig. 4.8, the spillover effects of the financial crises are investigated by the power contribution analysis (Akaike 1968; Tanokura and Kitagawa 2004), as discussed in Chap. 3.

Assume that a causation arises from short-term fluctuations. In particular, in financial markets, the trend of an asset price is regarded as the gradually changing long-term fluctuations caused by characteristics specific to the asset, such as fundamental and economic factors, and short-term cyclical fluctuations around the trend can sensitively be influenced by short-term cyclical fluctuations of any other asset prices, regardless of the specific characteristics. For example, the tendency of the sovereign risk of Germany has recently increased to be in line with that of Greece, even though their economic conditions are different. Moreover, such a short-term cyclical fluctuation often occurs as a short-term price adjustment. Therefore, a short-term cyclical fluctuation can be a risk factor with uncertainty and may lead to a future change in the long-term trend direction. Capturing short-term fluctuations of financial markets is important in risk management.

For each SCDS regional distribution-free index, we focus on the short-term cyclical fluctuations around its trend. In order to extract the trend component from an index, we use the freely available web-based time series analysis software, Web DECOMP ([http://ssnt.ism.ac.jp/inets/inets\\_eng.html](http://ssnt.ism.ac.jp/inets/inets_eng.html)) based on the seasonal adjustment model (Gersch and Kitagawa 1983; Kitagawa and Gersch 1984), reviewed in Chap. 2. In practice, although the rate of return and the spread change based on two consecutive prices are often used to analyze short-term fluctuations, they depend significantly on the previous price. On the other hand, the advantage of using the seasonal adjustment model is that the detrended cyclical component can be objectively estimated and is not dependent on the features of the asset.

Next, we focus the analysis on the following four periods: from July 2, 2007 to September 12, 2008 (post-subprime crisis), from September 15, 2008 to October 30, 2009 (post-Lehman shock), from November 2, 2009 to August 31, 2011 (post-Greece crisis), and September 1, 2011 to June 11, 2012 (crisis contagious phase). For each period, we obtain the detrended cyclical component by extracting the trend component from each SCDS regional distribution-free index by DECOMP. Then, for each period, we fit a five-dimensional autoregressive (AR) model to the five detrended regional distribution-free indices.

Table 4.3 shows the variances (diagonal) and correlation coefficients (off-diagonal) of the noises for the periods of post-subprime (top left), post-Lehman (top right), post-Greece (bottom left), and contagious phase (bottom right). In the top-left panel, which shows the variances and correlation coefficients for the post-subprime period, the significantly high correlation coefficient 0.91 between the developed regional distribution-free indices, i.e., the DE and DP indices, was found. Then, the top-right panel, which shows the variances and correlation coefficients for the post-Lehman period, shows small changes of the correlations and larger variances for all

**Table 4.3** Variances (*diagonal*) and correlation coefficients (*off-diagonal*) of the noise of five SCDS regional distribution-free indices for the periods of post-subprime (*top left*), post-Lehman (*top right*), post-Greece (*bottom left*), post-Lehman (*bottom right*) and contagious phase (*bottom right*)

Post-subprime	DE index	DP index	EA index	LA index	EM index	Post-Lehman	DE index	DP index	EA index	LA index	EM index
DE index	7E-11					DE index	2E-08				
DP index	0.91	2E-11				DP index	0.86	3E-09			
EA index	0.15	0.13	2E-07			EA index	-0.06	-0.07	2E-06		
LA index	0.09	0.09	0.28	1E-06		LA index	-0.18	-0.21	0.35	2E-05	
EM index	0.02	0.02	0.12	0.03	5E-04	EM index	-0.01	-0.01	0.14	0.05	8E-03
Post-Greece	DE index	DP index	EA index	LA index	EM index	Contagious phase	DE index	DP index	EA index	LA index	EM index
DE index	4E-07					DE index	8E-07				
DP index	0.64	3E-09				DP index	0.30	2E-09			
EA index	-0.69	-0.34	7E-07			EA index	0.54	0.41	5E-07		
LA index	-0.47	-0.30	0.62	3E-06		LA index	0.06	0.19	0.08	8E-06	
EM index	0.13	0.10	0.00	0.06	4E-03	EM index	0.07	0.06	0.14	0.01	2E-03

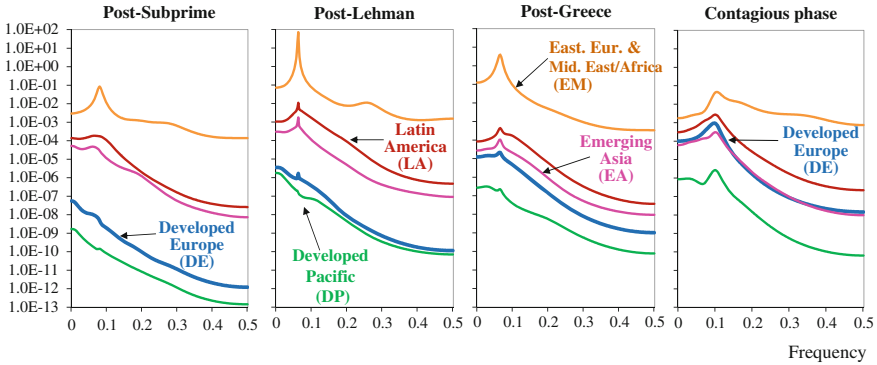


**Fig. 4.10** Power spectrum on a logarithmic scale of five SCDS regional distribution-free indices for the periods of post-subprime (*leftmost*), post-Lehman (*second leftmost*), post-Greece (*second rightmost*), and contagious phase (*rightmost*)

regional distribution-free indices than the previous period. Moreover, as the correlation coefficients of the emerging regional distribution-free indices, i.e., the EM, EA, and LA indices, with the developed regional distribution-free indices, i.e., the DE and DP indices, became negative, the emerging regional distribution-free indices started diverging from the developed regional distribution-free indices. For the post-Greece period in the bottom-left panel, this tendency strengthened as the correlations between the developed regional distribution-free indices and, the EA and LA indices became increasingly negative. Moreover, the positive correlation between the EA and LA indices strengthened. Finally, in the bottom-right panel for the period of contagious phase, the correlations between the developed regional distribution-free indices and, the EA and LA indices became reversed, and the correlations for all regional distribution-free indices became positive. This implies that the contagious effect from the European debt crisis was eventually established.

Let us investigate the changes in the power spectra of five regional distribution-free indices, as shown in Fig. 4.10. For the post-subprime period of the leftmost panel, the power spectra were polarized in the form of the developed regions (DE and DP indices) versus the emerging regions (LA, EA, and EM indices). Then, during the post-Lehman period of the second leftmost panel, all power spectra became larger. For the post-Greece period of the second rightmost panel, the slightly increasing power spectrum of the DE index (blue line) became closer to that of the EA index (pink line), whereas the power spectrum of the EM index (yellow line) decreased. For the period of contagious phase in the rightmost panel, the power spectrum of the DE index almost exceeded the power spectrum of the EA index.

Next, in order to detect the causation on the European debt crisis, we calculate the generalized power contributions (%) (3.13) in Chap. 3, for each period. Figure 4.11 shows the graph matrix of the power contributions (%) of five regional distribution-free indices with the power spectra. From top row to bottom row, the periods of post-subprime, post-Lehman, post-Greece, and contagious phase are shown, and the

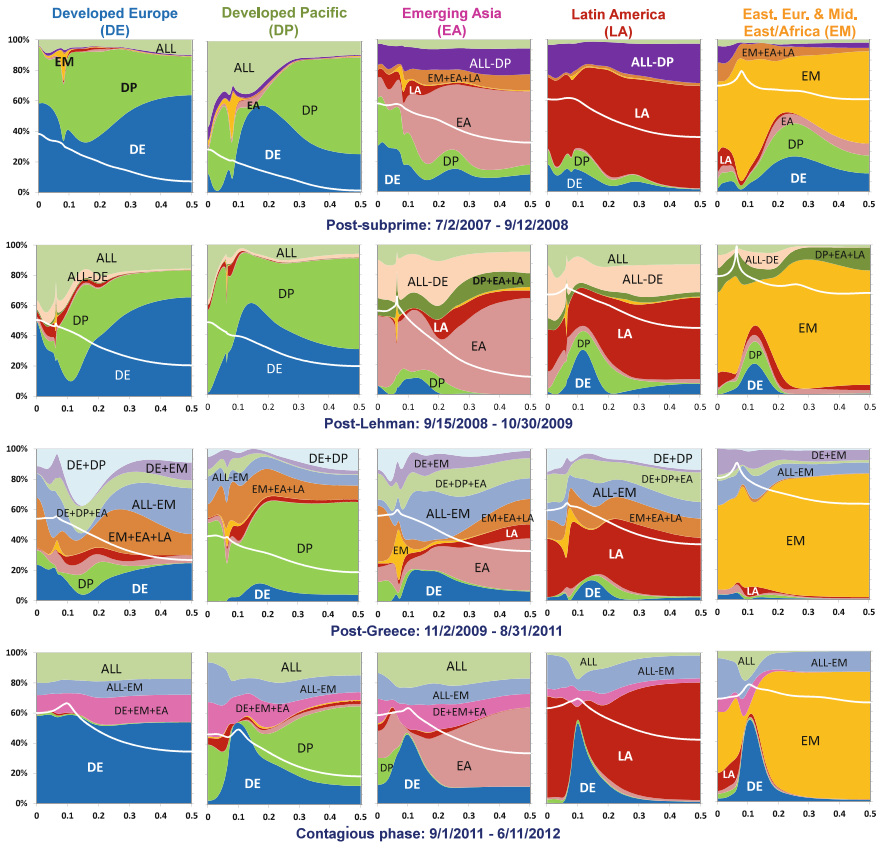


**Fig. 4.11** Power contributions (%) with the power spectrum on a logarithmic scale (*white line*) of five SCDS regional distribution-free indices for the periods of post-subprime (*top row*), post-Lehman (*second row*), post-Greece (*third row*), and contagious phase (*bottom row*). A+B: the simultaneous contribution of the correlated noises of A and B, ALL-B: the simultaneous contribution of the correlated noises of all five indices (ALL) excluding B

power contributions (%) for the Developed Europe (DE), Developed Pacific (DP), Emerging Asia (EA), Latin America (LA), and Eastern Europe & Middle East/Africa (EM) indices, are shown from left to right. In each graph, the proportion of each contributor within the power spectrum (*white line*) is shown at each frequency. Since the frequency refers to the number of cycles per day, the lower the frequency, the longer the fluctuation period.

For example, the top-left graph shows the power contributions of indices influencing the DE index for the post-subprime period. The blue area indicates the contribution of the DE index itself and the green area indicates that of the DP index. Therefore, the contributions of the developed regional distribution-free indices, i.e., the DP and DE indices occupied approximately 90% of the total power of the

fluctuations of the DE index, for all frequencies. On the other hand, the small light green area represents the simultaneous contribution from all five indices (ALL) to the DE index.

Then, based on the leftmost graph on the second row, the contribution of ALL to the DE index increased for the post-Lehman period. In the post-Greece period (third row), the correlated noise contributions, such as EM+EA+LA (combination of EM, EA, and LA indices), ALL-EM (ALL but the EM index), and DE+DP, to not only the DE index but also to all of the SCDS regional distribution-free indices excluding the EM index increased significantly. This implies that the SCDS regional distribution-free indices mostly become sensitive to each other during the post-Greece period. Then, in the period of contagious phase (bottom row), the sharp increases in the contribution from the DE index (blue area) around the frequency of 0.1 (approximately 10-day cycle of fluctuation) can be found for all regions. Interestingly, the contributors of the correlated noises became concentrated on only three contributors, i.e., ALL, ALL-EM, and DE+EM+EA for all regions. Note that the contagious effects of the European debt crisis became established during the period of contagious phase.

In order to summarize the results obtained by the power contribution analysis, we focus on the frequency domain around the peak of the power spectrum for each SCDS regional distribution-free index, which largely dominates the fluctuations of the index. Figure 4.12 shows the top three contributors around the peak of the power spectrum of each SCDS regional distribution-free index. The frequency domain considered for the post-subprime, post-Lehman, and post-Greece periods is from 0.06 to 0.065, which expresses an approximately 15-day cycle of fluctuation. On the other hand, the frequency domain considered for the period of contagious phase, from 0.0975 to 0.105, expressing a 10-day cycle of fluctuation, is slightly higher than that for the previous three periods.

In the post-subprime period on the top panel, the top contributor was the index itself for all regional distribution-free indices, excluding the EA index. The contribution of the developed regional distribution-free indices, such as the DE (blue bar) and DP (green bar) indices, are among the top three for all distribution-free indices. Then, during the post-Lehman period, shown in the second panel from the top, the contribution of the developed regional distribution-free indices significantly weakened for emerging regional distribution-free indices. During the post-Greece period, shown in the second panel from the bottom, the contributions of correlated noises, such as ALL-EM (dark blue bar) and DE+EM (light purple bar), increased. All regional distribution-free indices became sensitive to each other. Finally, during the contagious phase, shown in the bottom panel, the top three contributors became the same for all regional distribution-free indices: DE (blue), ALL (gray), and DE+EM+EA (light green). In particular, the contribution of the DE index, i.e., the influence of the European debt crisis, occupied more than 50 % of the power spectra of all regional distribution-free indices. The European debt crisis has spread worldwide.

Note that, in this analysis, the scale of economy of each country in a region is not considered as we focus on the crisis spillovers of a country with a small economy on the other countries with larger economies in the region, such as the European debt crisis. However, the SCDS regional distribution-free index can absorb

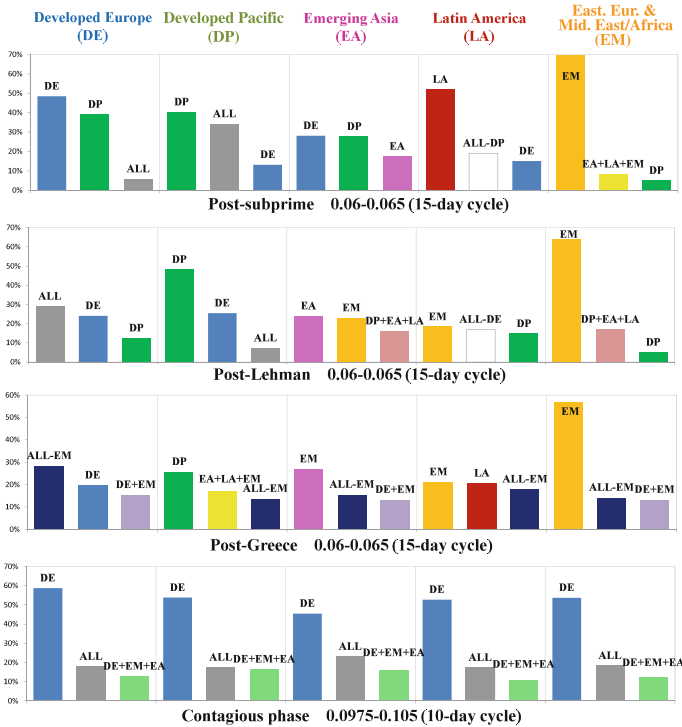


**Fig. 4.12** Top three contributors around the peak of the power spectrum of each SCDS regional distribution-free index for the periods of post-subprime (*top*), post-Lehman (second from *top*), post-Greece (second from *bottom*), and contagious phase (*bottom*)

the influence to some extent by its spread distribution-free effect. In addition, in Sect. 4.3.1, we will construct the GDP growth regional distribution-free index and analyze the relationship between the SCDS regional distribution-free index and the GDP growth regional distribution-free index.

To represent a different aspect of regional sovereign risk, various ways of application of the method for constructing a distribution-free index to SCDS markets, can be considered. For example, the method can be applied to weighted SCDS spreads based on an economic scale.

## 4.2 Measuring the Impact of the US Subprime Crisis on Japanese Financial Markets

The US subprime crisis sparked the subsequent financial crises. In this section, we investigate the spillover effect from the US subprime crisis on the Japanese financial markets. The Japanese corporate CDS market is treated as a credit risk indicator

representing Japanese corporations. Similar to the SCDS market in the previous section, the spread distributions of the Japanese corporate CDS issues are skewed and heavy-tailed, and the number of observations often fluctuates and even vanishes at certain times because the market is fast-growing and immature. We construct a distribution-free index for the Japanese corporate CDS by applying the method presented in Chap. 2.

In the case of corporate CDS, for a practical reason, the co-movement of the CDS spreads of the issues with the same credit rating can often be observed. Therefore, we assume that a CDS spread follows the specific distribution of the rating of the referencing company. Here, we categorize the CDS reference entities into four rating classes and construct a CDS rating-based distribution-free index for each rating. It is found that the higher the rating class, the higher the CDS rating-based distribution-free indices. Then, a composite Japanese corporate CDS distribution-free index for the entire market is constructed in a rating-weighted form. We regard this Japanese corporate CDS distribution-free index as a proxy for the Japanese corporate credit risk.

In order to examine the influence of the US subprime crisis on Japanese markets, we investigate the causations between the Japanese corporate CDS distribution-free index and other Japanese market indices, such as the Nomura-BPI overall index (fixed income), TOPIX (equity), and JPYUSD (Japanese yen exchange rate against US dollar) by the power contribution analysis (Akaike 1968; Tanokura and Kitagawa 2004), described in Chap. 3.

After the disclosure of the US subprime crisis, the Japanese domestic markets became significantly influential with respect to each other, and the Japanese corporate CDS distribution-free index we constructed, provides an indicator of the Japanese corporate credit risk, fully reflecting the fluctuations of the Japanese financial markets.

Note that this section presents a complementary analysis of the application in Tanokura et al. (2012).

### ***4.2.1 Japanese Corporate CDS Market and Rating Classes***

We use the middle spreads of Japanese yen-denominated corporate CDS spreads of the 5-year standard contract provided by Bloomberg LP, for the period from May 29, 2001 to January 29, 2010. There are at most 327 CDS issues referencing Japanese corporations in the sense that at least one middle spread of a bid and an offer exists during the period.

The spread distributions of Japanese corporate CDS are skewed and heavy-tailed. Since the histograms are too skewed to show an overall view, Fig. 4.13 shows only approximately the left-most 10% of the total bins along the horizontal axis. Nevertheless, the histograms are significantly skewed and heavy-tailed at each point in time.

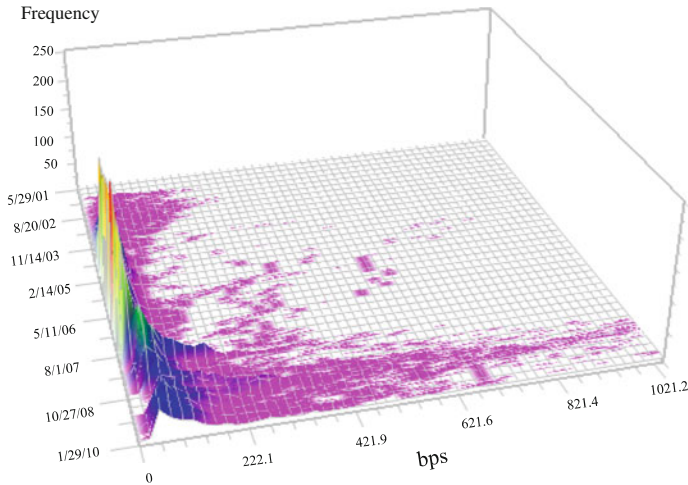


**Fig. 4.13** Histograms of Japanese corporate CDS spreads for approximately the left-most 10% of the total range. The SCDS spread in bps (from *left to right*), the time (from *upper rear to lower front*), and the number of observations (*vertical scale*). *Source* Bloomberg LP, and Tanokura et al. (2012)

For the practical reason that the CDS spreads where the referencing corporations have the same credit rating often co-move, we assume that a CDS spread follows a distribution specific to the rating to which the reference entity belongs. Rating data provided by the major rating agencies in Japan, i.e., R&I, JCR, Moody's, and Standard & Poor's, are used. Since the ratings across agencies in similar categories, such as AAA and Aaa, can be regarded to be practically the same, we uniquely define four rating classes, i.e., [AAA+AA], [A], [BBB], and [Lower than BBB], as shown in Table 4.4. Moreover, by determining the rating prioritization of the agencies as shown in the bottom row of Table 4.4, which is usually recognized in the Japanese market, one available rating class including that of the parent company, is assigned to each referencing corporation. Note that some CDS contracts may have certain periods with no ratings and that the rating class of a referencing corporation varies over time. For each rating class, the number of observations varies over time and becomes zero on certain trading days, as shown in Fig. 4.14. The largest, second largest, third largest, and smallest average proportions of the number of observations are 46.5% for class [A], 36.4% for class [AAA+AA], 15.6% for class [BBB], and 1.5% for class [Lower than BBB] (which is less than 10 observations), respectively.

Major corporations are included in each rating class. Class [AAA+AA] includes Toyota Motor Corp., NTT, and major utility companies such as Tokyo Electric Power Co. A general construction company, the Obayashi Corp., is included in class [A]. All Nippon Airways Co. in the air transportation industry belongs to class [BBB]. However, Japan Airlines Intl. Corp. in the same industry was revised downward from class [BBB] to class [Lower than BBB] on September 13, 2005. The other examples

**Table 4.4** Four rating classes based on major agency ratings and the rating prioritization

	R & I	JCR	Moody's	Standard & Poor's
[AAA+AA]	AAA AA+, AA, AA-	AAA AA+, AA, AA-	Aaa Aa1, Aa2, Aa3	AAA AA+, AA, AA-
[A]	A+, A, A-	A+, A, A-	A1, A2, A3	A+, A, A-
[BBB]	BBB+, BBB, BBB-	BBB+, BBB, BBB-	Baa1, Baa2, Baa3	BBB+, BBB, BBB-
[Lower than BBB]	BB+, BB, BB- B+, B, B- CCC+, CCC, CCC- CC, D	BB+, BB, BB- B+, B, B- CCC CC, C, D	Ba1, Ba2, Ba3 B1, B2, B3 Caa1, Caa2, Caa3 Ca, C	BB+, BB, BB- B+, B, B- CCC+, CCC, CCC- CC, R, SD, D
Rating prioritization	1	2	3	4

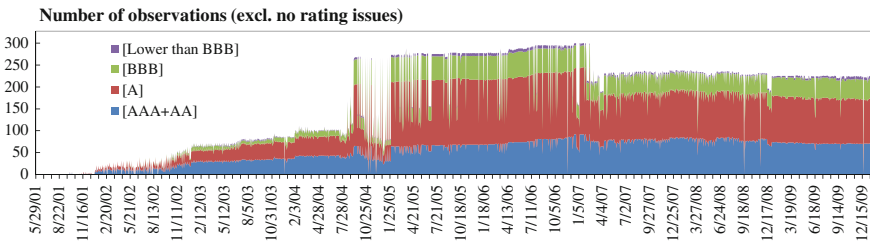


**Fig. 4.14** Breakdown of the number of spread observations by rating class (excluding the issues when they are not rated)

that should be mentioned, are the corporations which were often revised. Softbank Corp. in the information and communication industry was revised downward from class [BBB] to class [Lower than BBB] on November 30, 2001 and then was revised upward to class [BBB] on March 29, 2002. Another financial business company, AIFUL Corp., which drew attention due to its debt problem, was revised downward from class [A] to class [BBB] on January 30, 2009 and was again revised downward to class [Lower than BBB] on December 24, 2009. Moreover, the International Swaps and Derivatives Association (ISDA) announced the occurrence of a credit event at AIFUL Corp. at the end of 2009.

### 4.2.2 Japanese CDS Rating-Based Distribution-Free Index Construction

As mentioned in Chap. 2, Tanokura et al. (2012) applied a trend component model with Gaussian or Cauchy observation noises, namely, the Gaussian or the Cauchy trend estimation models (2.51) to Japanese corporate CDS spreads. As a further

improvement of the trend estimation, this book proposes a trend component model with Gaussian observation noises with a time-varying variance, namely, the GTV trend estimation model (2.52). Let us compare the three types of trend estimation model. Here, the trend order is set to one. For each type, we calculate  $AIC_\lambda^0$  in (2.61) by changing the parameter  $\lambda$  of the Box-Cox transformation (2.47) in Chap. 2 (Box and Cox 1964), for each rating class. Table 4.5 shows  $AIC_\lambda^0$  for major  $\lambda$ s of three types of trend estimation model for each rating class. Note that for each rating class,  $AIC_\lambda^0$  of the Cauchy trend estimation model is significantly smaller than that of the Gaussian trend estimation model for all  $\lambda$ . This implies the importance of the tails of the spread distributions of the Japanese corporate CDS.

For class [AAA+AA] in the leftmost panel of Table 4.5,  $AIC_\lambda^0$  becomes better in order of the Gauss, Cauchy, and GTV trend estimation models for all  $\lambda$ . On the other hand, for class [BBB] in the middle panel,  $AIC_\lambda^0$  becomes better in order of the Gauss, GTV, and Cauchy trend estimation models for all  $\lambda$ . For classes [A] and [Lower than BBB], the trend estimation model that obtains the minimum  $AIC_\lambda^0$  varies over  $\lambda$ .

Generally, the AIC is a relative measure of goodness of fit, and not an absolute measure, that expresses the discrepancy between the model describing a fluctuating phenomenon in question and observations, which is a realization of the model. Therefore, the reasonable model for the phenomenon to be analyzed should be carefully determined.

In the rightmost panel of Table 4.5 showing the total of  $AIC_\lambda^0$  for each  $\lambda$ , the minimum of  $AIC_\lambda^0$  is the Cauchy trend estimation model for  $\lambda = -0.5$ . This Box-Cox transformation is a reciprocal root square when the constant terms are ignored.

Let us compare the estimations of the Cauchy and GTV trend estimation models for  $\lambda = -0.5$ . As an example, Fig. 4.15 shows the estimated result of the Cauchy trend estimation model (top) and that of the GTV trend estimation model (bottom) for class [AAA+AA]. For both types of trend estimation model, although the frequent oscillation of the spread fluctuations and the short-term fluctuation of the number of observations yield diversified residual terms, the residual term of the GTV trend estimation model becomes smaller than that of the Cauchy trend estimation model. The estimation of the GTV trend estimation model is smoother than that of the Cauchy trend estimation model for the relatively long absence of the observations at the beginning of the analysis period.

Here, the optimal  $\lambda = -0.5$  of the Cauchy trend estimation model for all rating classes is determined and the trend estimation is performed by the sequential Monte Carlo filter presented in Chap. 2 (Kitagawa 2010; Kitagawa and Gersch 1996; Doucet et al. 2001).

Then, each CDS rating-based distribution-free index is obtained by the inverse Box-Cox transformation of the optimal trend (2.62). For example, Fig. 4.16 shows the CDS rating-based distribution-free index for class [AAA+AA] ([AAA+AA] index) with the CDS spread distributions for the entire period (top) and detailed periods of interest (bottom). The month-end data are shown for simplicity. The [AAA+AA] index (blue line) is mostly located close to the 50 percentile (red dotted line), and significantly heavy upside tails after the Lehman shock in the fall of 2008 reflect the

**Table 4.5**  $AIC_{\lambda}^0$  for major  $\lambda$ s of the Gauss, Cauchy, and GTV trend estimation models for four rating classes, and the total of  $AIC_{\lambda}^0$

$\lambda$	[AAA+AA]			[A]			[BBB]			[Lower than BBB]			Total		
	Gauss	Cauchy	GTV	Gauss	Cauchy	GTV	Gauss	Cauchy	GTV	Gauss	Cauchy	GTV	Gauss	Cauchy	GTV
1	12,657	9,976	8,843	17,287	13,049	14,056	23,805	18,129	20,412	28,421	26,115	25,104	82,170	67,270	68,415
0.5	9,512	6,584	5,904	11,974	8,523	8,050	15,841	10,676	10,717	22,608	18,616	18,212	59,935	44,398	42,883
0	8,179	4,908	4,587	10,503	7,040	6,954	13,759	8,644	9,235	20,432	14,499	16,854	52,873	35,092	37,629
-0.5	7,853	4,447	4,216	10,229	6,797	6,933	13,002	8,157	8,865	19,683	13,935	16,205	50,768	33,336	36,219
-1	8,226	4,725	4,639	10,740	7,017	7,662	13,350	8,110	10,342	20,039	15,170	17,182	52,354	35,023	39,825

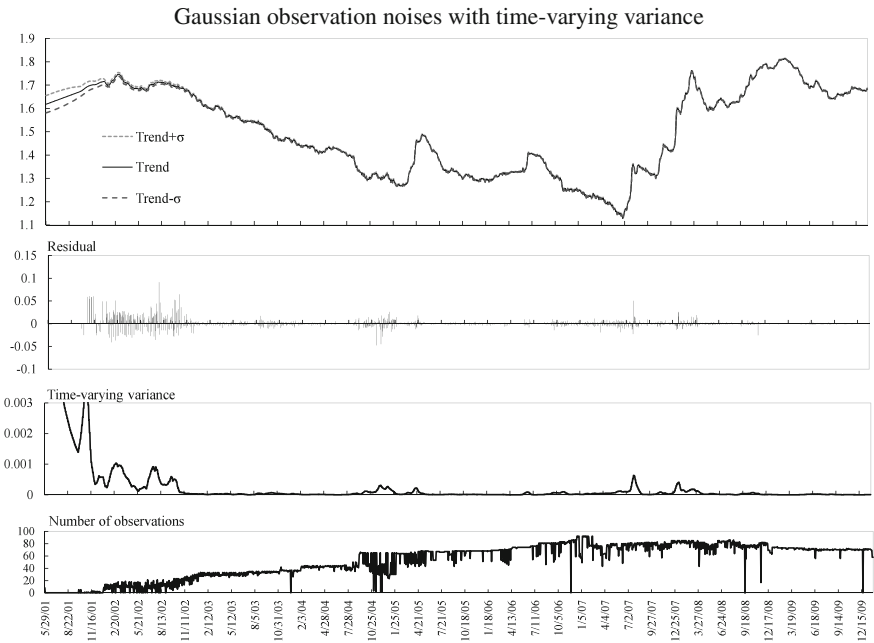
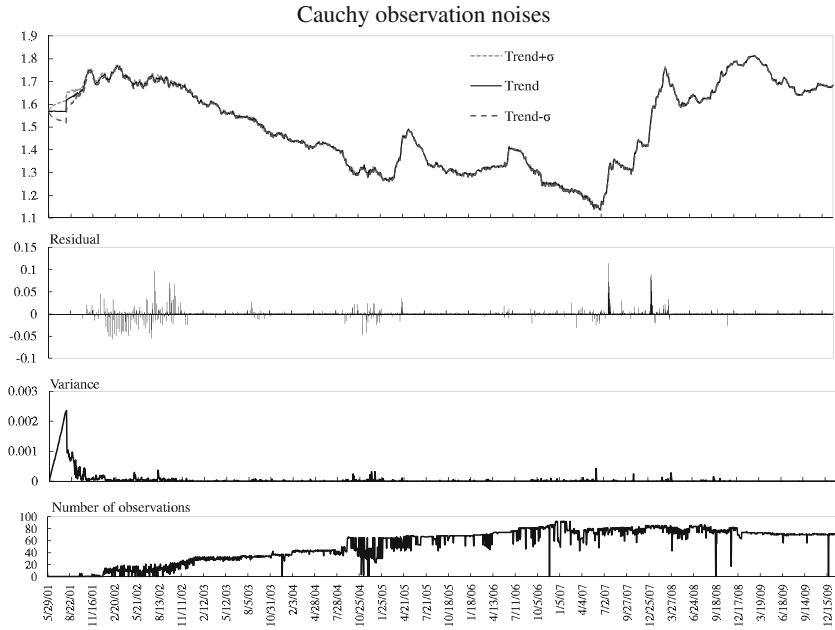


**Fig. 4.15** Visualized characteristics of the optimal trend for class [AAA+AA]. *Top* trend estimation model with Cauchy observation noises (*source* Tanokura et al. 2012), *bottom* trend estimation model with Gaussian observation noises with time-varying variance. The estimated trend, the residual term, the time-varying variance, and the number of observations are shown in each panel from top to bottom

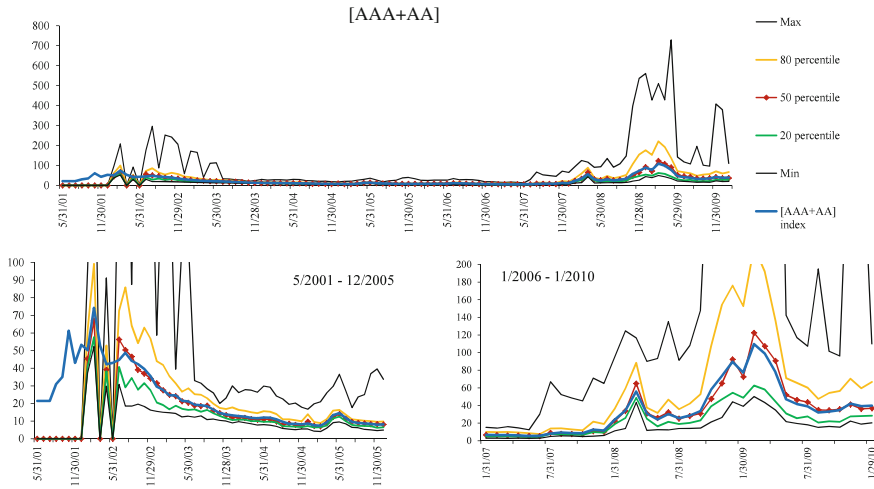


**Fig. 4.16** [AAA+AA] index (blue line) with the CDS spread distributions for the entire period (top) and detailed periods of interest (bottom) for class [AAA+AA]

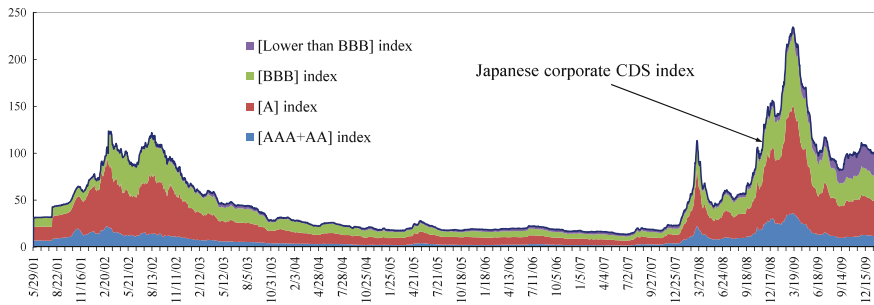


**Fig. 4.17** Japanese corporate CDS distribution-free index defined as the aggregated four CDS rating-based distribution-free indices with the rating weights

scale of the global financial crisis. As a whole, the CDS rating-based distribution-free index for each rating class is positioned appropriately.

In order to provide an overview of the Japanese corporate credit risk based on the four CDS rating-based distribution-free indices, we construct a composite index in a rating-weighted form, namely, the Japanese corporate CDS distribution-free index, which is defined as the aggregated value of the CDS rating-based distribution-free index multiplied by the rating weight proportional to the number of entities included, as shown in Fig. 4.17. Note that the rating weights are not based on the existence of their spreads but based on the rating information on the reference entities of the CDS issues, as the missing observations are interpolated.

Figure 4.18 shows the Japanese corporate CDS distribution-free index and the four CDS rating-based distribution-free indices. Comparison of the levels of four CDS rating-based distribution-free indices reveals that as the credit risk increases, the

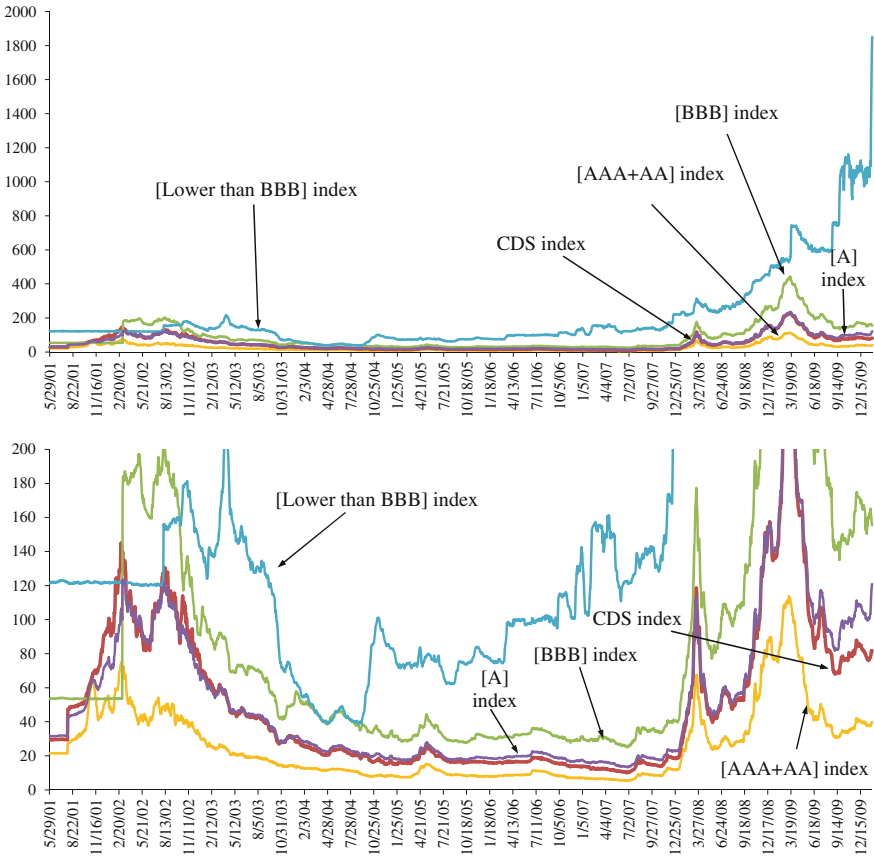


**Fig. 4.18** Japanese corporate CDS distribution-free index (red line) and four CDS rating-based distribution-free indices: overall view (top) and close-up view (bottom)

index increases. The CDS rating-based distribution-free indices are well balanced, reflecting the market views on the credit risk of the CDS entities concerned. The Japanese corporate CDS distribution-free index (red line) is generally located near the [A] index (purple line) in a balanced manner. The upside tails of the distributions have been distorted since the disclosure of the US subprime problem in mid-2007 until the cooling the global financial crisis in mid-2009 for all indices. However, the stand-alone steep appreciation of the [Lower than BBB] index since then, reflects the credit risk specific to this lowest rating class.

### 4.2.3 Causation Between Japanese Financial Markets

In order to investigate the effectiveness of the Japanese corporate CDS distribution-free index based on four CDS rating-based distribution-free indices, we examine

the influence of the US subprime crisis on the Japanese domestic markets by the power contribution analysis (Akaike 1968; Tanokura and Kitagawa 2004), presented in Chap. 3.

As the Japanese domestic market indices, the TOPIX (TPX) for the equity market, the Nomura-BPI overall index (BPI) for the fixed income market, the JPYUSD: Japanese yen exchange rate against US dollar (JPUS), and the Japanese corporate CDS distribution-free index (CDS) are analyzed. TPX, BPI, and JPUS are provided by Bloomberg LP.

The analysis focuses on the following two periods: the pre-subprime period from February 1, 2005 to June 29, 2007 (595 trading days) and the post-subprime period from July 2, 2007 to January 29, 2010 (630 trading days). Similar to the previous section, in each period, the detrended cyclical component series from each index are extracted by Web DECOMP based on the seasonal adjustment model (Gersch and Kitagawa 1983; Kitagawa and Gersch 1984), reviewed in Chap. 2. As

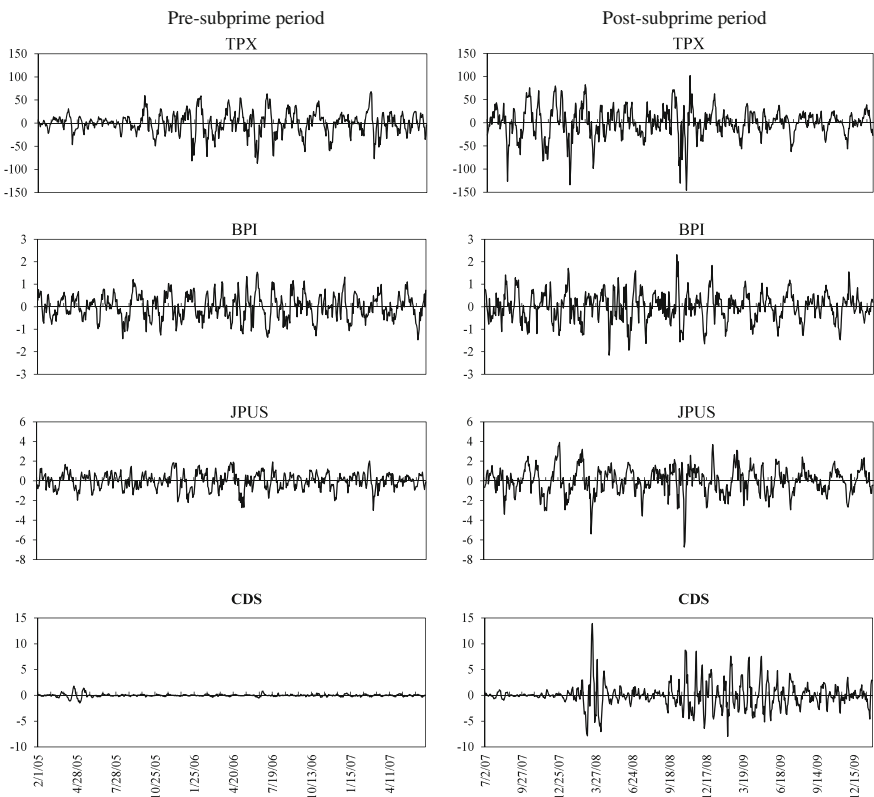


**Fig. 4.19** Detrended cyclical components of the TOPIX (TPX), the Nomura-BPI index (BPI), the JPYUSD foreign exchange rate (JPUS), and the Japanese corporate CDS distribution-free index (CDS) for the pre-subprime (*left*) and post-subprime (*right*) periods. *Source* Tanokura et al. (2012)

**Table 4.6** Variances (*diagonal*), covariances (*upper off-diagonal*), and correlation coefficients (*lower off-diagonal*) of the noises for the pre-subprime (*top*) and post-subprime (*bottom*) periods

Pre-subprime	TPX	BPI	JPUS	CDS
TPX	213.2400	-1.8910	1.0095	0.0421
BPI	-0.368	0.1241	-0.0273	-0.0028
JPUS	0.125	-0.139	0.3083	0.0006
CDS	0.021	-0.056	0.008	0.0194
Post-subprime	TPX	BPI	JPUS	CDS
TPX	367.6600	-3.9471	9.2850	-8.5279
BPI	-0.480	0.1837	-0.1367	0.0916
JPUS	0.575	-0.379	0.7093	-0.2154
CDS	-0.320	0.154	-0.184	1.9374

Source Tanokura et al. (2012)

shown in Fig. 4.19, all four detrended cyclical component series became volatile after the crisis.

A multivariate AR model is separately fitted to the four detrended index series for the pre- and post-subprime periods. As shown in Table 4.6, which shows the variances (diagonal), covariances (upper off-diagonal), and correlations (lower off-diagonal) of the noises for both periods, all variances, covariances, and correlations became significantly larger in size and their tendencies strengthened after the occurrence of the crisis. In particular, the correlation coefficients of CDS with the other three indices, which were extremely small for the pre-subprime period, increased dramatically for the post-subprime period.

Figure 4.20 shows the power spectrum for each detrended index for the pre-subprime (dashed line) and post-subprime (solid line) periods. Compared with the case of the pre-subprime period, the power spectrum for the post-subprime period significantly increased for each index, especially for CDS, and the peaks of the power spectrum became sharpened and strengthened at the lower frequency domain.

By calculating the generalized power contributions (%) (3.13), the influential components of the power spectrum for each index are investigated. As shown in the graph matrix of Fig. 4.21, in each graph, each power spectrum is decomposed into ten terms consisting of four independent noises and six correlated noises. Although the index combinations of the correlated noise for the pre-subprime period are not always consistent with those for the post-subprime period, the components of ALL (orange area), ALL-CDS (light green area), and TPX+BPI (light pink area) are common to both periods. For all indices, the contribution of each index, which largely occupied the index itself for the pre-subprime period, decreased for the post-subprime period. Moreover, the contribution of CDS to the other indices increased for the post-subprime period, especially in the specific frequency domain around 0.05 (approximately 20-day cycle of fluctuation).

Recall (3.12) in Chap. 3, i.e., the power spectrum of the  $r$ th component  $y_n(r)$  of the  $l$ -dimensional stationary time series  $y_n$  at frequency  $f$  was expressed as

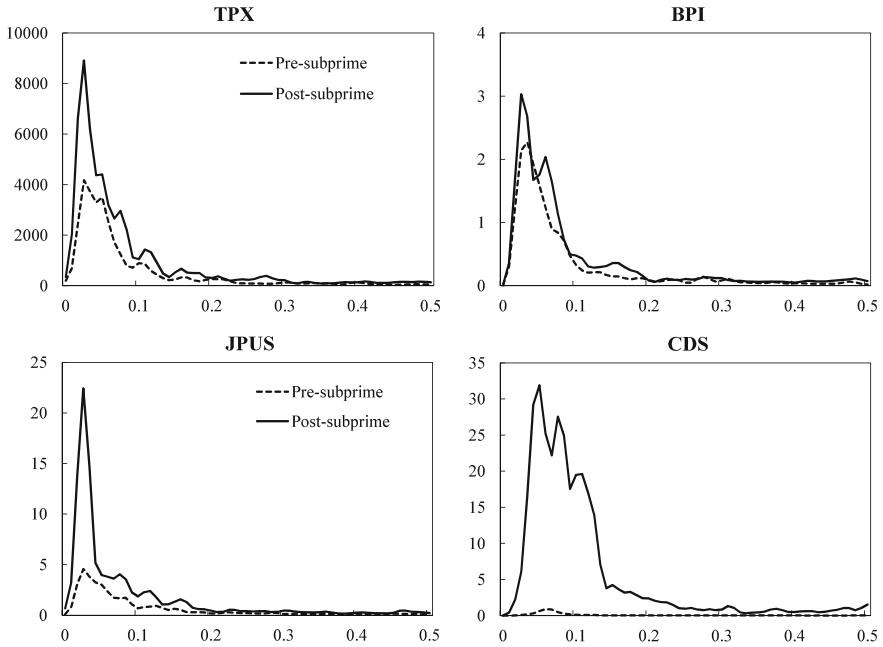


**Fig. 4.20** Power spectrum of each detrended index for the pre-subprime (*dashed line*) and post-subprime (*solid line*) periods. *Source* Tanokura et al. (2012)

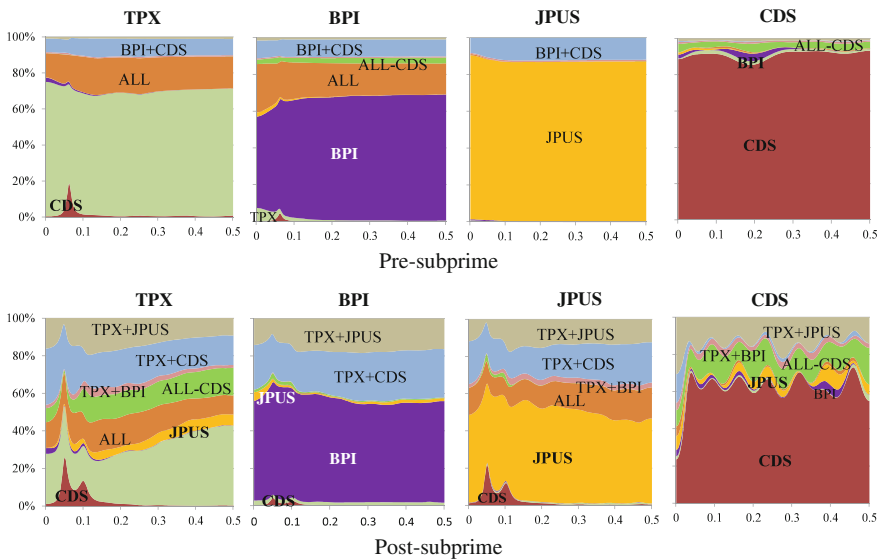


**Fig. 4.21** Power contributions (%) for the pre-subprime (*top*) and post-subprime (*bottom*) periods. *Source* Tanokura et al. (2012)

$$P_{rr}(f) = \sum_{k=0}^{l-2} \sum_{j=1}^{k+1} q_{l-(k+1)+j,j} \sum_{h=1, h \neq r}^l \sum_{n=1, n \neq r}^l c_{rjk}(h)c_{rjk}(n)^* + \sum_{j=1}^l q_{jj}|b_{rj}(f)|^2.$$

The former term expresses  $l(l-1)/2$  correlated noises resulting from correlations between  $l$  noise components and the latter term expresses  $l$  independent noises resulting from single noise components.

Here, let  $P_f(I_i, I_j)$  denote the noise influence of index  $I_i$  on index  $I_j$ , and  $K_i$  denote  $l(l-1)/2$  combinations of indices consisting of a correlated noise, for example,  $I_1 + I_2$  and  $I_2 + I_3$ . Then, the power spectrum of an index  $I_r$  at frequency  $f$  is rewritten as

$$P_{rr}(f) = \sum_{i=1}^{l(l-1)/2} P_f(K_i, I_r) + \sum_{j=1}^l P_f(I_j, I_r).$$

The expression of the former correlated noise and that of the latter independent noise are replaced with  $P_f(K_i, I_r)$ ,  $i = 1, \dots, l(l-1)/2$ , and  $P_f(I_j, I_r)$ ,  $j = 1, \dots, l$ , respectively. Therefore, the generalized power contribution of the correlated noise and the independent noise to an index  $I_r$  are expressed as

$$C_f(K_i, I_r) = \sum_{i=1}^{l(l-1)/2} P_f(K_i, I_r)/P_{rr}(f) \quad \text{and} \quad C_f(I_j, I_r) = \sum_{j=1}^l P_f(I_j, I_r)/P_{rr}(f),$$

respectively.

In order to effectively summarize the results of the power contribution analysis, we score the indices in terms of power contribution. In other words, we allocate the amount of the power contribution to each contributing index. Since the power contribution of the correlated noise is a many-to-one causation, we consider allocating the amount of power contribution to each concerned contributing index evenly. For example, in the case of power contribution  $C_f(I_i + I_j, I_r)$ , half of  $C_f(I_i + I_j, I_r)$  is assigned to  $I_i$  as  $C_f(I_i, I_r)$  and half is assigned to  $I_j$  as  $C_f(I_j, I_r)$ . On the other hand, since the power contribution of the independent noise is a one-to-one causation, the power contribution  $C_f(I_j, I_r)$  is simply assigned to the contributing index  $I_j$  as  $C_f(I_j, I_r)$ .

In this way, all power contributions are assigned to concerned contributing indices. Then, the sum of the assigned contribution,  $C_f(I_i, I_r)$ , expresses the contributing score of index  $I_i$  to index  $I_r$  at frequency  $f$ . The total contribution  $C(I_i, I_r)$  to an index  $I_r$  is the aggregated contributing score over all frequencies. Finally,  $l \times l$  total contributions  $C(I_i, I_j)$ ,  $i, j = 1, \dots, l$ , are obtained.

Note that the two total contributions  $C(I_i, I_j)$  and  $C(I_j, I_i)$  between  $I_i$  and  $I_j$ , which measure the degree of contributions from  $I_i$  to  $I_j$  and the degree of contributions from  $I_j$  to  $I_i$ , respectively, are not always the same.

Table 4.7 shows the total contributions (%) for the pre-subprime and post-subprime periods, and the ratio of the total contribution for the post-subprime period

**Table 4.7** Total contributions (%) for pre-subprime and post-subprime periods, and the ratio of the total contribution for the post-subprime to pre-subprime periods

Pre-subprime	TPX	BPI	JPUS	CDS	Post-subprime	TPX	BPI	JPUS	CDS	Post/pre	TPX	BPI	JPUS	CDS
TPX	73.7	7.5	1.0	3.1	TPX	54.0	23.4	21.3	14.8	TPX	0.7	3.1	21.7	4.8
BPI	10.5	76.1	6.9	3.7	BPI	8.7	49.9	5.0	7.3	BPI	0.8	0.7	0.7	2.0
JPUS	5.1	6.5	85.8	2.2	JPUS	19.7	12.1	58.4	15.4	JPUS	3.8	1.9	0.7	6.9
CDS	10.6	9.9	6.4	91.0	CDS	17.5	14.6	15.3	62.5	CDS	1.7	1.5	2.4	0.7
Total	100.0	100.0	100.0	100.0	Total	100.0	100.0	100.0	100.0					

to that for the pre-subprime period. For the pre-subprime period,  $C(\text{CDS}, \text{TPX}) = 10.6\%$  and  $C(\text{TPX}, \text{CDS}) = 3.1\%$ . For the post-subprime period,  $C(\text{CDS}, \text{TPX})$  increased to  $17.5\%$  and  $C(\text{TPX}, \text{CDS})$  increased to  $14.8\%$ . Therefore, as shown in the right panel, the contribution of CDS to TPX increased 1.7-fold, and the total contribution of TPX to CDS increased 4.8-fold. Similarly, the total contribution of CDS, to BPI and JPUS increased 1.5-fold and 2.4-fold, respectively, while the total contributions of BPI and JPUS, to CDS increased 2.0-fold and 6.9-fold, respectively. Since the total contributions to the other indices were relatively weak, CDS (Japanese corporate CDS distribution-free index) can be considered as highly sensitive to the fluctuations caused by the other domestic indices, even though the total contributions from the other indices shown in the left and middle panel, were relatively small.

The total contribution of TPX to JPUS significantly increased 21.7-fold, whereas the total contribution of JPUS to TPX was 3.8-fold. On the other hand, the total contribution of BPI to all indices decreased, except for that to CDS which increased from 3.7 to 7.3%. Note that the fluctuation of BPI (fixed income), became less likely to reflect fluctuations of TPX (equity), and JPUS (foreign exchange rate). Moreover, the total contribution from an index to the index itself weakened by a factor of 0.7 for every index.

After the disclosure of the US subprime crisis, the Japanese domestic markets became influential with respect to each other and the Japanese corporate CDS distribution-free index we constructed, can be an indicator of Japanese corporate credit risk, fully reflecting the fluctuations of the Japanese financial markets.

### 4.3 Other Applications: Usability of the Distribution-Free Index

In order to examine the usability of a distribution-free index, in this section, we provide two applications. First, we construct GDP growth regional distribution-free indices using the real GDP growth data of 63 countries. The clear polarization in the form of developed regions versus emerging regions in terms of GDP growth regional distribution-free indices, is detected. Moreover, as the relation between the GDP growth regional distribution-free index and the SCDS regional distribution-free index constructed in Sect. 4.1, strengthened during the period of the global economic crisis, estimating the economic growth after carefully examining sovereign risks becomes indispensable in economic policy decision making. Second, we construct the Japanese SCDS distribution-free index using SCDS curves referencing Japan, consisting of the spreads of 11 kinds of maturities. The Japanese SCDS distribution-free index can be regarded as an underlying SCDS spread level, reflecting a domestic credit strength, and is usable for pricing.

### 4.3.1 *Constructing a GDP Growth Regional Distribution-Free Index*

The financial crisis triggered by the US subprime loan crisis in 2007 eventually led to a global economic crisis that affected simultaneously not only emerging countries but also developed countries all over the world. Due to the increasing globalization of the world economy, countries have become more exposed to cross-border economic risks. Moreover, observing a global trend of the world economy becomes significantly important because an economic crisis of a country often spills over to economies of other countries starting with neighbor countries to even distant countries. The European debt crisis can be cited as an example.

As estimating the economic growth for a country plays an important role in economic policy decision making and managing investment strategy, it is crucial to determine the current state of the economy of the country. However, this is not easy because there is usually some lag, e.g., a few months, between events and the official announcement of economic figures. Therefore, it is necessary to make the fullest possible use of available information on the economy. As such, we consider using a statistical method effectively.

We focus on the quarterly year-on-year growth rate (%) data of the real GDP of 63 countries, provided by CEIC, for the period from the first quarter of 1996 to the second quarter of 2012. As shown in Fig. 4.22, the number of observations gradually increases because there were some countries with no available official data for the early period of analysis. On the other hand, in June 2012, which is the end of the analysis period, there were only 30 observations available at that time due to the lag of the announcement. It is necessary to make the fullest possible use of the observations.

Here, we classify the countries into eight regions and the United States, as shown in Table 4.8, which is similar to the classification in Table 4.1 for comparison. The \* symbol indicates that a country belongs to advanced economies, whereas other countries belong to emerging and developing economies, according to the IMF country classification. The region, e.g., Northern, Western, Southern Europe, or Developed

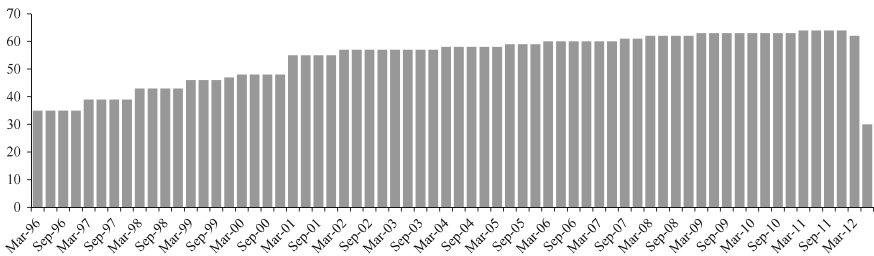


**Fig. 4.22** Number of countries with available real GDP growth observations

**Table 4.8** Regional classification of 63 countries

Region (no. of countries)	Country
Northern Europe (6)	Denmark*, Finland*, Ireland*, Norway*, Sweden*, UK*
Western Europe (6)	Austria*, Belgium*, France*, Germany*, Netherlands*, Switzerland*
Southern Europe (5)	Greece*, Italy*, Malta*, Portugal*, Spain*
Eastern Europe (16)	Bulgaria, Croatia, Czech*, Estonia*, Hungary, Kazakhstan, Latvia*, Lithuania*, Poland, Romania, Russia, Serbia, Slovakia*, Slovenia*, Turkey, Ukraine
Middle East/Africa (7)	Bahrain, Egypt, Israel*, Saudi Arabia, South Africa, Tunisia
Developed Pacific (4)	Australia*, Hong Kong*, Japan*, New Zealand*
Emerging Asia (9)	China, India, Indonesia, Korea*, Malaysia, Philippines, Singapore*, Taiwan*, Thailand
Latin America (9)	Argentina, Brazil, Chile, Colombia, Ecuador, Mexico, Panama, Peru, Venezuela
–	USA*

The \* symbol indicates an advanced economy, whereas other countries are emerging and developing economies, according to the IMF country classification

Pacific, consists of countries in advanced economies, whereas countries in Latin America belong to emerging and developing economies.

Figure 4.23 shows the time series of the GDP growth histograms. The histogram at March 1996 is at the rear and that at June 2012 is at the front. The range of the GDP growth covers from  $-25$  to  $37\%$  as a whole. We highlight the countries, or regions to which most of the countries belong, conspicuously in the tails of the distributions (yellow circle). The highlighted Emerging Asia in the lower tail of the distributions around 1998 reflects the influence of the Asian financial crisis in 1997. Similarly, the influence of the Latin American crisis triggered by the excessive debt of Argentina in 2001 can be found in the highlighted Latin America in 2002. The sharply twisted distribution in the first half of 2009 clearly reflects the magnitude of the impact of the global economic crisis. The highlighted Eastern Europe in the lower tail in 2009 indicates that this region was economically devastated by the crisis. Moreover, the existence of Greece in the lower tails around 2011 to 2012 is due to the debt crisis of the country. Thus, the influences of the financial crises on the regional economy, including the concerned country, cannot be ignored.

Let us consider the distributions of real GDP growth by region. In order to emphasize the twisting of the distribution, Fig. 4.24 shows an overhead view of the histograms of real GDP growth for Latin America in the top panel and that for Southern Europe in the bottom panel. Both distributions exhibit a similar transition, whereas the distribution for Southern Europe is tighter than that for Latin America as a whole.

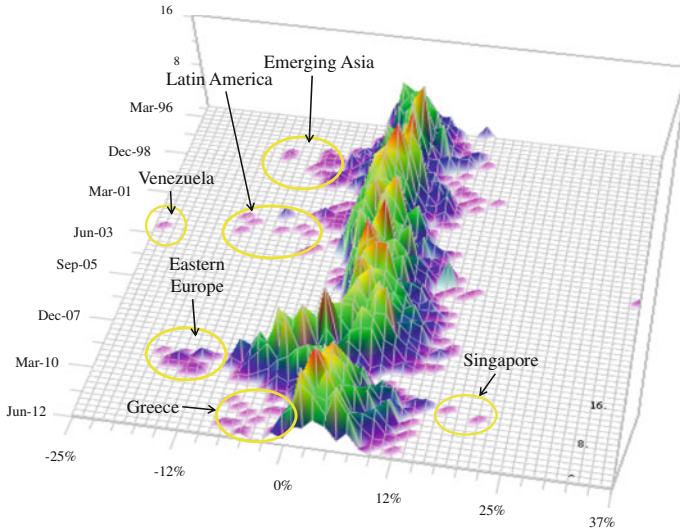


**Fig. 4.23** Real GDP growth (%) histograms of 63 countries. The real GDP growth (from left to right), the time (from upper rear to lower front), and the number of observations (vertical scale). Conspicuous countries or regions in the tails of the distributions are highlighted (yellow circle). Source CEIC

However, as shown in Table 4.8, the countries in Southern Europe are all advanced economies and those in Latin America are all emerging and developing economies.

Recall that the method for constructing a distribution-free index presented in Chap. 2 can be used for examining the observation distribution. Since the Box-Cox transformation (2.47) (Box and Cox 1964) is applied to positive values of observation, the real GDP growth data ranging from negative to positive are not directly applicable. Therefore, we first transform the observations to be in a positive domain by the following distribution invariant function.

Let  $g_i(n)$ ,  $i = 1, \dots, j(n)$ , denote the real GDP growth of a country  $i$  in a region at time  $n$ , where  $j(n)$  denotes the number of country observations in the region at time  $n$  and  $n = 1, \dots, N$ . We transform  $g_i(n)$  to a positive domain by the following parallel shift:

$$p_i(n) = g_i(n) + C, \tag{4.1}$$

where  $C$  is an appropriate constant such that  $C > \min_i(g_i(n))$  for  $n = 1, \dots, N$ . Then, the Box-Cox transformation can be applied to  $p_i(n)$ . Note that the GDP growth regional distribution-free index is eventually defined by the inverse of the distribution invariant function (4.1) of the inverse Box-Cox transformed values of the optimal trend.

Next, we search for the optimal  $\lambda$  of the Box-Cox transformation for  $p_i(n)$ . From Table 4.9, which shows  $AIC_{\lambda}^0$  for major  $\lambda$ s by region including all countries (All),

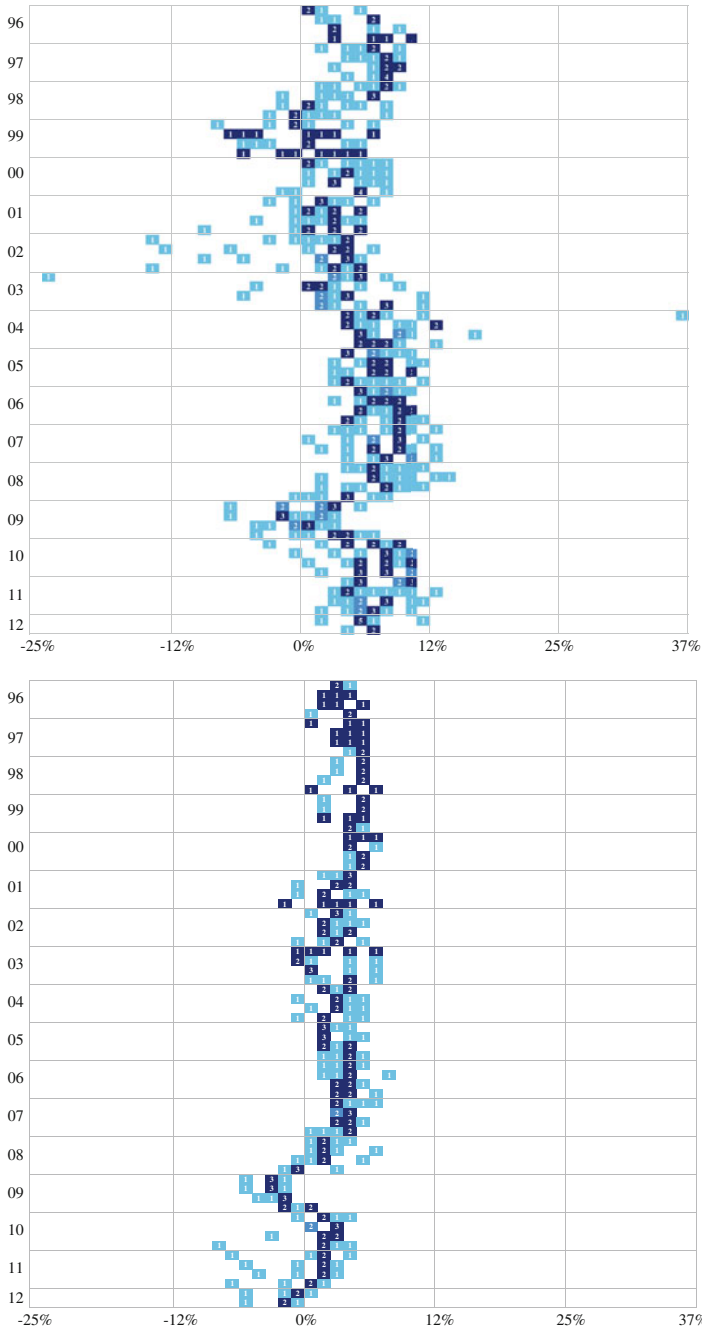


**Fig. 4.24** Overhead view of GDP growth histograms for Latin America (*top*) and Southern Europe (*bottom*). The numbers in the cells indicate the number of countries

**Table 4.9**  $AIC_{\lambda}^0$  for major  $\lambda$ s by region

$\lambda$	All	North. Europe	West. Europe	South. Europe	East. Europe	Developed Pacific	Emerging Asia	Mid. East/Africa	Latin America
1	298	304	251	262	406	329	445	285	363
0.5	214	229	184	205	285	248	301	217	273
0	225	232	185	209	299	252	306	216	307
-0.5	262	241	197	214	325	258	322	219	413
-1	366	253	205	225	359	268	339	231	606

the minimum  $AIC_{\lambda}^0$  are at  $\lambda = 0.5$  for all regions, excluding Middle East/Africa. However,  $AIC_{\lambda}^0$  at  $\lambda = 0.5$  for Middle East/Africa is the second minimum with a small difference from the first minimum. Therefore, for all nine regions, we determine the optimal  $\lambda = 0.5$ , which is a square transformation when the constant term is ignored. Based on these results, the distribution of observations is similar for each region. Therefore, we assume that the real GDP growth of a country follows the distribution specific to the region and construct a GDP growth regional distribution-free index.

Then, the optimal trend for each region is estimated. For example, the estimated trend for Southern Europe is shown in Fig. 4.25. The figure shows, from top to bottom, the estimated trend with  $\pm\sigma$ , the residual term, the estimated time-varying variance, and the number of observations. Although a relatively large residual term can be found at March 2009 due to the turning point of the trend which can be caused by the global economic crisis, the overall estimation is good. Moreover, it is natural to observe the large swing of the time-varying variance during the period of the crisis.

By the inverse transformation of the distribution invariant function (4.1) of the inverse Box-Cox transformed values of the optimal trend (2.62), we obtain the GDP growth regional distribution-free index for each region. In Fig. 4.26, the relationship between the GDP growth distribution-free index of Southern Europe (SE index: blue line) and the original GDP growth distributions, are shown. The SE index is generally close to the mean (black dotted line). However, the diversified changes of the distribution are flexibly reflected, in particular, since December 2009 just after the disclosure of the deficit problem in Greece. Similarly, other eight GDP growth regional distribution-free indices including that for all countries (All index), are constructed.

Figure 4.27 shows all GDP growth regional distribution-free indices. The vertical lines across the two panels express, from left to right, the revelation of the US subprime crisis, the Lehman shock, and the disclosure of the Greece debt crisis. We categorize the Northern, Western and Southern Europe, and Developed Pacific indices, plus the USA, as the developed regional distribution-free indices, and categorize the other Middle East/Africa, Eastern Europe, Emerging Asia, and Latin America indices, as the emerging regional distribution-free indices. Note that the USA uses the GDP growth observations.

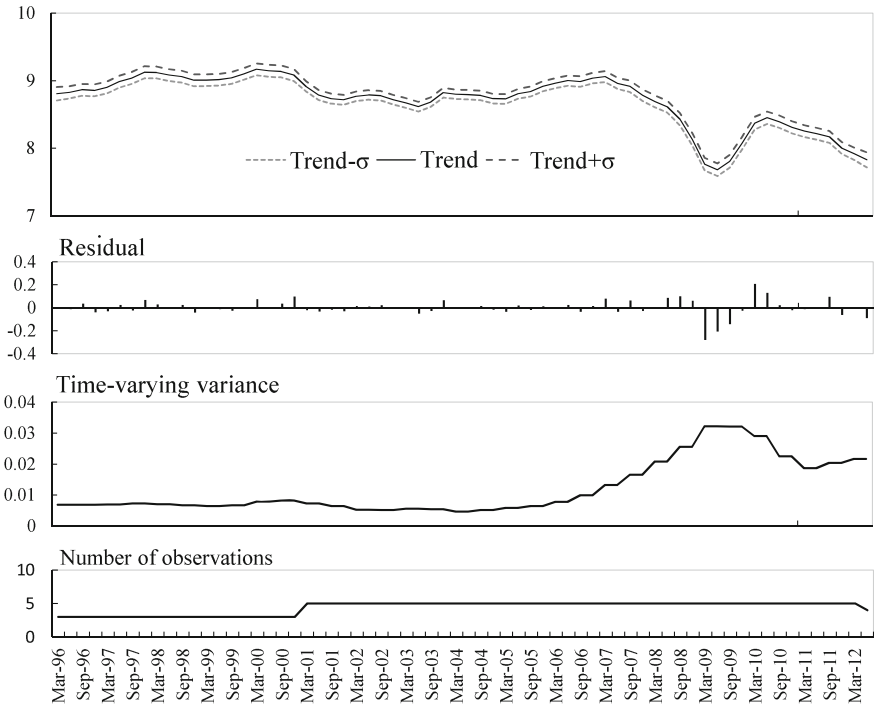


**Fig. 4.25** Visualization of the characteristics of the optimal trend for Southern Europe. The estimated trend, the residual term, the time-varying variance, and the number of observations are shown from top to bottom

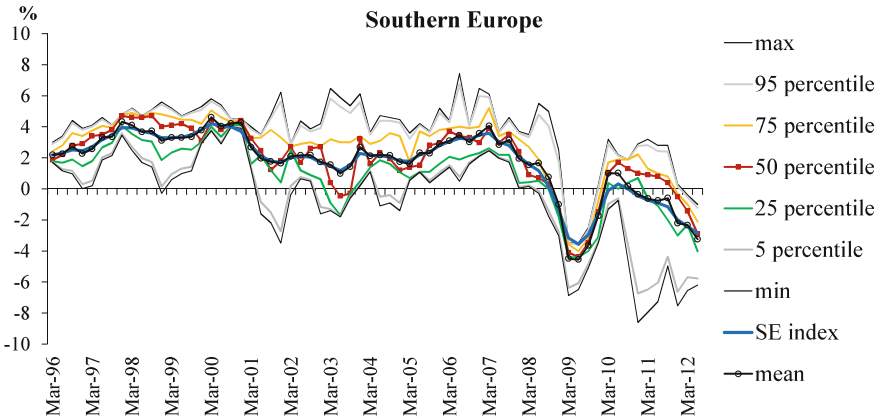


**Fig. 4.26** GDP growth distribution-free index of Southern Europe (SE index) with the distribution of GDP growth

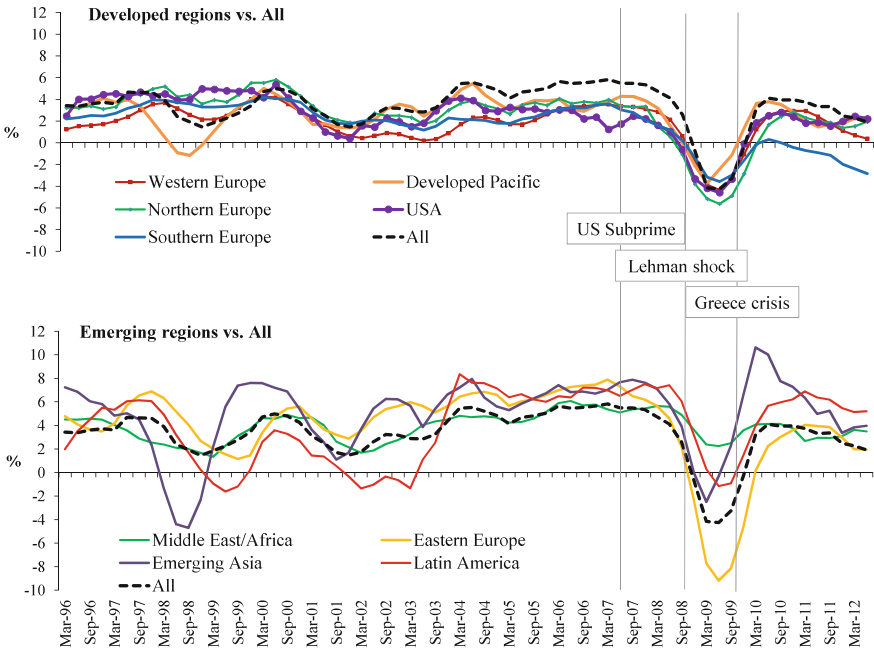


**Fig. 4.27** Developed regional distribution-free indices for the Northern, Western and Southern Europe, and Developed Pacific indices, plus the USA versus the All index (*top*), and emerging regional distribution-free indices for the Middle East/Africa, Eastern Europe, Emerging Asia, and Latin America indices versus the All index (*bottom*). The vertical lines express, from left to right, the revelation of the US subprime crisis, the Lehman shock, and the disclosure of the Greece debt crisis

The top panel compares the developed regional distribution-free indices with the All index. The drop to the minimum level in 1998 of the Developed Pacific index (orange line) reflected the influence of Hong Kong due to the Asian financial crisis. Note that, since 2000, most developed regional distribution-free indices have performed under the All index (black dashed line). In particular, the current lowest downward performance of the Southern Europe index (blue line) can reflect the seriousness of the prolonged Greece debt crisis. The All index, which can be regarded as a global trend of the world economy, has reversed the upward trend from the bottoming out, since June 2010, along with the SE index (blue line).

In the bottom panel of Fig. 4.27, the emerging regional distribution-free indices and the All index are compared. The large magnitudes of the fluctuations of the emerging regional distribution-free indices are quite impressive. The emerging regional distribution-free indices had revolved around the All index (black dashed line) until 2003, and then, they mostly performed better than the All index, except the Eastern Europe index (yellow line) for the period of the global economic crisis from 2008 to 2009.

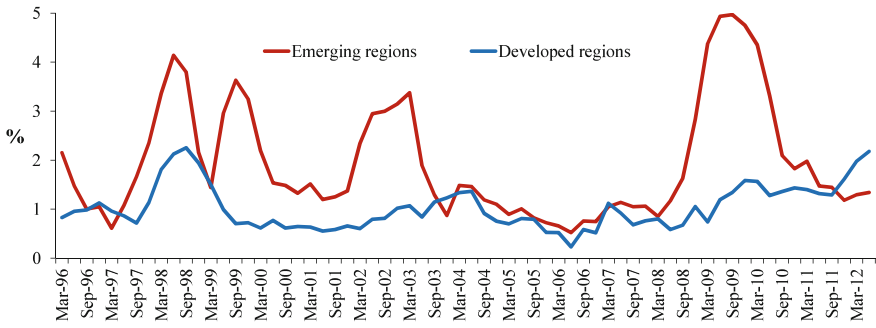


**Fig. 4.28** Time series of standard deviations of the developed and emerging regional distribution-free indices

The clear polarization in the form of developed regional distribution-free indices versus emerging regional distribution-free indices across the All index through the analysis period, is noteworthy. Although this polarization was interrupted by the global economic crisis from 2008 to 2009, it has currently recovered.

Figure 4.28 shows the time series of standard deviations of the developed and emerging regional distribution-free indices. The sharply-widened variations for both developed and emerging regional distribution-free indices were observed in 1998, reflecting the Asian financial crisis. However, since then, the independent peak of variation of emerging regional distribution-free indices (red line) occurred in September 1999, in March 2003, and in September 2009. Whereas, the variation of developed regional distribution-free indices (blue line), which had been relatively smaller than the variation of emerging regional distribution-free indices, exhibited a gradual upward trend during the global economic crisis. The variation of developed regional distribution-free indice largely exceeded the variation of emerging regional distribution-free indices in December 2011, and in June 2012 almost reached the level of its peak in 1998. This implies the significant influence of the prolonged Greece debt crisis on developed regional economies.

Let us observe the relation between a regional economy and a regional sovereign risk. As an indicator of regional sovereign risk, we use the SCDS regional distribution-free index, provided on a quarterly base, which was constructed in Sect. 4.1.

Figure 4.29 shows the GDP growth regional distribution-free (DF) index (red line) and the SCDS regional distribution-free (DF) index (blue line) by region for the period from March 2004 to June 2012.

Although the scale is different by region, for the pre-subprime period from March 2004 to June 2007, no obvious relations between the GDP growth DF index and the SCDS DF index were observed for all regions. Then, during the post-subprime period from September 2007 to September 2009, the bottoming out of the GDP growth DF index occurred at the same quarter as the peak of the SCDS DF index for Developed Pacific, whereas, for other seven regions, the bottoming out of the GDP



**Fig. 4.29** Comparison of the GDP growth distribution-free (DF) index (red) with the SCDS distribution-free (DF) index (blue: RHS) for eight regions

growth DF index occurred one or two quarters later than the peak of the SCDS DF index. For the post-Greece period from December 2009 to June 2011, the relatively stable transition of the SCDS DF index was found for emerging regions, such as Eastern Europe, Emerging Asia, Middle East/Africa, and Latin America, whereas the gradual increase of the SCDS DF index was observed for developed regions, such as Northern and Western Europe, and Developed Pacific, reflecting the steep increase of the SCDS DF index of Southern Europe. On the other hand, the V-shaped regional recovery from the global economic crisis in terms of the GDP growth DF index, turned downward for all regions. Lastly, in the period of crisis contagious phase from September 2011 to June 2012, the fluctuation of the SCDS DF index for emerging regions along with that for Southern Europe, implies the spillover effect from the European debt crisis. On the other hand, the regional economy varied over region. The gradual regional economic recovery in terms of the GDP growth DF index was observed in Developed Pacific and Middle East/Africa, whereas the economic downturn was found in Western, Southern, and Eastern Europe, and Latin America.

We calculate correlations between the GDP growth regional distribution-free index and the SCDS regional distribution-free index by region for the periods of pre-subprime (from March 2004 to June 2007), post-subprime (from September 2007 to September 2009), post-Greece (from December 2009 to June 2011), and contagious phase (from September 2011 to June 2012), as shown in Table 4.10.

Here, we focus on the size of correlation. The region with the size of correlation more than 0.5, which was Western Europe and Latin America for the pre-subprime period, extended across all eight regions for the post-subprime period, which includes the global economic crisis. This implies the serious influence of the crisis on the global economy, which caused soaring sovereign risks. Then, for the post-Greece period, the region with the size of correlation more than 0.5 was only Western Europe including Germany, indicating that the concerns on the European credit uncertainty expanded to this region despite its regional economic recovery. For the period of contagious phase, the region with the size of correlation more than 0.5 was all regions excluding Northern and Western Europe, implying that the influence of the European debt crisis on the regional economies spilled over into even outside of Europe.

Note that the relation between the regional economy and the regional sovereign risk significantly strengthened during the period of the global economic crisis from 2008 to 2009. At that time, since an improvement of the regulatory framework of the financial system and a reconsideration of economic theory were actually required, the economic circumstances have changed substantially since then. In economic policy decision making of a country, it becomes indispensable to estimate the economic growth after carefully examining sovereign risks. Further analysis is left for future study.

Thus, the wider applicable area of the method for constructing a distribution-free index can be expected.

**Table 4.10** Correlation between the GDP growth regional distribution-free index and the SCDS regional distribution-free index for eight regions for the periods of pre-subprime, post-subprime, post-Greece, and contagious phase

	North. Europe	West. Europe	South. Europe	East. Europe	Developed Pacific	Emerging Asia	Mid. East /Africa	Latin America
Pre-subprime	-0.04	-0.73	-0.37	-0.46	0.46	0.02	-0.40	0.57
Post-subprime	-0.82	-0.82	-0.82	-0.74	-0.94	-0.81	-0.55	-0.52
Post-Greece	0.45	0.80	0.04	-0.31	-0.20	-0.03	-0.27	-0.37
Contagious phase	0.18	-0.35	-0.66	0.57	-0.64	0.59	0.63	0.73

### 4.3.2 Constructing a Japanese SCDS Distribution-Free Index Using SCDS Curves

Usually, CDS contracts with various maturities are traded, such as six months, three years, five years, or ten years. Some contracts, like the standard 5-year contract, may be liquid, whereas others may not. As mentioned in the previous section, an SCDS spread can be regarded as a market evaluation of the country’s credit. Therefore, the SCDS curve, which plots SCDS spreads referencing a country at a point in time against maturities, provides a market view on the country’s future credit risk at that time.

Figure 4.30 shows the daily time series of the SCDS curve referencing Japan, for the period from June 23, 2006 to December 31, 2014. From upper left to lower right, the maturity increases in length, and from upper right to lower left, the time becomes nearer to the end of the period of analysis. We use the composite middle spreads, provided by Markit, of US dollar-denominated SCDS contracts referencing Japan, with 11 different maturities: 6 months, 1 year, 2 years, 3 years, 4 years, 5 years, 7 years, 10 years, 15 years, 20 years, and 30 years.

As shown in the most left end of the surface in Fig. 4.30, which shows the SCDS curve at the end of December 2014, an SCDS curve usually has an upward slope as the length of maturity increases. Because the SCDS spread tends to become higher (riskier) for the longer maturity due to the higher uncertainty in order to protect against a credit event that may occur in the country.

There are missing spread observations of some maturities in the beginning of the period. A few sharp increases in the SCDS curve level are found. The first sharp increase occurred upon the bankruptcy of Lehman Brothers in the fall of 2008. The

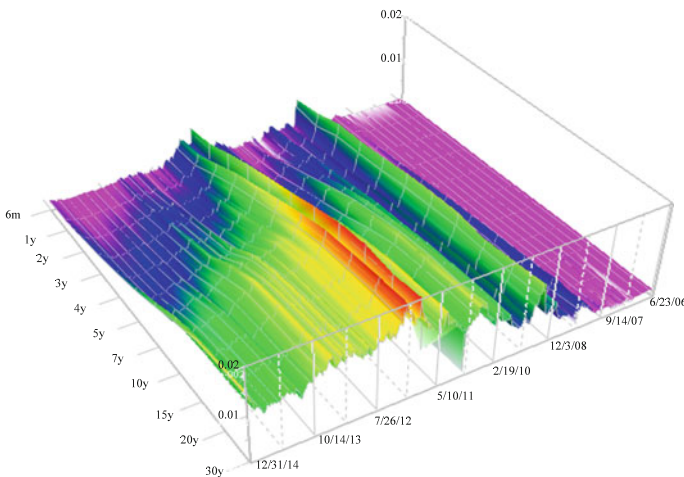


**Fig. 4.30** Time series of Japanese SCDS curve. The maturity (from upper left to lower right), the time (from upper right to lower left), and the spread (vertical scale), are shown. Source Markit

**Table 4.11**  $AIC_{\lambda}^0$  for major  $\lambda$ s

$\lambda$	1	0.5	0	-0.5	-1
$AIC_{\lambda}^0$	-29,529	-31,103	-31,143	-30,194	-25,835

conspicuously sharp increase starting from the beginning of 2010 gradually reached a peak at the beginning of October 2011, which may reflect the European debt crisis.

Let us consider estimating an underlying SCDS spread level using an SCDS curve at a point in time, assuming that an SCDS spread for each maturity is appropriately distributed around this level in response to external uncertain influences. Then the underlying SCDS spread level can be a basic spread for pricing, reflecting a domestic credit strength specific to the country at that time.

By applying the method for constructing a distribution-free index presented in Chap. 2, to the SCDS curves referencing Japan, consisting of the spreads of 11 different maturities, we construct the Japanese SCDS distribution-free index.

First, we calculate  $AIC_{\lambda}^0$  in (2.61) by changing the parameter  $\lambda$  of the Box-Cox transformation (2.47) (Box and Cox 1964) and search for the optimal  $\lambda$ . In Table 4.11 showing  $AIC_{\lambda}^0$  for major  $\lambda$ s, the minimum value of  $AIC_{\lambda}^0$  is obtained at  $\lambda = 0$ . In order to ensure validity of the optimal transformation, we also examine  $AIC_{\lambda}^0$  for the SCDS curves of other 73 countries, and the optimal  $\lambda = 0$  is obtained for 32% of countries. Considering these results, we select the logarithmic transformation ( $\lambda = 0$ ).

Next, the trend estimation using the optimal Box-Cox transformation is conducted. Figure 4.31 shows, from top to bottom, the estimated trend with  $\pm\sigma$ , the residual term, which is the difference between the mean of the log-transformed SCDS spreads and the estimated trend at each point in time, the estimated time-varying variance and the number of observations. Although there are a few missing spreads in the SCDS curve at some points in time, the optimal trend is smoothly estimated. The sharp peaks of the time-varying variance are often found from 2008 to 2009 due to the turning points of the trend, that may be caused by the global financial crisis. Generally, the trend is well estimated. By the inverse Box-Cox transformation of the optimal trend (2.62) in Chap. 2, the Japanese SCDS distribution-free index is obtained. Note that the information on the length of maturity is not taken into account in the estimation.

In order to figure out if the Japanese SCDS distribution-free index can be considered as an underlying SCDS spread level, we investigate the relationships between the Japanese SCDS distribution-free index and the SCDS spreads of 11 maturities, as shown in Fig. 4.32. In the top panel, the Japanese SCDS distribution-free index and the time series of the SCDS spreads with maturities of 6 months, 1 year, 2 years, 3 years, 4 years, 5 years, 7 years, 10 years, 15 years, 20 years, and 30 years are shown. In the middle and bottom panels, the difference between the index and spreads with maturities longer than or equal to 5 years, and the difference between the index and spreads with maturities shorter than 5 years, are shown, respectively. Note that a few sudden drops to zero in the top panel indicate missing spreads. For simplicity, the data based on the month-end are shown.

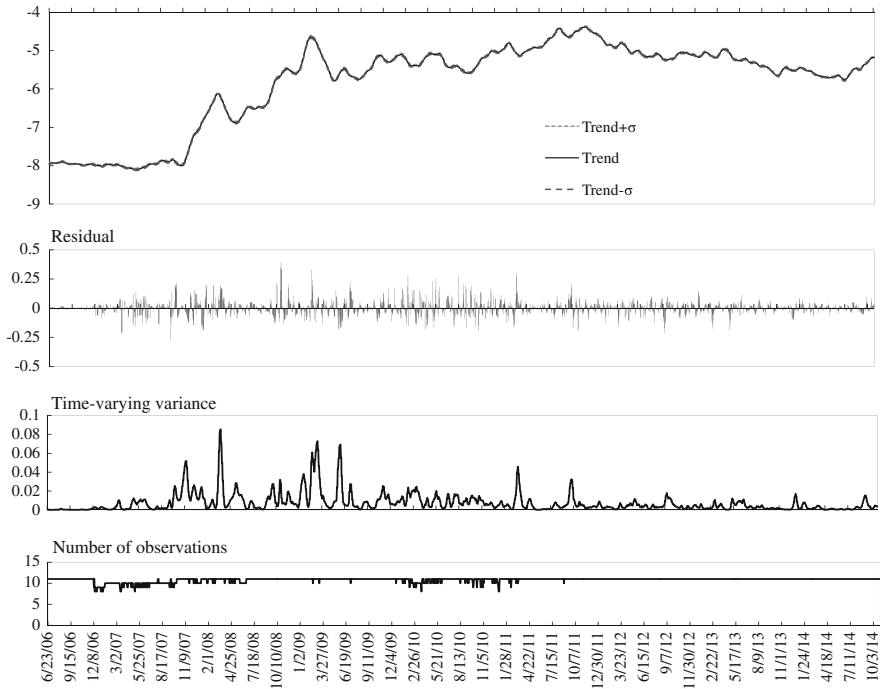


**Fig. 4.31** Visualization of the characteristics of the optimal trend for Japanese SCDS curves. The estimated trend, the residual term, the time-varying variance, and the number of observations are shown from top to bottom

For the period from June 2006 to the end of 2007, in the top panel, the Japanese SCDS distribution-free index (red dotted line) had an approximately 5-year spread (blue dotted line). In the middle panel, the spread differences between the Japanese SCDS distribution-free index and contracts with maturities longer than or equal to 5 years, were approximately less than 10 bps, while in the bottom panel, the spread differences between the index and contracts with maturities shorter than 5 years, were symmetrically more than -10 bps. As there were no significantly influential events on Japan before the global financial crisis, the underlying spread level can be naturally considered equivalent to the standard 5-year spread, which is most liquid, and the SCDS spreads for other maturities were priced in a balanced manner.

In 2008, as shown in the top panel, the Japanese SCDS distribution-free index was gradually shifted to have approximately a 4-year spread, but lower than the shift of a 5-year spread, reflecting the influence of the Lehman shock. Since then, the Japanese SCDS distribution-free index has stayed a more or less 4-year spread. Note that the standard 5-year contract has been priced riskier than the Japanese SCDS distribution-free index, reflecting the spillover effect from the crisis into the sovereign risk of Japan. Moreover, as shown in the middle panel, the spread differences between the Japanese SCDS distribution-free index and contracts with maturities longer than

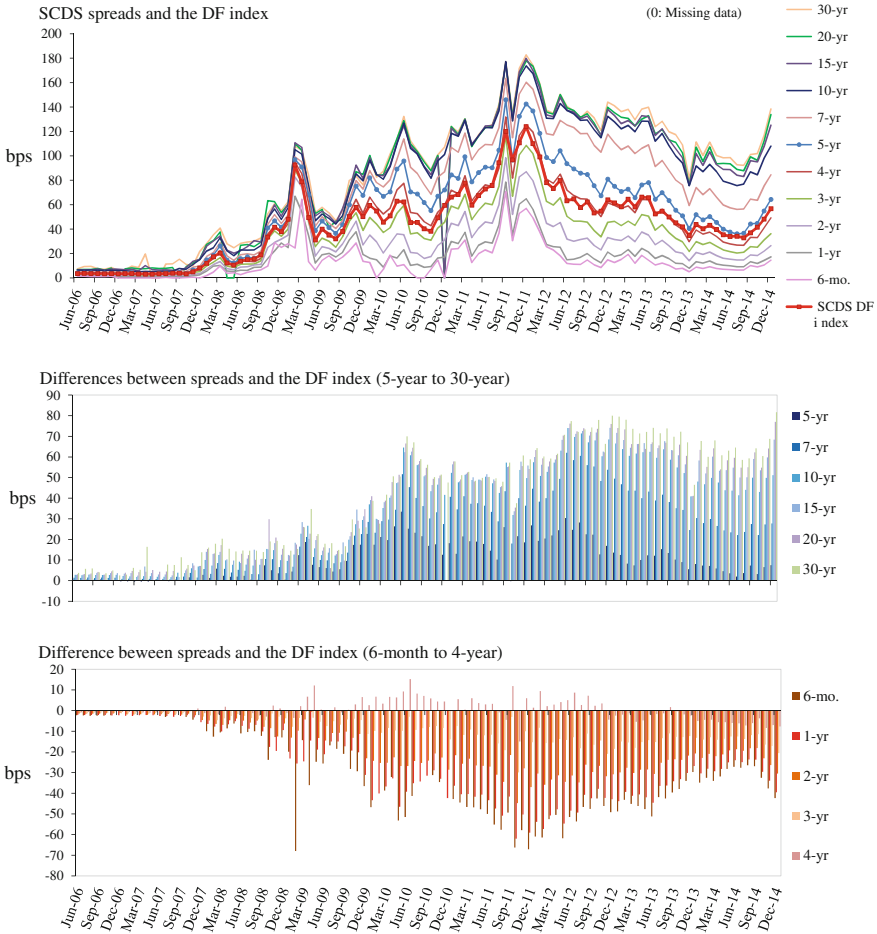


**Fig. 4.32** Relationships between the Japanese SCDS distribution-free index (SCDS DF index) and the SCDS spreads for maturities of 6 months, 1 year, 2 years, 3 years, 4 years, 5 years, 7 years, 10 years, 15 years, 20 years, and 30 years (top), the difference between the index and spreads with maturities longer than or equal to 5 years (middle), and the difference between the index and spreads with maturities shorter than 5 years (bottom). Source Markit

or equal to 5 years, rapidly increased in 2008, and then almost reached the maximum 80 bps of the 30-year contract, in December 2012. Symmetrically, as shown in the bottom panel, the spread differences between the index and contracts with maturities shorter than 5 years, decreased to almost reach the minimum  $-70$  bps of the 6-month contract, at the end of 2011.

The variations of spread differences in both middle and bottom panels since 2008, exhibits dynamic fluctuations responding to the external influences such as increasing uncertainty to the crisis. Neither spread differences had returned to the level before

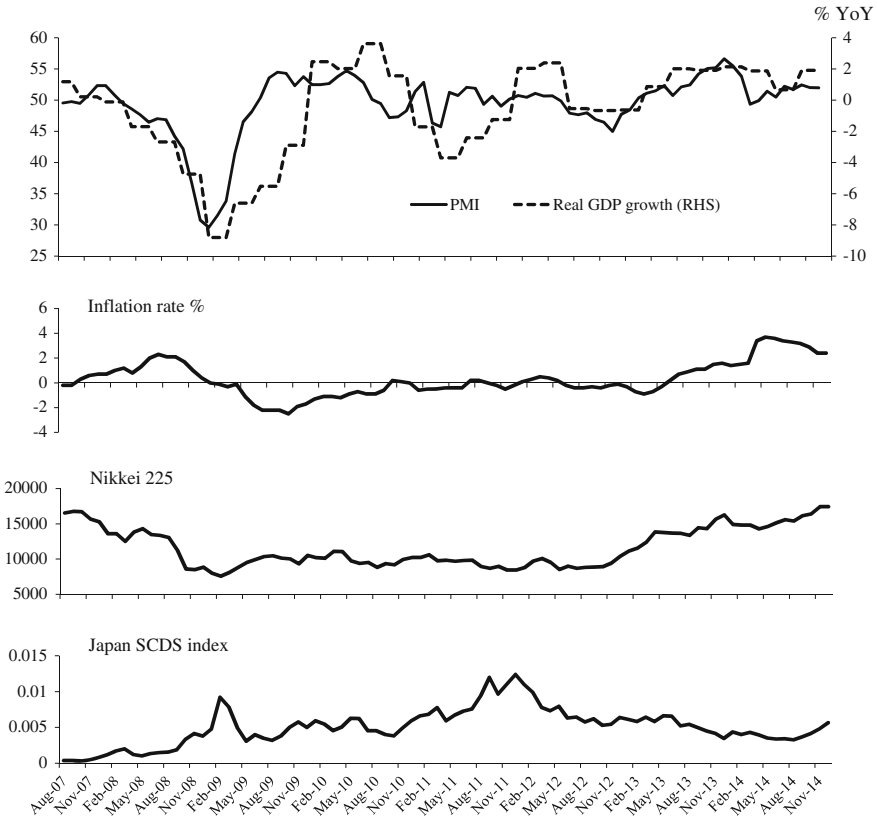


**Fig. 4.33** Purchasing Managers' Index (PMI: *solid line*) with the real GDP growth (*dashed line*) for Japan (*top*), the Japanese inflation rate (second from *top*), the Nikkei 225 (second from *bottom*), and the Japanese SCDS distribution-free index (*bottom*). *Source* Markit Economics Limited, OECD the Statistics Bureau of Japan, and the Nikkei

the US subprime crisis and the Japanese SCDS distribution-free index had never exceeded the 5-year spread level.

Next, let us investigate the relationships between the Japanese SCDS distribution-free index and the Japanese domestic indicators, representing the equity market and the economy. We focus on the period of analysis from August 2007 to December 2014 through the crises following the US subprime crisis. As shown in Fig. 4.33, as economic indicators, we use the seasonally adjusted Purchasing Managers' Index for the manufacturing sector of Japan (PMI) provided by Markit Economics Limited, and the inflation rate provided by the Statistics Bureau of Japan, and the Nikkei 225 provided by the Nikkei, representing the equity market. Note that the data provide a monthly base. As shown in the top panel, since the transition of PMI (solid line) is similar to that of the quarterly real GDP growth (dashed line) provided by OECD, we regard PMI as an economic indicator in this analysis.

**Table 4.12** Standard deviations (*diagonal*) and correlation coefficients (*off-diagonal*) of the noises for PMI (Purchasing Managers' Index), CPI (inflation rate), CDS (Japanese SCDS distribution-free index), and EQ (Nikkei 225)

	PMI	CPI	CDS	EQ
PMI	0.94			
CPI	-0.33	0.16		
CDS	-0.23	0.08	0.001	
EQ	0.24	-0.08	-0.06	205

Compared with the sharp V-shaped recovery of PMI (solid line), from the bottom at January 2009 to the mid-2009 due to the global economic crisis, which is shown in the top panel, both the recovery from the relatively steep decline of the Nikkei 225 in the second from bottom panel, and the peak out of the Japanese SCDS distribution-free index in the bottom panel, occurred in February 2009, i.e., one month later. Whereas, as shown in the second from top panel, the inflation rate bottomed out in October 2009. This may reflect that the shock of the crisis remained for approximately one year. The gradual upward trend in the Japanese SCDS distribution-free index since May 2009 was observed in the bottom panel. In other words, the underlying sovereign risk has gradually strengthened.

In order to investigate causations by the power contribution analysis (Akaike 1968; Tanokura and Kitagawa 2004) presented in Chap. 3, for each index, we focus on the short-term cyclical fluctuation around the trend. Using the software DECOMP based on the seasonal adjustment model (Gersch and Kitagawa 1983; Kitagawa and Gersch 1984) reviewed in Chap. 2, the detrended cyclical component is obtained by extracting the long-term trend from each index, as shown in Fig. 4.34. Various-shaped fluctuations of detrended cyclical components are observed.

Table 4.12 shows the standard deviations (diagonal) and correlation coefficients (off-diagonal) of the noises for PMI (Purchasing Managers' Index), CPI (inflation rate), CDS (Japanese SCDS distribution-free index), and EQ (Nikkei 225). The almost nonexistent correlation between EQ and CDS, that between EQ and CPI, and that between CDS and CPI are noteworthy. In particular, the almost nonexistent correlation between EQ and CDS contrasts the negative correlation between TOPIX and the Japanese corporate CDS distribution-free index for the post-subprime period, shown in Table 4.6 of Sect. 4.2. This may reflect the difference of productive characteristic between sovereign CDS referencing a country, and corporate CDS referencing a corporation. The positive correlation between EQ and PMI, and the negative correlation between CDS and PMI, are relatively strong. Interestingly, the correlation between economic indices, CPI and PMI, is negative.

We calculate the power contributions (%) (3.13), presented in Chap. 3. As shown in the graph matrix of Fig. 4.35, in each graph, each power spectrum on a logarithmic scale (white line), is decomposed into ten terms consisting of four contributions of independent noise, and six contributions of correlated noise.

There are a few outstanding common contributions of correlated noises such as ALL (yellow area), ALL-EQ (orange area), and ALL-CDS (green area). The

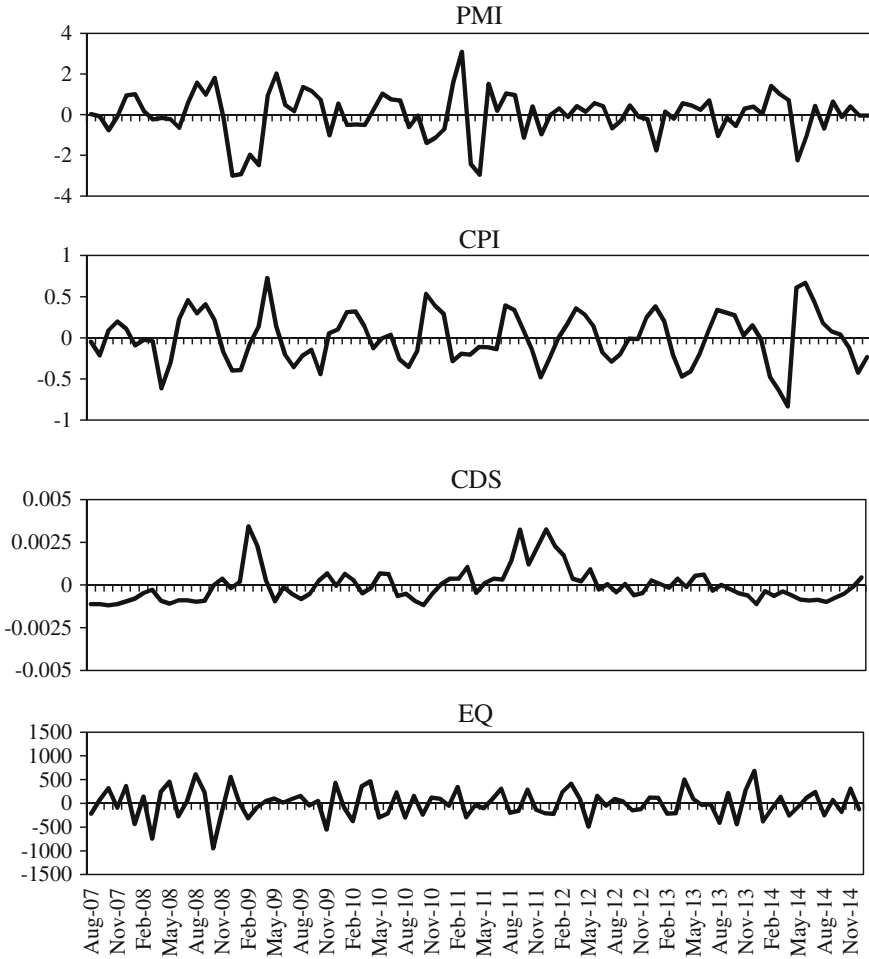


**Fig. 4.34** Detrended cyclical components of PMI (Purchasing Managers' Index), CPI (inflation rate), CDS (Japanese SCDS distribution-free index), and EQ (Nikkei 225) for Japan

contribution of the correlated noise ALL was large for PMI and CPI, whereas ALL-CDS contributed largely to PMI and CDS.

The contributions of independent noise, including the index itself, occupied approximately 50– 80 % for all indices. The economic indices, PMI and CPI, are largely due to EQ (red area) at some frequencies. In particular, CDS is largely affected by the independent noises of other indices, and the contribution of all independent noises reached 80% of the power spectrum. In other word, the fluctuations of CDS were likely to reflect the specific fluctuation of each index. In contrast, the contribution of CDS is relatively small for the other indices. Considering the productive characteristic of SCDS, dealing with sovereign risk on Japan, it is reasonable that

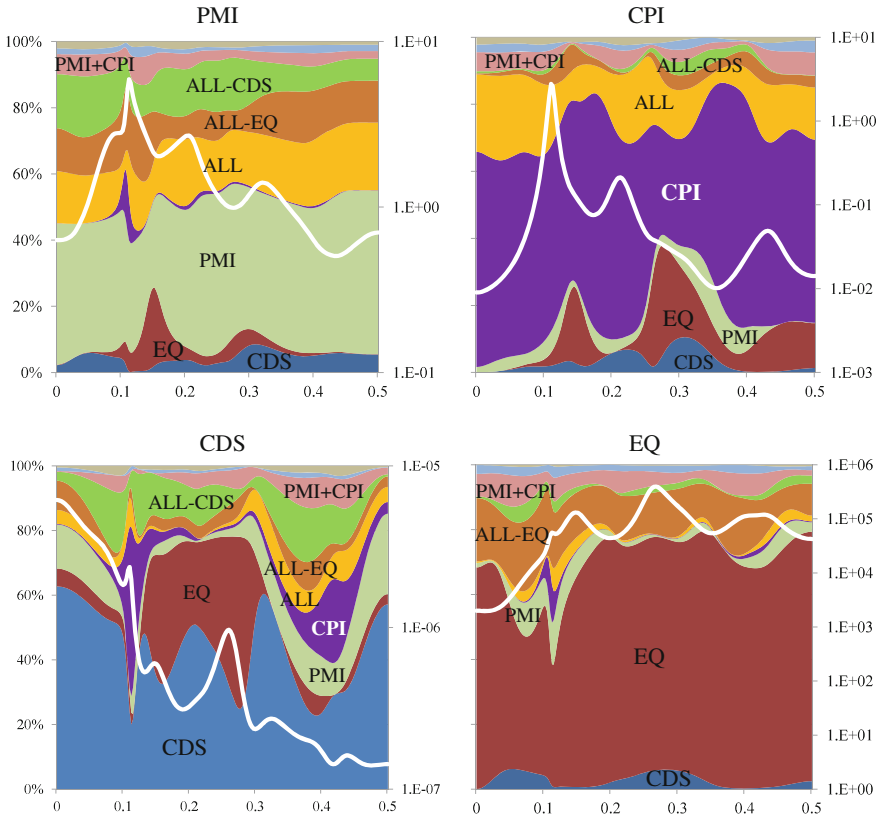


**Fig. 4.35** Power contributions (%) with the power spectrum on a logarithmic scale (*white line*) of PMI, CPI (inflation rate), CDS (Japanese SCDS distribution-free index) and EQ (Nikkei 225) for Japan

CDS (Japanese SCDS distribution-free index) is very sensitive to the fluctuations of the other domestic indices, such as Japanese financial markets and economy, which may cause a higher sovereign risk for the country. Therefore, the Japanese SCDS distribution-free index can be recognized as the indicator reflecting uncertain fluctuations in the equity market and the economy of the country.

Considering the peaks of the power spectra, we focus on the following two frequency domains: the frequency domain from 0.11 to 0.15 (approximately 8-month cycle of fluctuation), which includes the second peaks of EQ and CDS, and the peaks of PMI and CPI, and the frequency domain from 0.205 to 0.2675 (approximately 4-month cycle of fluctuation), which includes peaks of all indices. Then, as introduced in Sect. 4.2, we calculate the total contributions (%) of each index for both frequency domains, as shown in Table 4.13.

The total contributions of CDS, to CDS itself and EQ, which was 39.3 and 8.8 % for the frequency domain from 0.11 to 0.15, increased to 44.2 and 9.5 %, respectively,

**Table 4.13** Total contributions (%) for frequency domains from 0.11 to 0.15 (*left*) and from 0.205 to 0.2675 (*right*)

Frequency domain:	0.11–0.15				0.205–0.2675			
	(8-month cycle)				(4-month cycle)			
	CDS	EQ	PMI	CPI	CDS	EQ	PMI	CPI
CDS	39.3	8.8	11.6	8.4	44.2	9.5	10.2	11.1
EQ	20.3	55.1	19.9	18.0	38.9	72.7	13.2	15.9
PMI	12.1	22.4	48.5	12.1	9.3	9.9	62.1	12.2
CPI	28.3	13.7	20.0	61.5	7.6	7.9	14.5	60.8
Total	100.0	100.0	100.0	100.0	100.0	100.0	100.0	100.0

for the frequency domain from 0.205 to 0.2675. Similarly, the total contributions of EQ, to CDS and EQ increased, respectively. On the other hand, the total contributions of PMI, to CDS itself and EQ, which was 12.1 and 22.4% for the frequency domain from 0.11 to 0.15, decreased to 9.3 and 9.9%, respectively, for the frequency domain from 0.205 to 0.2675. Similarly, the total contributions of CPI, to CDS and EQ decreased, respectively. Note that the influences of the economic indices, PMI and CPI, on EQ and CDS, strengthened for the longer cycle of fluctuation. In particular, the total contribution of CPI increased for all indices.

The largest total contributor to CDS apart from CDS itself, was EQ for both frequency domains, whereas the largest total contributor to EQ excluding EQ itself was PMI for both frequency domains. As for the economic indices, the largest total contributor to PMI apart from PMI itself, was CPI for both frequency domains, whereas the largest total contributor to CPI excluding CPI itself was EQ for both frequency domains. Moreover, the total contribution of EQ to the other indices excluding CDS increased. The significant influence of EQ on all indices is found.

On the other hand, although the total contributions of CDS to the other indices were weak for both frequency domains, CDS was largely influenced by the other indices for the longer cycle of fluctuation. In other word, CDS is relatively sensitive to the fluctuations of other domestic indices. Note that, regardless of the contribution amount, the influence from the market-related indices, CDS and EQ, on the economic indices, PMI and CPI, cannot be ignored.

Based on the above-mentioned investigations, we consider the Japanese SCDS distribution-free index as an underlying SCDS spread level reflecting a domestic credit strength specific to Japan. The usability of this index for pricing can be proposed under the following assumptions:

1. The information on the length of maturity is factored into the SCDS spread of each concerned maturity.
2. An SCDS spread for each maturity is quoted by adding (or deducting) an extra spread corresponding to the length of maturity to (or from) the SCDS distribution-free index. The extra spread can be evaluated based on external influences such as other country's sovereign risks, the investor's forecast, or the international views on financial markets and economies.

The fluctuations of the extra spread, and the reversion of the slope of the SCDS curve, which is occasionally observed when the referencing country is in a critical situation for political or economical problems, should be investigated. We leave these modeling for future studies.

In this section, we examined the usability of a distribution-free index in two applications: constructing a GDP growth regional distribution-free index and a Japanese SCDS distribution-free index.

Finally, we believe that the applications presented in this chapter, verify the effectiveness of a distribution-free index, and confirm that applying our method to data with insufficient information, such as fast-growing or immature financial markets and economic indicators of emerging economies, can be effective. The wider applicable area of the method for constructing a distribution-free index can be expected.

## References

- Akaike, H.: On the use of a linear model for the identification of feedback systems. *Ann. Inst. Statist. Math.* **20**, 425–439 (1968)
- Akaike, H.: Information theory and an extension of the maximum likelihood principle. In: Parzen, E., Tanabe, K., Kitagawa, G. (eds.) *Selected Papers of Hirotugu Akaike*, pp. 199–213. Springer, New York (1998)
- Box, G.E.P., Cox, D.R.: An analysis of transformations. *J. R. Stat. Soc. Ser. B* **26**(2), 211–252 (1964)
- Cossin, D., Hricko, T., Daniel, A.-N., Zhijiang, H.: Exploring for the determinants of credit risk in credit default swap transaction data: is fixed-income markets' information sufficient to evaluate credit risk? *FAMA Research Paper*, 65 (2002)
- Doucet, A., de Freitas, N., Gordon, N.: *Sequential Monte Carlo Methods in Practice*. Springer, New York (2001)
- Fung, H.-G., Sierra, G.E., Yau, J., Zhang, G.: Are the U.S. stock market and credit default swap market related? Evidence from the CDX indices. *J. Altern. Invest.* **11**(1), 43–61 (2008)
- Gersch, W., Kitagawa, G.: The prediction of time series with trends and seasonalities. *J. Bus. Econ. Stat.* **1**(3), 253–264 (1983)
- Kitagawa, G.: *Introduction to Time Series Modeling*. CRC Press, Boca Raton (2010)
- Kitagawa, G., Gersch, W.: A smoothness priors-state space modeling of time series with trend and seasonality. *J. Am. Stat. Assoc.* **79**(386), 378–389 (1984)
- Kitagawa, G., Gersch, W.: *Smoothness Priors Analysis of Time Series*. In: *Lecture Notes in Statistics*, vol. 116, Springer, New York (1996)
- Konishi, S., Kitagawa, G.: *Information Criteria and Statistical Modeling*. Springer, New York (2008)
- Tanokura, Y., Kitagawa, G.: Modeling influential correlated noise sources in multivariate dynamic systems. In: Hamza, M.H. (ed.) *Modelling and Simulation: Fifteenth IASTED International Conference Proceedings*, pp. 19–24. ACTA Press, CA (2004)
- Tanokura, Y., Tsuda, H., Sato, S., Kitagawa, G.: Constructing a credit default swap index and detecting the impact of the financial crisis. In: Bell, W.R., Holan, S.H., McElroy, T.S. (eds.) *Economic Time Series: Modeling and Seasonality*, pp. 359–380. CRC Press, Boca Raton (2012)

# Index

## A

AIC, [v](#), [2](#), [16](#), [29–31](#), [51](#), [68](#)  
AIC <sub>$\lambda$</sub> <sup>0</sup>, [31](#), [33](#), [51](#), [68](#), [81](#), [91](#)  
Akaike's power contribution, [vi](#), [4](#), [35](#), [36](#),  
[38](#), [40](#), [43](#), [46](#)  
AR model, [9](#), [15](#), [59](#)  
Auto-covariance, [6](#)  
Auto-covariance function, [6](#), [7](#)  
Autoregressive model, [9](#), [59](#)

## B

Box–Cox transformation, [v](#), [1](#), [2](#), [13](#), [28](#), [29](#),  
[31](#), [33](#), [50](#), [68](#), [81](#), [91](#)  
Box–Cox transformed, [v](#), [2](#), [30](#), [51](#)

## C

Cauchy distribution, [23](#), [29](#)  
Cauchy observation noise, [28](#)  
Cauchy trend estimation model, [29](#), [67](#), [68](#)  
CDS, [2](#), [49](#), [90](#)  
CDS rating-based distribution-free index,  
[65](#), [68](#), [71](#), [72](#)  
Chi-squared ( $\chi^2$ ) distribution, [17](#), [18](#)  
Cholesky decomposition, [44](#)  
Conditional distribution, [24](#), [25](#)  
Conditional mean, [8](#), [24](#), [29](#)  
Conditional variance covariance matrix, [8](#),  
[24](#), [29](#)  
Corporate CDS, [27](#), [31](#), [64](#), [65](#)  
Correlated noise, [39](#), [43](#), [45](#), [63](#), [74](#), [76](#), [95](#)  
Correlation coefficients, [74](#), [95](#)  
Correlation matrix, [40](#), [42](#)  
Covariance, [74](#)  
Credit default swap, [2](#), [49](#)  
Cross spectrum, [36](#)

Cross spectrum matrix, [36](#), [37](#), [39](#)  
Cross-covariance, [7](#)  
Cross-covariance function, [7](#), [36](#)  
Cross-covariance matrix, [7](#), [37](#)  
Cross-spectral density function, [36](#)

## D

DECOMP (Web DECOMP), [10](#), [22](#), [59](#), [73](#),  
[95](#)  
Detrended cyclical component, [10](#), [22](#), [59](#),  
[73](#), [95](#)  
Distribution-free index, [v](#), [1](#), [2](#), [5](#), [10](#), [13](#), [30–](#)  
[32](#), [35](#), [49](#), [50](#), [57](#), [65](#), [78](#), [81](#), [88](#), [91](#),  
[99](#)  
Double exponential distribution, [17](#), [18](#)  
Dow Jones Industrial Average, [13](#)

## E

Exponential distribution, [18](#)  
Extended Kalman filter, [24](#)

## F

Fixed interval smoothing algorithm, [2](#), [16](#),  
[17](#)  
Fourier transform, [36](#), [37](#)  
Frequency domain approach, [4](#), [35](#)

## G

Gaussian distribution, [2](#), [8](#), [14](#), [16](#), [20](#), [27](#), [31](#)  
Gaussian observation noise, [28](#), [32](#)  
Gaussian state-space model, [22](#), [24](#)  
Gaussian trend estimation model, [29](#), [67](#), [68](#)

GDP growth regional distribution-free index, 49, 64, 78, 81, 83, 86, 88  
 Generalized power contribution, vi, 1, 4, 10, 35, 38, 40, 43, 44, 46, 61, 74, 76  
 GTV trend estimation model, 29, 30, 33, 68

## H

Heavy-tailed distribution, v, 2, 23, 50, 65

## I

Independent noise, 39, 43, 45, 74, 76, 96  
 Inflation rate, 94  
 Inverse Box–Cox transformation, v, 2, 13, 30, 33, 52, 68, 91  
 Inverse Box–Cox transformed, 31, 81, 83  
 iTraxx SovX Asia Pacific, 57  
 iTraxx SovX CEEMA, 57  
 iTraxx SovX Western Europe, 56, 57

## J

Jacobian, 31  
 Japanese consumer price index for spinach, 19, 22  
 Japanese corporate CDS distribution-free index, v, 65, 71–73, 78  
 Japanese SCDS distribution-free index, 49, 91, 94, 98  
 JCR, 66  
 JPYUSD, 65, 73

## K

Kalman filter, 2, 8, 16, 17, 24, 29, 33

## L

Lag operator, 15, 20, 21  
 Log-likelihood, 26, 30, 31  
 Logarithmic transformation, 17

## M

Markit iTraxx SovX indices, 57  
 Maximum likelihood estimate, 26  
 Maximum likelihood method, 16, 29, 33  
 Mean, 6  
 Mean value function, 6, 7, 13, 20  
 Missing observations, v, 2, 8, 27, 29, 52, 57, 71, 90  
 Moody's, 66  
 Moving average, 13

Multivariate AR model, 4, 36, 37, 74  
 Multivariate autoregressive model, 4, 36  
 Multivariate feedback system, 1, 4, 10, 35, 40

## N

Nikkei 225, 7, 94  
 Nomura-BPI overall index, 65, 73  
 Non-Gaussian distribution, 13, 23, 28, 30  
 Non-Gaussian filter, 19, 24, 25, 29  
 Non-Gaussian observation noise, 28  
 Non-Gaussian state-space model, 23, 24  
 Nonlinear non-Gaussian state-space representation, 25  
 Nonlinear state-space model, 25  
 Nonstationary non-Gaussian multivariate time series, v, 1, 2  
 Nonstationary time series, 7, 16, 22  
 Nonstationary time series model, 10, 13

## O

Observation model, 8, 9, 20  
 Observation noise, 8, 18, 20, 23

## P

Power contribution, 22, 49, 50, 59, 63, 65, 73, 76, 95  
 Power spectral density function, 36  
 Power spectrum, 36, 37, 39, 44, 61, 63, 74, 76, 95, 97  
 Purchasing Managers' Index (PMI), 94

## R

R&I, 66  
 Random walk model, 14  
 Real GDP growth, 78–81, 94

## S

SCDS, 2, 49, 50, 65, 90, 98  
 SCDS curve, 78, 90, 99  
 SCDS regional distribution-free index, 3, 50, 52, 53, 56, 59, 63, 64, 78, 86, 88  
 Seasonal adjustment model, 13, 19, 21, 22, 59, 73  
 Seasonal component, 19, 20  
 Seasonal component model, 20, 21  
 Seasonality, 19  
 Sequential Monte Carlo filter, 25, 26, 29, 68

Short-term cyclical fluctuation, vi, 4, 5, 7, 10, 22  
Smoothing algorithm, 19, 24, 25, 29  
Sovereign CDS, 2, 49, 50  
Standard & Poor's, 66  
Standard deviation, 95  
State vector, 8, 24  
State-space model, v, 8, 9, 15–17, 22, 23, 26, 29  
Stationary AR component model, 20  
Stationary component, 20  
Stationary time series, 6, 36  
Statistical Financial Risk Monitor (Stat-FiRM), 10  
System model, 8, 9  
System noise, 8, 17, 23

**T**

Time difference operator, 14, 15  
Time domain approach, 4, 35

Time-varying variance, v, 16, 18, 23, 29, 33, 51, 83, 91  
Time-varying variance model, 13, 24, 25, 29, 33  
TOPIX, 65, 73  
Total contribution, 76, 78, 97  
Trend, v, vi, 4, 7, 13  
Trend component, 14, 17, 20, 30, 59  
Trend component model, 14, 15, 20, 67  
Trend model, v, 1, 14, 15, 17, 28, 30, 32

**V**

Variance, 6, 74  
Variance covariance matrix, 4, 8, 35–40, 42–45

**W**

Weakly stationary, 6  
White noise, 8, 14, 36